



VCU

Virginia Commonwealth University
VCU Scholars Compass

Theses and Dissertations

Graduate School

2013

ASSESSMENT OF THE FEASIBILITY OF CO-ADMINISTRATION OF PHENOLIC DIETARY COMPOUNDS WITH PHENYLEPHRINE TO INCREASE ITS BIOAVAILABILITY

Zhenxian Zhang
Virginia Commonwealth University

Follow this and additional works at: <https://scholarscompass.vcu.edu/etd>



Part of the [Pharmacy and Pharmaceutical Sciences Commons](#)

© The Author

Downloaded from

<https://scholarscompass.vcu.edu/etd/539>

This Dissertation is brought to you for free and open access by the Graduate School at VCU Scholars Compass. It has been accepted for inclusion in Theses and Dissertations by an authorized administrator of VCU Scholars Compass. For more information, please contact libcompass@vcu.edu.

© Zhenxian Zhang, 2013
All Rights Reserved

**ASSESSMENT OF THE FEASIBILITY OF CO-ADMINISTRATION OF PHENOLIC
DIETARY COMPOUNDS WITH PHENYLEPHRINE TO INCREASE ITS
BIOAVAILABILITY**

A dissertation submitted in partial fulfillment of the requirements for the degree of
Doctor of Philosophy at Virginia Commonwealth University

By

Zhenxian Zhang

Master of Science, The University of Toledo, OH, USA

Bachelor of Engineering, China Pharmaceutical University, Jiangsu, China

Director: Dr. Phillip M. Gerk,
Associate Professor, Department of Pharmaceutics

Virginia Commonwealth University
Richmond, Virginia
August, 2013

ACKNOWLEDGEMENTS

This dissertation would not be possible without the guidance of my committee members, help from my friends, support from my family, and funding from VCU School of Pharmacy and Graduate School. I would like to take this opportunity to express my deepest gratitude to everyone that has supported me during my past four years as a Ph.D. student.

Firstly, I would like to thank my advisor, Dr. Phillip M. Gerk, for his guidance and criticism in my research.

I would also like to thank all my committee members for their suggestions and continuous help through my research. Dr. Jurgen Venitz helped me understanding Pharmacokinetics and Pharmacodynamics which is an important part of my research. He also provided precious advice in the clinical trial design. I am very grateful to Dr. William H. Barr and Dr. Masahiro Sakagami's input in my research. They have always been so patient with my questions. Last but not least, I would like to thank Dr. Joseph K. Ritter and Dr. MaryPeace McRae for their guidance.

In addition, I would like to thank Dr. Matthew S. Halquist for his help in LC-MS/MS instrument operation and method development.

I would like to thank Dr. Aditi Mulgaonkar for sharing her enzyme kinetics knowledge and research resources with me. I would like to thank Morse Faria for his help in LC-MS/MS method development and HPLC method validation. I would like to thank Dr. Lei Wang for his advice in metabolite synthesis and purification. I would also like to thank all my fellow graduate students for their encouragement and support during my four years as a Ph.D. student.

Special thanks go to my family and friends for their love, support, and encouragement.

TABLE OF CONTENTS

LIST OF TABLES	I
LIST OF FIGURES	III
LIST OF ABBREVIATIONS	VI
ABSTRACT.....	IX
CHAPTER 1	1
CLINICAL SIGNIFICANCE AND PHARMACOKINETIC PROBLEM OF PHENYLEPHRINE.....	1
1.1 CLINICAL SIGNIFICANCE AS ORAL NASAL DECONGESTANT	1
1.2 PHYSICOCHEMICAL PROPERTIES AND PHARMACOLOGY	2
1.3 EFFICACY AND SAFETY	3
1.4 ANALYTICAL METHODS.....	4
1.5 PHARMACOKINETICS OF PHENYLEPHRINE IN HUMANS	7
1.6 LOW BIOAVAILABILITY AND EXTENSIVE PRE-SYSTEMIC METABOLISM.....	11
1.7 PREDOMINANT METABOLIC PATHWAYS: SULFATION AND OXIDATIVE DEAMINATION	15
1.8 COMMON APPROACHES TO IMPROVE ORAL BIOAVAILABILITY.....	16
1.9 THE STRATEGY TO INCREASE ORAL BIOAVAILABILITY OF PHENYLEPHRINE: INHIBITION OF PRE-SYSTEMIC SULFATION	17
1.10 SUMMARY	19
CHAPTER 2	21
OBJECTIVE AND SPECIFIC AIMS	21

2.1 OBJECTIVE AND HYPOTHESIS.....	21
2.1.1 Objective.....	21
2.1.2 Hypothesis.....	21
2.2 SPECIFIC AIMS.....	21
2.2.1 Specific Aim I.....	21
2.2.2 Specific Aim II.....	22
2.2.3 Specific Aim III.....	22
CHAPTER 3.....	23
SCREENING POTENTIAL INHIBITORS FOR PRE-SYSTEMIC SULFATION OF PHENYLEPHRINE WITH LS180 CELL MODEL	23
3.1 INTRODUCTION.....	23
3.2 MATERIALS AND METHODS	24
3.2.1 Chemicals and Reagents	24
3.2.2 Apparatus	25
3.2.3 Screening of Potential Inhibitors	25
3.2.4 LS180 Cell Culture	31
3.2.5 Characterization of the Sulfation Activity in LS180 Cells	31
3.2.6 HPLC Method for Phenylephrine	32
3.2.7 Linearity of Incubation Time and Concentration-dependent Study	33
3.2.8 Optimized Inhibition Assay	34
3.2.9 Data Description and Statistical Analysis.....	34
3.3 RESULTS	35
3.4 DISCUSSION AND CONCLUSIONS.....	42

CHAPTER 4..... 47

CHEMICAL SYNTHESIS AND CHARACTERIZATION OF R-(-)-PHENYLEPHRINE

SULFATE AND R-(-)-ETILEFRINE SULFATE 47

4.1 INTRODUCTION..... 47

4.2 MATERIALS AND METHODS 54

4.2.1 Chemicals and Reagents 54

4.2.2. Apparatus 54

4.2.3 Reaction I..... 56

4.2.4 Reaction II..... 58

4.2.5 Identification and Characterization of PE/ET Sulfate 59

4.2.6 Chemical Hydrolysis of PE/ET Sulfate 59

4.3 RESULTS 61

4.4 DISCUSSION AND CONCLUSIONS..... 69

CHAPTER 5..... 73

LC-MS/MS METHOD DEVELOPMENT FOR SIMULTANEOUS QUANTITATION OF

PHENYLEPHRINE AND ITS METABOLITES 73

5.1 INTRODUCTION..... 73

5.2 MATERIALS AND METHODS 76

5.2.1 Chemicals and Reagents 76

5.2.2 Apparatus 76

5.2.3 Application of the Preliminary LC-MS/MS Method..... 77

5.2.4 LC-MS/MS Method Development 77

5.3 RESULTS AND DISCUSSION..... 85

CHAPTER 6.....	89
THE EFFECT OF POTENTIAL INHIBITORS ON MONOAMINE OXIDASE A/B ACTIVITY.....	89
6.1 INTRODUCTION.....	89
6.2 MATERIALS AND METHODS	92
6.2.1 Chemicals and Reagents	92
6.2.2 Apparatus	93
6.2.3 HPLC Method for Kynuramine and 4-Hydroxyquinoline.....	93
6.2.4 Preliminary Studies.....	96
6.2.5 Optimized Enzyme Kinetic Assay and K_m Determination	97
6.2.6 Inhibition Screening and IC_{50} Determination	97
6.3 RESULTS	100
6.3.1 HPLC Method Validation.....	100
6.3.2 Preliminary Studies.....	102
6.3.3 Optimized Enzyme Kinetic Assay and K_m Determination	106
6.3.4 Inhibition Screening and IC_{50} Determination	108
6.4 DISCUSSION AND CONCLUSIONS.....	115
CHAPTER 7.....	121
OVERALL CONCLUSIONS AND FUTURE DIRECTIONS.....	121
REFERENCES.....	127
VITA.....	141

LIST OF TABLES

TABLE 1.1. HPLC METHODS FOR PHENYLEPHRINE IN PHARMACEUTICAL FORMULATIONS AND BIOLOGIC FLUIDS	6
TABLE 1.2. PHARMACOKINETIC PARAMETERS OF PHENYLEPHRINE IN CLINICAL TRIALS	9
TABLE 1.3. URINARY EXCRETION OF PHENYLEPHRINE METABOLITES AS PERCENTAGE OF ADMINISTERED DOSE.....	13
TABLE 3.1. CHEMICAL PROPERTIES OF POTENTIAL INHIBITORS [8]	28
TABLE 3.2. PHARMACOKINETIC PROPERTIES OF POTENTIAL INHIBITORS.....	29
TABLE 3.3. EFFECTS OF PHENOLIC DIETARY COMPOUNDS ON PHENYLEPHRINE DISAPPEARANCE	40
TABLE 3.4. EFFECTS OF COMBINATIONS OF PHENOLIC DIETARY COMPOUNDS ON PHENYLEPHRINE DISAPPEARANCE	41
TABLE 4.1. HPLC PURITY TEST FOR PHENYLEPHRINE SULFATE	61
TABLE 4.2. HPLC PURITY TEST FOR ETILEFRINE SULFATE	62
TABLE 5.1. GRADIENT ELUTION FOR LC METHOD	80
TABLE 5.2. MRM TRANSITIONS FOR PE METABOLITES, PE AND THEIR INTERNAL STANDARDS ...	82
TABLE 5.3. OPTIMIZED MASS SPECTROMETER PARAMETERS	82
TABLE 5.4. INHIBITION OF PHENYLEPHRINE SULFATE FORMATION WITH DIETARY COMPOUNDS IN LS180 CELLS.....	85
TABLE 5.5. COMPARISON OF PHENYLEPHRINE DISAPPEARANCE AND SULFATE FORMATION WITH DIETARY COMPOUNDS IN LS180 CELLS	85
TABLE 6.1. GRADIENT ELUTION FOR KYNURAMINE AND 4-HYDROXYQUINOLINE.....	93
TABLE 6.2. SOLUBILITY AND MAXIMUM SINGLE DOSE OF PHENOLIC DIETARY COMPOUNDS	99
TABLE 6.3. INTRA-ASSAY ACCURACY AND PRECISION FOR KYNURAMINE	100

TABLE 6.4. INTRA-ASSAY ACCURACY AND PRECISION FOR 4-HYDROXYQUINOLINE	100
TABLE 6.5. INTER-ASSAY ACCURACY AND PRECISION FOR KYNURAMINE.....	101
TABLE 6.6. INTER-ASSAY ACCURACY AND PRECISION FOR 4-HYDROXYQUINOLINE.....	101
TABLE 6.7. SAMPLE PROCESSING STABILITY FOR KYNURAMINE	101
TABLE 6.8. SAMPLE PROCESSING STABILITY FOR 4-HYDROXYQUINOLINE	102
TABLE 6.9. IC ₅₀ AND HILL COEFFICIENT FOR MAO-A INHIBITION BY PHENOLIC COMPOUNDS...	113
TABLE 6.10. IC ₅₀ AND HILL COEFFICIENT FOR MAO-B INHIBITION BY PHENOLIC COMPOUNDS.	115

LIST OF FIGURES

FIGURE 1.1. STRUCTURES OF PHENYLEPHRINE ENANTIOMERS	2
FIGURE 1.2. PROPOSED METABOLIC PATHWAYS OF PHENYLEPHRINE.....	14
FIGURE 1.3. DISPOSITION SCHEME FOR RESEARCH PROJECT GOALS	20
FIGURE 3.1. STRUCTURES OF POTENTIAL SULT INHIBITORS SELECTED FROM FDA’S “GRAS” LIST, EAFUS, OR DIETARY COMPOUNDS	27
FIGURE 3.2. REMAINING 1-NAPHTHOL AND 1-NAPHTHOL SULFATE FORMATION OVER 2 HRS IN LS180 CELLS.....	36
FIGURE 3.3. FRACTION OF REMAINING PHENYLEPHRINE OVER 40 HRS IN LS180 CELLS.....	37
FIGURE 3.4. PHENYLEPHRINE DISAPPEARANCE OVER A BROAD RANGE OF CONCENTRATIONS IN LS180 CELLS.....	38
FIGURE 4.1. SYNTHETIC ROUTE FOR PHENYLEPHRINE/ETILEFRINE SULFATE BY PROTECTING THE SECONDARY HYDROXYL GROUP WITH JONES OXIDATION.....	51
FIGURE 4.2. SYNTHETIC ROUTE FOR PHENYLEPHRINE/ETILEFRINE SULFATE BY PROTECTING THE SECONDARY HYDROXYL GROUP WITH ESTERIFICATION.....	53
FIGURE 4.3. REACTION I FOR SYNTHESIS OF TRIFLUORO-ACETIC ACID 1-(3-HYDROXY-PHENYL)-2- [METHYL-(2,2,2-TRIFLUORO-ACETYL)-AMINO]-ETHYL ESTER/TRIFLUORO-ACETIC ACID 2- [ETHYL-(2,2,2-TRIFLUORO-ACETYL)-AMINO]-1-(3-HYDROXY-PHENYL)-ETHYL ESTER	56
FIGURE 4.4. POTENTIAL BY-PRODUCTS FROM REACTION I	57
FIGURE 4.5. REACTION II FOR SYNTHESIS OF PHENYLEPHRINE/ETILEFRINE SULFATE	58
FIGURE 4.6. ¹ H-NMR SPECTRUM FOR PHENYLEPHRINE SULFATE	63
FIGURE 4.7. ¹³ C-NMR SPECTRUM FOR PHENYLEPHRINE SULFATE	64
FIGURE 4.8. HPLC PURITY TEST FOR PHENYLEPHRINE SULFATE	65

FIGURE 4.9. ¹ H-NMR SPECTRUM FOR ETILEFRINE SULFATE	66
FIGURE 4.10. ¹³ C-NMR SPECTRUM FOR ETILEFRINE SULFATE	67
FIGURE 4.11. HPLC PURITY TEST FOR ETILEFRINE SULFATE	68
FIGURE 5.1. COLUMN SWITCHING TECHNIQUE FOR LC-MS/MS METHOD	79
FIGURE 5.2. STRUCTURES OF INTERNAL STANDARDS FOR 3-HYDROXYMANDELIC ACID AND PHENYLEPHRINE	79
FIGURE 5.3. GRADIENT CURVE FOR LC METHOD	80
FIGURE 5.4. REPRESENTATIVE CHROMATOGRAPH OF PHENYLEPHRINE SULFATE, 3- HYDROXYMANDELIC ACID, AND HOMOVANILIC ACID (I.S.) IN NEGATIVE ION MODE	83
FIGURE 5.5. REPRESENTATIVE CHROMATOGRAPH OF PHENYLEPHRINE AND ETILEFRINE (I.S.) IN POSITIVE ION MODE	84
FIGURE 6.1. KYNURAMINE CONVERTED TO 4-HYDROXYQUINOLINE VIA 3-(2-AMINOPHENYL)-3- OXO-PROPIONALDEHYDE.....	92
FIGURE 6.2. TIME DEPENDENCE FOR OXIDATIVE DEAMINATION OF KYNURAMINE WITH MAO-A	103
FIGURE 6.3. TIME DEPENDENCE FOR OXIDATIVE DEAMINATION OF KYNURAMINE WITH MAO-B	104
FIGURE 6.4. MAO CONCENTRATION DEPENDENCE FOR OXIDATIVE DEAMINATION OF KYNURAMINE WITH MAO-A.....	105
FIGURE 6.5. MAO CONCENTRATION DEPENDENCE FOR OXIDATIVE DEAMINATION OF KYNURAMINE WITH MAO-B	106
FIGURE 6.6. CONCENTRATION DEPENDENCE FOR OXIDATIVE DEAMINATION OF KYNURAMINE WITH MAO-A.....	107

FIGURE 6.7. CONCENTRATION DEPENDENCE FOR OXIDATIVE DEAMINATION OF KYNURAMINE WITH MAO-B	108
FIGURE 6.8. INHIBITION OF MAO-A ACTIVITY BY PHENOLIC DIETARY COMPOUNDS	109
FIGURE 6.9. INHIBITION OF MAO-B ACTIVITY BY PHENOLIC DIETARY COMPOUNDS	110
FIGURE 6.10. DETERMINATION OF IC ₅₀ FOR CURCUMIN, GUAIACOL, ISOEUGENOL, PTEROSTILBENE, RESVERATROL, AND ZINGERONE ON MAO-A ACTIVITY	112
FIGURE 6.11. DETERMINATION OF IC ₅₀ FOR CURCUMIN, GUAIACOL, ISOEUGENOL, PTEROSTILBENE, AND RESVERATROL ON MAO-B ACTIVITY	114

LIST OF ABBREVIATIONS

ALDH	Aldehyde dehydrogenase
APS	Adenosine 5'-phosphosulfate
AR	Aldehyde reductase
ATP	Adenosine-5'-triphosphate
AUC _{0-∞}	Area under the plasma drug concentration-time curve
AUC _{extrap}	Extrapolated AUC from last point to infinity
AUMC _{0-∞}	Area under the moment curve
C _{max}	Observed peak concentration
CE	Collision energy
CL _{con}	Conjugation clearance
CL _{mao}	Oxidative deamination clearance
CL _{ren}	Renal clearance
CL _{tot}	Total clearance
CN	Cyano
CXP	Collision cell exit potential
DFN	Difference from nominal
DMEM	Dulbecco's modified Eagle's medium
DMSO	Dimethyl sulfoxide
DP	Declustering potential
EAFUS	Everything Added to Food in the United States
EC	Electrochemical
EP	Entrance potential

ESI	Electrospray ion
ET	Etilefrine
F_a	Fraction of the oral dose absorbed
F_{oral}	Oral bioavailability
FDA	The Food and Drug Administration
FLU	Fluorescence
GI	Gastrointestinal
GRAS	Generally recognized as safe
HBSS	Hank's balanced salt solution
HILIC	Hydrophilic interaction liquid chromatography
HPLC	High-performance liquid chromatography
IC_{50}	The concentration of an inhibitor at which the enzyme activity is reduced by half
I.S.	Internal standard
k_a	Absorption rate constant
K_m	The Michaelis-Menten constant
K_i	Dissociation constant for an inhibitor of enzyme
LC	Liquid chromatography
LC-MS/MS	Liquid chromatography-mass spectrometry
LLOD	The low limit of detection
LLOQ	The low limit of quantification
LS180	Human colon adenocarcinoma epithelial cell line
MAO	Monoamine oxidase
MAT	Mean absorption time

mRNA	Messenger ribonucleic acid
MRM	Multiple reaction monitoring
MRT	Systemic mean residence time
MS	Mass spectrometry
NMR	Nuclear magnetic resonance
ODS	Octadecylsilane
PAPS	3'-Phosphoadenosine-5'-phosphosulfate
PE	Phenylephrine
PEG	Polyethylene glycol
PFP	Pentafluorophenyl
PK	Pharmacokinetic
RSD	Relative standard deviation
SPE	Solid-phase extraction
SULT	Sulfotransferase
$t_{1/2, \text{term}}$	Terminal half-life
T_{max}	Time at observed peak concentration
TLC	Thin-layer chromatography
UGT	Uridine 5'-diphospho-glucuronosyltransferase
UV	Ultraviolet
V_{max}	The maximum rate achieved at saturating substrate concentrations
$V_{\text{d}_{\text{pss}}}$	Volume of distribution at pseudo-steady-state
$V_{\text{d}_{\text{ss}}}$	Volume of distribution at steady-state
WCX	Weak cation-exchange

ABSTRACT

ASSESSMENT OF THE FEASIBILITY OF CO-ADMINISTRATION OF PHENOLIC DIETARY COMPOUNDS WITH PHENYLEPHRINE TO INCREASE ITS BIOAVAILABILITY

By Zhenxian Zhang, M.S.

A dissertation submitted in partial fulfillment of the requirements for the degree of
Doctor of Philosophy at Virginia Commonwealth University

Virginia Commonwealth University, 2013

Major Director: Phillip M. Gerk, Pharm.D., Ph.D.
Associate Professor
Department of Pharmaceutics, School of Pharmacy

R-(-)-Phenylephrine (PE) is the most commonly used nonprescription oral nasal decongestant in the United States. It is a selective α_1 -adrenergic receptor agonist and has many years of safe usage. However, the efficacy of PE is controversial, due to its extensive pre-systemic metabolism, which leads to low and variable oral bioavailability ($38 \pm 9\%$, mean \pm SD). Sulfation plays a very important role in pre-systemic metabolism of PE. The sulfation of PE occurs at its phenolic group, which is the preferred structural feature of many sulfotransferase (SULT) substrates. Compounds with phenolic groups have similar structures to PE, which may share the same SULT isoforms with PE and have the potential to inhibit PE sulfation. Co-administration of the phenolic compounds from the Food and Drug Administration's (FDA)

“Generally Recognized as Safe” (GRAS) list, Everything Added to Food in the United States (EAFUS), or dietary supplements along with PE could be an effective strategy to inhibit the pre-systemic sulfation of PE. The primary side effect of PE is hypertension. Since monoamine oxidase (MAO) inhibitors may increase the risk of hypertension, they should not be taken with PE.

In order to increase the oral bioavailability and eventually improve the efficacy of PE, this research project aimed to investigate the feasibility of inhibiting the pre-systemic sulfation of PE with phenolic dietary compounds. Considering the safety issue, this research project also aimed to investigate whether these phenolic dietary compounds have inhibitory effects on MAO-A/B.

A human colon adenocarcinoma epithelial cell line (LS180), which shows sulfation activity, was used as a model to test the effect of these phenolic compounds on the sulfation of PE. The extent of disappearance of PE was significantly ($p < 0.05$) decreased to the following (mean \pm SEM, as % of control) when incubated with phenolic dietary compounds in LS180 cells for 14 - 19 hrs: curcumin $24.5 \pm 14.0\%$, guaiacol $51.3 \pm 8.0\%$, isoeugenol $73.9 \pm 4.3\%$, pterostilbene $70.6 \pm 4.2\%$, resveratrol $14.2 \pm 28.0\%$, zingerone $52.4 \pm 14.6\%$, and the combinations eugenol + propylparaben $42.6 \pm 8.4\%$, vanillin + propylparaben $37.0 \pm 11.2\%$, eugenol + propylparaben + vanillin + ascorbic acid $31.1 \pm 10.9\%$, eugenol + vanillin $57.5 \pm 20.6\%$, and pterostilbene + zingerone $36.5 \pm 7.0\%$. The combinations of curcumin + resveratrol and curcumin + pterostilbene + resveratrol + zingerone almost completely inhibited PE disappearance.

PE sulfate formation was inhibited $67.0 \pm 4.2\%$ (mean \pm SEM, as % of control) by guaiacol and $71.7 \pm 2.6\%$ by pterostilbene + zingerone. The combinations of curcumin + resveratrol and curcumin + pterostilbene + resveratrol + zingerone inhibited $\geq 99\%$ of PE sulfate formation. These results were consistent with those from analysis of the disappearance of PE in LS180 cells.

These phenolic inhibitors for sulfation were also tested to see whether they have any inhibitory effects on MAO-A or B. Significant inhibition was found with curcumin, guaiacol, isoeugenol, pterostilbene, resveratrol, and zingerone on both MAO-A and B. Further kinetic studies were conducted to investigate the concentration of an inhibitor at which the enzyme activity is reduced by half (IC_{50}) (mean \pm SEM) of these inhibitors. The most potent inhibitor for MAO-A was resveratrol ($0.313 \pm 0.008 \mu\text{M}$) followed by isoeugenol ($3.72 \pm 0.20 \mu\text{M}$), curcumin ($12.9 \pm 1.3 \mu\text{M}$), pterostilbene ($13.4 \pm 1.5 \mu\text{M}$), zingerone ($16.3 \pm 1.1 \mu\text{M}$), and guaiacol ($131 \pm 6 \mu\text{M}$). The most potent inhibitor for MAO-B was pterostilbene ($0.138 \pm 0.013 \mu\text{M}$), followed by curcumin ($6.30 \pm 0.11 \mu\text{M}$), resveratrol ($15.8 \pm 1.3 \mu\text{M}$), isoeugenol ($102 \pm 5 \mu\text{M}$), and guaiacol ($322 \pm 27 \mu\text{M}$). Since these phenolic compounds all have relatively low oral bioavailability, any MAO inhibition which could occur systemically is expected to be limited. Most inhibitory effects on MAO-A and B if any would be limited to the GI tract and liver.

In conclusion, several compounds and combinations showed inhibition on PE sulfation in LS180 cell model, which may have potential to inhibit the pre-systemic sulfation of PE to improve its oral bioavailability. These compounds also showed the unexpected inhibition on human MAO-A and B with different potency, which could guide the selection of phenolic dietary compounds for further studies, along with the sulfation inhibition results and their pharmacokinetic (PK) properties such as bioavailability.

CHAPTER 1

CLINICAL SIGNIFICANCE AND PHARMACOKINETIC PROBLEM OF PHENYLEPHRINE

1.1 CLINICAL SIGNIFICANCE AS ORAL NASAL DECONGESTANT

Sympathomimetic amines: PE, phenylpropanolamine, pseudoephedrine, and ephedrine are commonly used oral nasal decongestants and have a long history [1, 2]. Oral PE, phenylpropanolamine, and pseudoephedrine were approved as over-the-counter nasal decongestants by FDA in 1976 [3]. Ephedrine activates both α - and β - adrenergic receptors. Many adverse effects with ephedrine may be related to its non-selective adrenergic properties [4]. Phenylpropanolamine and pseudoephedrine predominantly occupied the market until 2000. Phenylpropanolamine was withdrawn from the market because of its possible side effect (hemorrhagic stroke) and also its abuse [5, 6]. Due to the illegal manufacture of methamphetamine from pseudoephedrine, the retail stores in the United States have to put pseudoephedrine products “behind the counter”, require photo identification for sales, and keep personal information in a log for at least 2 years, as required by the Combat Methamphetamine Epidemic Act of 2005 [7]. PE is now the predominant nonprescription orally administered nasal decongestant. Oral PE has been used for many years as a systemic nasal decongestant at 10 mg dose to treat nasal or sinus congestion for the common cold, flu, allergic rhinitis, and sinusitis [3].

1.2 PHYSICOCHEMICAL PROPERTIES AND PHARMACOLOGY

The physicochemical properties of PE are listed as follows: small, polar, molecular weight of 167.21. The logP value is 0.117 ± 0.269 at 25 °C [8]. The logD value is -2.13 at pH 7.0 and 25 °C [8]. The estimated pKa values of hydroxyphenyl and amine groups are 9.8 and 9.2, respectively [8]. PE is ionized at physiological pH and thereby highly hydrophilic. The structure of PE is shown in **Figure 1.1**. Since PE has a single chiral carbon atom, there is a pair of enantiomers: *R*-(-)-PE and *S*-(+)-PE. The *R*-(-)-form activates α_1 -adrenergic receptors and is commercially used [2, 9]. Unlike catecholamines, PE does not contain a hydroxyl group at the 4-position on the benzene ring. Because of the lack of the 4-hydroxyl group, PE is not a substrate of catechol-*O*-methyltransferase in the gastrointestinal tract, liver, and blood circulation, which explains less extensive pre-systemic metabolism, longer half-life and duration of action with PE compared to catecholamines such as dopamine, epinephrine, and norepinephrine [10].

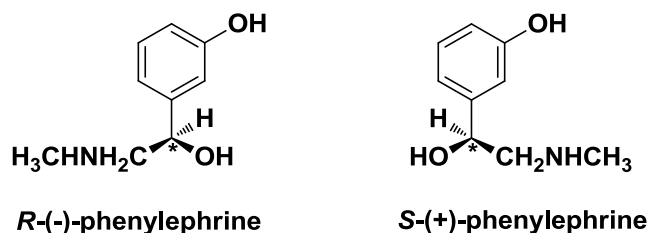


Figure 1.1. Structures of Phenylephrine Enantiomers

The structures show the chiral center of PE is a carbon atom, generating a pair of enantiomers: *R*-(-)-PE and *S*-(+)-PE.

PE has promising pharmacological activity as a nasal decongestant. The mechanism is that PE stimulates the α_1 -adrenergic receptors expressed in peripheral vascular smooth muscle, causing vasoconstriction in the arterioles of nasal and sinus mucosa. Therefore, the nasal blood flow declines and nasal congestion is reduced [11]. PE is a relatively selective α_1 -

adrenergic receptor agonist, but also a weak α_2 -adrenergic receptor agonist. It has negligible β -adrenergic effects [7]. Instead of the indirect action on regulating endogenous catecholamines, the action produced by PE is through direct activation of α -adrenergic receptors. Due to its direct α -adrenergic agonist effect, PE is much more potent on vasoconstriction than indirect decongestants [7].

1.3 EFFICACY AND SAFETY

The efficacy of oral PE is controversial, due to its extensive pre-systemic metabolism which leads to low and variable oral bioavailability [12, 13]. A clinical efficacy study based on the effects of oral PE on nasal airway resistance shows that 10 mg PE is not significantly different from a placebo. A 25 mg dose PE reduces the maximal nasal airway resistance significantly compared to a placebo [3]. These findings also demonstrate that the lack of efficacy may be associated with inadequate plasma concentrations. In this study, the patient-reported effects of PE on congestion relief do not show consistent improvement compared with placebo [3].

There is no severe safety issue with PE after being used for so many years. At a high dose level (50 mg), PE may cause increases in arterial blood pressure and declines in heart rate [14]. But at the approved therapeutic dose as oral nasal decongestant (10 mg), PE has limited effects on the cardiovascular system. Due to its hydrophilicity, which leads to low diffusional permeability, PE has less chance to cause central nervous system stimulation [7]. The primary side effect of PE is hypertension. Using MAO inhibitors together with PE should be avoided because they may increase the risk of hypertension by enhancing the hypertensive effect of α_1 -adrenergic agonists. MAO inhibitors can inhibit pre-systemic and systemic metabolism of PE, resulting in the elevated level of PE in the systemic circulation [15]. Furthermore, the

metabolism of endogenous sympathomimetic amines in circulation and tissue could be inhibited by systemic exposure to MAO inhibitors [16].

1.4 ANALYTICAL METHODS

In the early days, fluorimetry, gas chromatography, and liquid scintillation were used to determine PE levels in either biologic samples or pharmaceutical formulations [17-20]. Owing to the non-specificity of radioactivity measurement, and the inconvenience of gas chromatography usage, the application of high-performance liquid chromatography (HPLC) coupled with ultraviolet (UV), fluorescence (FLU), electrochemical (EC) detector, or mass spectrometry (MS) became more popular to quantitatively analyze PE. **Table 1.1** summarizes the HPLC methods in the literature. These studies cover a variety of matrices, including extraction from different dosage forms such as nasal drops/spray, oral syrup/capsules/sachets, or injection, as well as biologic fluids like serum, plasma, or aqueous humor. Based on the complexity of serum and plasma, solid-phase extraction (SPE) is applied to clean up the samples. Since PE is a very polar compound with a phenyl ring, phenyl cartridges are appropriate for this purpose [21, 22]. Another choice is weak cation-exchange (WCX) cartridge, which is used since PE is positively charged below pH 9 [23]. Also due to this property, ion-pairing strategy for separation is performed successfully several times. One of these studies even shows that adding ion-pairing reagents to the samples instead of mobile phase can increase the retention time of PE as well [24]. Some special columns, for example, cyano (CN), polyethylene glycol (PEG), pentafluorophenyl (PFP), and hydrophilic interaction liquid chromatography (HILIC) columns, are selected in order to have better retention for PE [25-30]. The low limit of detection (LLOD) and the low limit of quantification (LLOQ) vary among different methods, with the lowest limit of quantification as 0.051 ng/mL in human serum [29].

None of the assays in the literature directly analyze PE metabolites. One of the studies detected PE sulfate and glucuronide by hydrolyzing them with enzymes to the parent compounds and then measuring the parent compounds [14]. Another study separated the radio-labeled PE and metabolites by column chromatography, solvent extraction, and thin-layer chromatography (TLC) and analyzed the fractions by liquid scintillation [19].

Table 1.1. HPLC Methods for Phenylephrine in Pharmaceutical Formulations and Biologic Fluids

Matrix	Sample Preparation	Analytical Separation Method	Column	Detection	LLOD (ng/mL)	LLOQ (ng/mL)	Reference
Dilute nose drops		Ion pairing	C18	UV			Ghanekar <i>et al.</i> 1978 [31]
Dilute nasal spray		Ion pairing	ODS	UV			Wilson <i>et al.</i> 1985 [32]
Extraction from capsules		Ion pairing	C8	UV			Schieffer <i>et al.</i> 1984 [33]
Human plasma	SPE (phenyl)		C18	FLU	0.5		Chien <i>et al.</i> 1985 [21]
Aqueous solution			C18	UV			Gupta <i>et al.</i> 1986 [34]
Human plasma				EC			Martinsson <i>et al.</i> 1986 [35]
Dilute cough-cold products		Ion pairing	ODS	UV			Lau <i>et al.</i> 1989 [36]
Human serum	Deproteinizing	Ion pairing	ODS	FLU		5	Yamaguchi <i>et al.</i> 1994 [37]
Human serum	SPE (phenyl)	Ion pairing	C18	EC		0.35	Vuma <i>et al.</i> 1995 [22]
Human plasma	SPE (WCX)	Ion pairing	ODS	EC		2	Gumbhir <i>et al.</i> 1996 [23]
Human aqueous humor		Ion pairing	CN	UV		61	Galmier <i>et al.</i> 2000 [25]
Extraction from capsules			PEG	UV	120	400	Garc'ia <i>et al.</i> 2002 [26]
Extraction from capsules and sachets				UV	120		Mari'n <i>et al.</i> 2002 [38]
Extraction from capsules			PEG	UV		2780	Mari'n <i>et al.</i> 2004 [27]
Water with the ion-pairing reagents	Ion-pairing agent		C18	MS			Gao <i>et al.</i> 2005 [24]
Extraction from sachets			CN	UV	4.6	15.3	Olmo <i>et al.</i> 2005 [28]
0.9% Sodium chloride injection			C18	UV			Kiser <i>et al.</i> 2007 [39]
Human plasma	SPE (C18)		PFP	MS		0.051	Pt'a'cek <i>et al.</i> 2007 [29]
Dilute syrup		Ion pairing	C8	UV			Amer <i>et al.</i> 2008 [40]
Extraction from sachets		Ion pairing	C18	FLU	60	200	Dousa <i>et al.</i> 2010 [30]
Extraction from sachets		HILIC	HILIC	FLU	70	230	Dousa <i>et al.</i> 2010 [30]

SPE: solid-phase extraction; WCX: weak cation-exchange; HILIC: hydrophilic interaction liquid chromatography; ODS: octadecylsilane; CN: cyano; PEG: polyethylene glycol; PFP: pentafluorophenyl; UV: ultraviolet; FLU: fluorescence; EC: electrochemical; MS: mass spectrometry; LLOD: the low limit of detection; LLOQ: the low limit of quantification.

1.5 PHARMACOKINETICS OF PHENYLEPHRINE IN HUMANS

According to the literature, only a few studies have been conducted to investigate the PK properties of PE in humans. Two papers published by Bogner *et al.* and Cavallito *et al.* compared the plasma concentration-time profiles and urinary excretion of radio-labeled PE after PE hydrochloride (immediate-release tablet) and PE tannate (sustained-release tablet) which were orally administered to subjects [41, 42]. The disadvantage is that the measurement of total radioactivity cannot separate the parent drug from its metabolites in plasma and urine. Furthermore, PE hydrochloride and PE tannate were labeled randomly by exposure to tritium gas, which adds to the complexity of the radioactive forms in plasma and urine [41, 42]. Both studies conclude that the sustained-release dosage form maintains plasma radioactivity levels longer than the immediate-release dosage form [41, 42]. Another analytical article determined the serum level of the combination of parent and conjugated PE (after acidic hydrolysis) by HPLC with a FLU detector [37]. The pilot PK study with this acidic hydrolysis method was excluded for further PK analysis because the concentration represents the combination of PE and its conjugates.

Other clinical studies which quantitatively detected parent PE following a single dose are listed in **Table 1.2**. The plasma concentration-time profiles from the figures in these papers were obtained by the software DataThief III (Version 1.6). The PK parameters were calculated by a non-compartmental PK analysis. Area under the plasma drug concentration-time curve ($AUC_{0-\infty}$) and area under the moment curve ($AUMC_{0-\infty}$) were estimated by a linear trapezoidal method. Assuming the conjugates only eliminated by urinary excretion, the conjugation clearance (CL_{con}) was estimated by the amount of dose recovered in urine as conjugates divided by $AUC_{0-\infty}$. Assuming 3-hydroxymandelic acid only eliminated by urinary excretion, the oxidative

deamination clearance (CL_{mao}) was estimated by the amount of dose recovered in urine as 3-hydroxymandelic acid divided by $AUC_{0-\infty}$.

Hengstmann *et al.* measured the total radioactivity and separated free PE and its metabolites by column chromatography, solvent extraction, and TLC [19]. The sensitivity and specificity of these assays were not evaluated and could bring problems to the validity and reliability of the data and furthermore the PK parameters.

Later on, advanced technology like HPLC with EC detector and liquid chromatography-mass spectrometry (LC-MS/MS) was introduced to improve the sensitivity and specificity of PE analysis in clinical trials [29]. The variation in the bioanalytic methods may explain the difference in the PK parameters in these studies. The data from different studies with different assays are not comparable.

Table 1.2. Pharmacokinetic Parameters of Phenylephrine in Clinical Trials

Formulation	Intravenous Solution	Oral Solution	IR Tablet	Oral Solution	IR Tablet
Dose as PE base (mg)	0.842	0.986	8.21	16.4	10.0
*AUC _{0-∞} (ng*min/mL)	339	182	108		
*AUC _{extrap} (ng*min/mL)	42	30	6		
*AUC _{extrap} /AUC _{0-∞} (%)	12%	16%	6%		
*AUMC _{0-∞} (ng*min ² /mL)	67880	38167	8073		
C _{max} (ng/mL)		0.9	1.8	3.1	0.6
T _{max} (min)		75	36	40	30
*t _{1/2, term} (min)	181	130	78		
*CL _{tot} (mL/min)	2486				
*CL _{ren} (mL/min)	398	141			
*CL _{con} (mL/min)	206	2474			
*CL _{mao} (mL/min)	1414	1310			
*Vd _{pss} (L)	648				
*Vd _{ss} (L)	478				
*MRT (min)	192	210	75		
*MAT (min)		17			
*k _a (min ⁻¹)		0.06			
*F _{oral}		46%			
Reference	Hengstmann <i>et al.</i> 1982 [19]	Hengstmann <i>et al.</i> 1982 [19]	Ptacek <i>et al.</i> 2007[29]	Vuma <i>et al.</i> 1996 [22]	Schering-Plough Corporation 2007 [43]

AUC_{0-∞}: area under the plasma drug concentration-time curve; AUC_{extrap}: extrapolated AUC from last point to infinity; AUMC_{0-∞}: area under the moment curve; C_{max}: observed peak concentration; T_{max}: time at observed peak concentration; t_{1/2, term}: terminal half-life; CL_{tot}: total clearance; CL_{ren}: renal clearance; CL_{con}: conjugation clearance; CL_{mao}: oxidative deamination clearance; Vd_{pss}: volume of distribution at pseudo-steady-state; Vd_{ss}: volume of distribution at steady-state; MRT: systemic mean residence time; MAT: mean absorption time; k_a: absorption rate constant; F_{oral}: oral bioavailability. The parameters with asterisk (AUC_{0-∞}, AUC_{extrap}, AUC_{extrap}/AUC_{0-∞}, AUMC_{0-∞}, t_{1/2, term}, CL_{tot}, CL_{ren}, CL_{con}, CL_{mao}, Vd_{pss}, Vd_{ss}, MRT, MAT, k_a, and F_{oral}) were determined from the published images and text as described. Therefore, values differ from those reported in the articles.

The plasma protein binding for PE is not available in the literature. But it was reported that the binding to human serum albumin and plasma for etilefrine (ET) is $8.5 \pm 2.6\%$ and $23 \pm 4\%$, respectively, in the concentration range of 0.4 - 46 ng/mL [44]. ET has a structure similar to PE. PE is expected to have similar plasma protein binding. There is not enough information from the above data to determine whether PE exhibits linear or non-linear pharmacokinetics. Peak plasma levels showed inter-study variability, and were found between 30 and 75 min [19, 22, 29, 43]. Both the CL_{ren} after intravenous and oral administration were larger than the product of glomerular filtration rate by the unbound fraction of PE in plasma, which indicates net renal tubular secretion. The non-renal clearance was higher than hepatic blood flow of 1500 mL/min, which indicates the contribution of other organs to the extra-hepatic clearance. CL_{mao} was similar after intravenous and oral administration. CL_{con} was much higher after oral dose than that after intravenous dose. This indicates conjugation plays an important role in pre-systemic metabolism of PE. The volume of distribution at steady state exceeded total body water. This suggests the extensive distribution of PE in certain organs/tissues, possibly due to transporter-mediated uptake into tissues or extensive tissue binding. PE is ionized at the physiological pH. It is difficult for PE to penetrate into the tissues by passive diffusion. It is probably transferred into the tissues by active transporters. The structure of PE is similar to norepinephrine and dopamine, which are taken into neurons or extra-neuronal tissues by transporters like the norepinephrine transporter, dopamine transporter and organic cation transporters [45-47]. The distribution of PE into tissues may also be mediated by such transporters, potentially resulting in large volume of distribution at steady state.

1.6 LOW BIOAVAILABILITY AND EXTENSIVE PRE-SYSTEMIC METABOLISM

PE is almost completely absorbed with 95.3% of the oral dose at 24.6 mg recovered in urine [20]. Another study found 79.5% of the oral dose at 0.986 mg recovered in urine [19]. The rest could possibly be excreted by biliary excretion and recover in feces. Since PE has high solubility and high permeability, it is classified as Biopharmaceutics Classification System Class I compound. The oral bioavailability (F_{oral}) of PE was determined as $38 \pm 9\%$ (mean \pm SD, recalculated based on the individual data in the paper published by Hengstmann *et al.*) [19]. The low oral bioavailability of PE is likely due to pre-systemic metabolism. Urine contained 2.6% free PE, 45.7% conjugated PE, and 24.2% 3-hydroxymandelic acid after 0.986 mg oral dose [19]. Compared with the urinary recovery after 0.842 mg intravenous dose containing 16% free PE, 8.3% conjugated PE, and 56.9% 3-hydroxymandelic acid, it seems more PE undergoes conjugation by oral route and more PE converts to 3-hydroxymandelic acid by intravenous route [19]. The total excretion of administered dose after oral and intravenous administration was calculated by cumulative urinary excretion of ^3H -activity in **Table 1.3**, which is larger than the sum of the dose excreted as parent PE and each identified metabolite [19]. This indicates there are some unidentified metabolites recovered in urine. Another study detected four metabolites in urine after oral administration of 24.6 mg PE over 8 hrs, which were 30% 3-hydroxymandelic acid, 6% 3-hydroxyphenylglycol sulfate, 47% PE sulfate, and 12% PE glucuronide (**Table 1.3**) [20]. These results are consistent with those after 0.986 mg oral administration. The major routes for oral PE metabolism in humans are sulfation and oxidative deamination. After inhalation of 10, 24, and 34 mg PE by three subjects over 9 hrs, the components recovered in the urine were 24% 3-hydroxymandelic acid, 6% 3-hydroxyphenylglycol sulfate, 56% PE sulfate, and 5% PE glucuronide, which were similar to the oral route (**Table 1.3**) [20]. This indicates

that the lung also has extensive sulfation activity, which has been reported in the literature [48-50]. The proposed metabolic pathway for PE is shown in **Figure 1.2**.

The intestine may play an important role in pre-systemic PE metabolism. PE is a substrate of SULT1A3, which is highly expressed in human intestine, but absent in human and rodent liver [51]. In the past years, researchers paid more attention to the first-pass metabolism in the liver [52, 53]. Recently, the interest in pre-systemic intestinal metabolism is increasing [52, 53]. The intestinal availability of salbutamol is even less than the hepatic availability [52, 53]. Salbutamol has a structure similar to PE and mainly undergoes sulfation, which suggests intestinal metabolism is probably important for pre-systemic PE metabolism.

There are differences in metabolism of PE across animal species. After intraperitoneal injection of 250 µg PE into rats, 7% free PE, 5% 3-hydroxymandelic acid, 35% 3-hydroxyphenylglycol sulfate, 5% PE sulfate, and 4% PE glucuronide recovered in urine (**Table 1.3**) [20]. The metabolism of PE in rats is highly different from that in human. The evidence of the species difference of sulfation can also be found in the literature [54-57]. The species difference in sulfation is associated with the difference in gene and enzyme expression levels. Homologous sequences for SULT1A3 haven't been found in other species [58]. This indicates that animal models such as rat may not be a good choice for studying PE metabolism in humans. Thus, animal models such as rat have been excluded from the current study.

Table 1.3. Urinary Excretion of Phenylephrine Metabolites as Percentage of Administered Dose

Route of administration	Urinary Excretion of Administered Dose (%)				Rat Intraperitoneal Injection
	Intravenous Injection	Oral Solution	Human Oral Tablet	Inhalation	
Subject	3	10	3	3	3
Dose as PE base	0.842 mg	0.986 mg	24.6 mg	10, 24, 34 mg	250 µg
Urine collecting time	48 hrs	48 hrs	24 hrs	24 hrs	24 hrs
PE sulfate	8.3	45.7	47	56	5.0
PE glucuronide			12	5	4.0
3-Hydroxymandelic acid	56.9	24.2	30	24	5.0
3-Hydroxyphenylglycol sulfate	Not detected	Not detected	6	6	35.0
Free PE	16.0	2.6	0.3	1.5	7.0
Total excretion of administered dose	86.3	79.5	95.3	92.5	56.0
Reference	Hengstmann <i>et al.</i> 1982 [19]	Hengstmann <i>et al.</i> 1982 [19]	Ibrahim <i>et al.</i> 1983 [20]	Ibrahim <i>et al.</i> 1983 [20]	Ibrahim <i>et al.</i> 1983 [20]

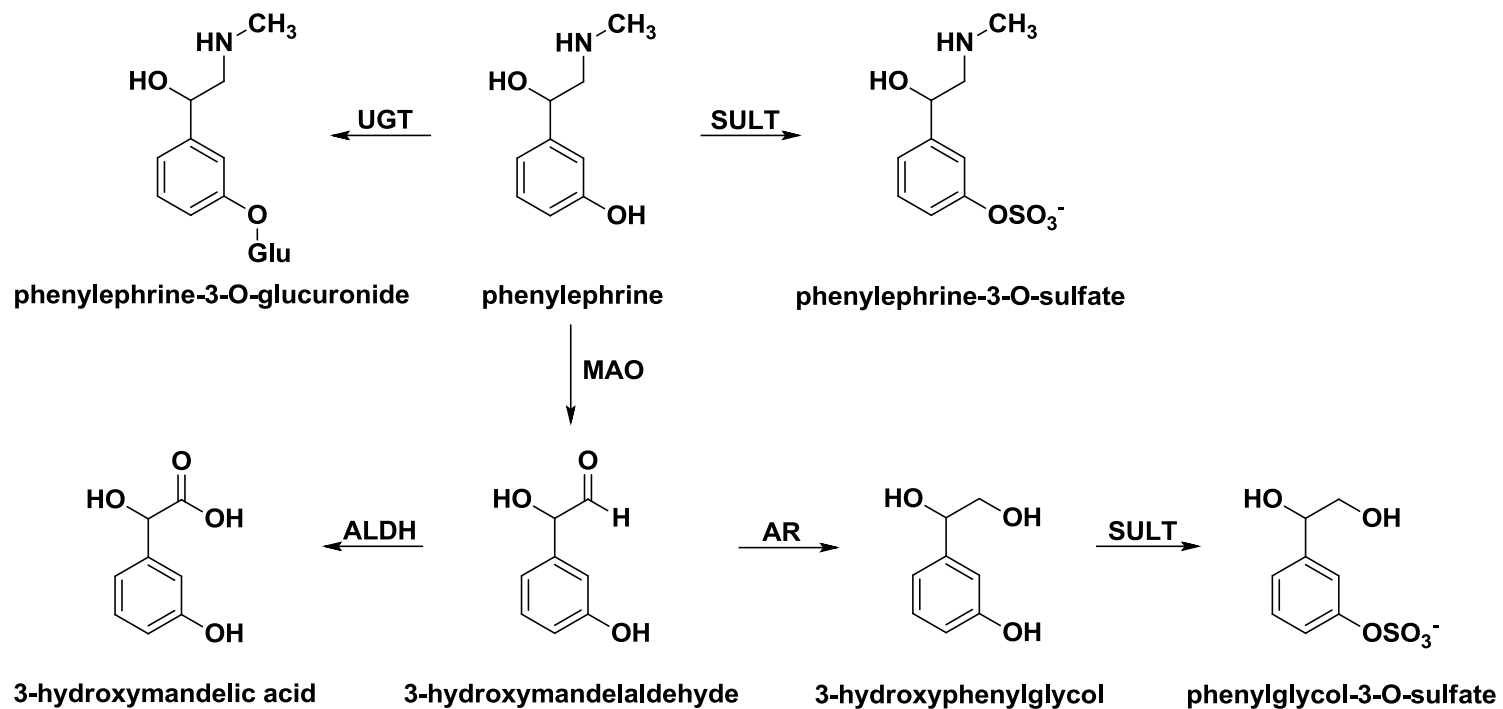


Figure 1.2. Proposed Metabolic Pathways of Phenylephrine

UGT: uridine 5'-diphospho-glucuronosyltransferase; SULT: sulfotransferase; MAO: monoamine oxidase; ALDH: aldehyde dehydrogenase; AR: aldehyde reductase.

1.7 PREDOMINANT METABOLIC PATHWAYS: SULFATION AND OXIDATIVE DEAMINATION

Sulfation and oxidative deamination are the two predominant metabolic pathways for PE [20]. Sulfation is an important conjugation reaction, which belongs to Phase II metabolism [51]. A sulfonate group is transferred from the cofactor 3'-phosphoadenosine-5'-phosphosulfate (PAPS) to hydroxyl or amino groups of the compounds under the catalysis of SULTs [51]. This reaction leads to more water-soluble metabolites, which facilitates excretion [51]. In general, sulfation is a high-affinity, low-capacity reaction compared to uridine 5'-diphosphoglucuronosyltransferase (UGT) [59]. The total amount of PAPS in the whole liver can be consumed in less than 2 min [59]. Substrate inhibition is very common for SULTs [60-63]. SULT has many isoforms in humans, most of which have substrate overlap. SULT activities are higher in the small intestine than in the stomach or colon. However, the activities in different segments of small intestine show differences [60]. SULTs are also expressed in the liver and the level of phenol SULT in the liver shows inter-individual variation [51]. Model substrates were used to test the SULT activities in the liver among various species (human, monkey, dog, rabbit, rat, mouse, guinea pig, and hamster), and the results show large species differences [51]. In rat, mouse, and rabbit only one form of ST1A (phenol SULT) has been reported so far [64].

PE is not a substrate of SULT1A1 when it was tested at 10 mM [65]. Monoamine-sulfating phenol transferase SULT1A3 was reported to be involved in the sulfation of PE [65]. SULT1A3 prefers bioamines such as PE, catecholamine and dopamine [66]. SULT1A3 is almost negligible in the liver, but has high expression levels in the colon and jejunum [67, 68]. Single nucleotide polymorphisms have been found for SULT1A3, but this does not significantly affect the Michaelis-Menten constant (K_m) value for its typical substrate and cofactor PAPS [58].

Oxidative deamination by MAO is a type of Phase I metabolism. MAO exists in almost all the tissues and is located in the outer membrane of mitochondria [69]. It can oxidize primary aliphatic and aromatic amines, as well as some secondary and tertiary amines [69]. Flavin adenine dinucleotide is the cofactor [69]. There are two isoforms of MAO: MAO-A and MAO-B [69]. Synephrine, a regioisomer of PE, is metabolized by both types of MAO and mainly by MAO-A [70]. Dopamine, which has structural similarity with PE, is metabolized by both MAO-A and MAO-B [71, 72].

1.8 COMMON APPROACHES TO IMPROVE ORAL BIOAVAILABILITY

In order to improve oral bioavailability, there are several common approaches in the literature such as modified formulations, pro-drugs and inhibiting pre-systemic metabolism by co-administration of enzyme inhibitors. Modified formulations with chitosan microsphere or cyclodextrin complex can only increase the solubility of poorly soluble drugs (unlike PE), but cannot inhibit the pre-systemic metabolism of the drug [73, 74]. So when the drug is absorbed in the intestine and then goes through the portal vein into the liver, it still gets metabolized, which lowers the oral bioavailability. These new formulations could not solve the problem of low oral bioavailability due to extensive pre-systemic metabolism. Pro-drugs can be synthesized to protect groups on the drug molecule which are easily metabolized by first-pass metabolism. But since the pro-drug would be a new chemical entity, the toxicity would be unknown and would need extensive and expensive investigation. The stability of the pro-drug in gastric fluid and blood is also unknown. Stability studies have to be done to prove it is an effective pro-drug, which is very resistant to the gastric fluid and can convert to the active drug in plasma. The effort also has to be put to synthesize the drug. Co-administration of enzyme inhibitors with the drug orally can inhibit pre-systemic metabolism of the drug and increase its oral bioavailability.

Ritonavir is used as an inhibitor of pre-systemic metabolism of lopinavir [75]. Among these approaches, co-administration of the inhibitors for pre-systemic metabolism is the most appropriate one for drugs with extensive pre-systemic metabolism, which will be discussed in the next section.

1.9 THE STRATEGY TO INCREASE ORAL BIOAVAILABILITY OF PHENYLEPHRINE: INHIBITION OF PRE-SYSTEMIC SULFATION

The efficacy of PE, the most commonly used over-the-counter oral nasal decongestant, is questioned because of its low and variable oral bioavailability, which appears to be due to its extensive pre-systemic metabolism [3, 19]. If the pre-systemic metabolism of PE can be inhibited, the variability of the oral bioavailability for PE can be reduced and the oral bioavailability of PE can be increased. Finally the efficacy can be better realized. As described above, more PE is conjugated mainly as sulfate by the oral route (45.7%) than that by the intravenous route (8.3%) [19]. Less PE is biotransformed to 3-hydroxymandelic acid by the oral route (24.2%) than after the intravenous route (56.9%) [19]. This indicates that sulfation may play a significant role in pre-systemic metabolism of PE. If the major pre-systemic metabolic pathway, i.e., sulfation, can be inhibited, the oral bioavailability of PE may be improved. The sulfation of PE occurs at its phenolic group, which is a common structural feature for many SULT substrates [51]. The compounds with phenolic groups have similar structures as PE and may share affinity for the same SULT isoforms with PE, which obtain the potential to inhibit sulfation of PE. Therefore, co-administration of phenolic compounds with PE can be an appropriate strategy to inhibit the pre-systemic sulfation of the drug.

Considering safety concerns, phenolic compounds from FDA's "GRAS" list, EAFUS, or dietary supplements are the first choice of potential inhibitors. GRAS substances are compounds

generally recognized as safe. Experts have already evaluated the safety of these compounds from many aspects such as systemic exposure, metabolism, pharmacokinetics and toxicology. For toxicology, many aspects are considered such as carcinogenicity, genotoxicity, reproductive toxicity, and the median lethal dose in animals. Adequate scientific information is available to prove their safety as food additives. EAFUS lists the substances used as food additives, some of which are included in FDA's "GRAS" list. The substances listed in EAFUS can be directly added into food. Dietary supplements are basically vitamins, minerals, botanicals, herbs, herbal extracts, amino acids, and various other natural compounds, most of which have been used for many years without reported safety issues. Many successful examples of applying dietary compounds to inhibit metabolism and finally improve the oral bioavailability can be found in the literature: when 2 g curcumin was orally administered alone to human subjects, the plasma concentration of the parent compound was very low or even below LLOQ [76]. But when orally co-administered with 20 mg piperine, the plasma concentration of curcumin was significantly increased between 0.25 and 1 hr. The oral bioavailability was increased by 20-fold by piperine [76]. Piperine is used as a feasible absorption/bioavailability enhancer for some compounds probably by improving absorption and decreasing metabolism [77]. Piperine was also found to enhance the plasma concentration and the oral bioavailability of resveratrol [78]. Co-administration of biochanin A with quercetin and (-)-epigallocatechin-3-gallate lead to an increase in the oral bioavailability of biochanin A in rats [79]. Thus, co-administration of phenolic compounds from FDA's "GRAS" list, EAFUS, or dietary supplements with PE could be a safe way to inhibit pre-systemic metabolism of PE.

1.10 SUMMARY

PE is widely used as oral nasal decongestant. It has been used safely for many years. But the efficacy of PE is controversial due to its low and variable oral bioavailability. The extensive pre-systemic metabolism contributes to the low and variable oral bioavailability of PE. Sulfation plays a very important role in pre-systemic metabolism of PE. The sulfation of PE occurs at its phenolic group, which is the preferred structural feature of many SULT substrates. Compounds with phenolic groups have similar structures to PE, which may share the same SULT isoforms with PE and have the potential to inhibit PE sulfation. Considering safety concerns for oral consumption, phenolic compounds from FDA's "GRAS" list, EAFUS, or dietary supplements are the first choice of potential inhibitors to inhibit the pre-systemic sulfation of PE. The primary side effect of PE is hypertension. Since MAO inhibitors may increase the risk of hypertension, they should not be taken with PE. Therefore, as the co-administered phenolic compounds to improve the oral bioavailability of PE, the inhibitory effects of these compounds on MAO are not desired. The disposition scheme for research project goals is shown in **Figure 1.3**.

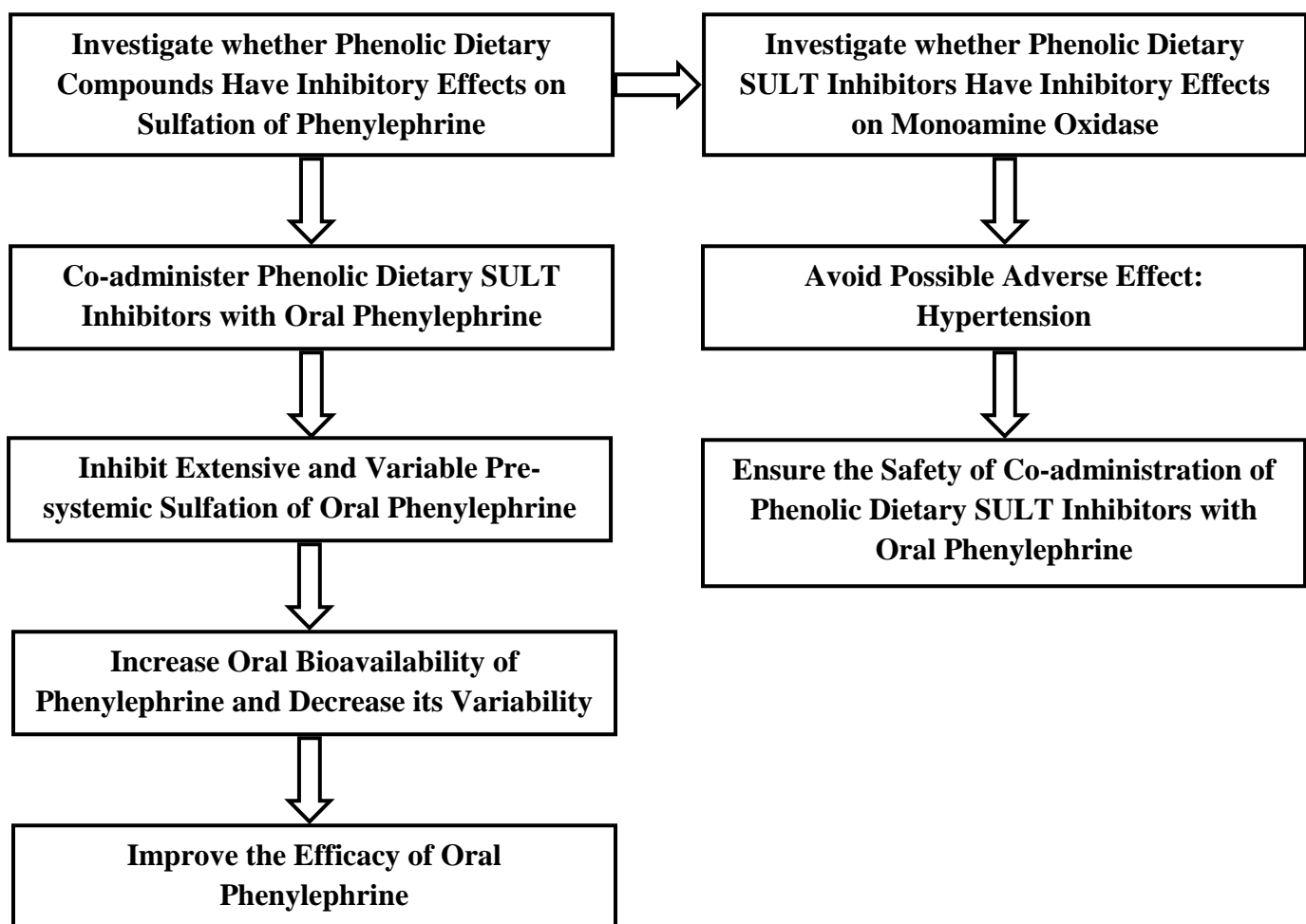


Figure 1.3. Disposition Scheme for Research Project Goals

CHAPTER 2

OBJECTIVE AND SPECIFIC AIMS

2.1 OBJECTIVE AND HYPOTHESIS

2.1.1 Objective

The objective of this project is to test the feasibility of using phenolic dietary compounds from FDA's "GRAS" list, EAFUS, or dietary supplements, as excipients to increase the oral bioavailability of PE: 1) Investigate whether phenolic dietary compounds inhibit the metabolism of PE using the *in vitro* LS180 cell model; 2) Investigate whether phenolic dietary compounds have any *in vitro* inhibitory effects on human MAO-A/B.

2.1.2 Hypothesis

Phenolic dietary compounds can inhibit pre-systemic sulfation of PE to improve its oral bioavailability, preferably with no or less inhibition on MAO metabolic activities.

2.2 SPECIFIC AIMS

2.2.1 Specific Aim I

Test phenolic dietary compounds for metabolic inhibition of PE in LS180 cell model via monitoring of PE disappearance.

- 1) Characterize the sulfation activity in LS180 cells with a model compound, 1-naphthol.
- 2) Develop an HPLC method to determine PE in both the extracellular incubation buffer media and LS180 cell lysates.

- 3) Determine the time- and concentration-dependent PE metabolism in LS180 cell model.
- 4) Determine the extent of PE disappearance in the presence of phenolic dietary compounds.

2.2.2 Specific Aim II

Chemically synthesize and characterize PE sulfate and ET sulfate for quantitative analysis of PE sulfate in LS180 cell model by LC-MS/MS.

- 1) Design the routes for chemical synthesis and synthesize PE sulfate as well as ET sulfate with “protecting group” strategy.
- 2) Identify and characterize PE sulfate and ET sulfate by nuclear magnetic resonance (NMR) and MS and test the purity of these newly synthesized compounds by HPLC.
- 3) Chemically hydrolyze PE sulfate and ET sulfate to determine their original concentrations.
- 4) Develop an LC-MS/MS method for simultaneous quantitative analysis of PE, PE sulfate, and 3-hydroxymandelic acid, and apply it to a preliminary sulfation inhibition study in LS180 cells.

2.2.3 Specific Aim III

Test selected phenolic compounds for inhibitory activities against MAO-A/B using kynuramine as a marker substrate, and determine their IC_{50} values.

- 1) Develop and validate an HPLC method with FLU and UV detection for simultaneous determination of kynuramine and its oxidative deamination product, 4-hydroxyquinoline.
- 2) Characterize the time- and MAO-A/B concentration-dependent kynuramine oxidative deamination and determine the K_m values.
- 3) Test the phenolic dietary compounds for MAO-A/B metabolic inhibition of kynuramine and determine the IC_{50} values.

CHAPTER 3

SCREENING POTENTIAL INHIBITORS FOR PRE-SYSTEMIC SULFATION OF PHENYLEPHRINE WITH LS180 CELL MODEL

3.1 INTRODUCTION

According to the sulfation activities of PE with SULT recombinant enzymes, PE appears to be a substrate of SULT1A3 but not SULT1A1 [51]. It is not now clear however whether other forms of SULT also contribute to the sulfation of PE. As mentioned earlier, SULT1A3 is expressed in humans but its homologous sequences have not been found in other species [58], and thus, animal models are not appropriate to study PE sulfation and its inhibition. In humans, SULT1A3 is very specific for exogenous and endogenous monoamine phenols and highly expressed in the jejunum and colon, but absent in the liver [67]. Catecholamine dopamine, which has structural similarities with PE, is a typical substrate for SULT1A3 with K_m value of 2.9 μM or 9.7 μM reported in the literature [61, 65]. Dopamine has a much lower affinity towards SULT1A1 [65].

Considering the safety issue, phenolic compounds are from FDA's "GRAS" list, EAFUS, or dietary supplements. GRAS substances are compounds generally recognized as safe. Experts have already evaluated the safety of these compounds from many aspects such as exposure, metabolism, pharmacokinetics and toxicology. Adequate scientific information is available to improve their safety as food additives. EAFUS listed the substances used as food additives, some

of which are included in FDA's "GRAS" list. The substances from EAFUS can be directly added into food. Dietary supplements are basically vitamins, minerals, botanicals, herbs, and amino acids, most of which have been used for many years with no safety problems. Therefore phenolic compounds, which have FDA's "GRAS" list, EAFUS, or dietary supplements status, are the first choice as the co-administered substances for PE.

3.2 MATERIALS AND METHODS

3.2.1 Chemicals and Reagents

Curcumin (mixture of curcumin, demethoxycurcumin and bisdemethoxycurcumin) and methylparaben, and quercetin hydrate were purchased from Acros Organics (Morris Plains, NJ). Ethyl vanillin, 1-naphthol, naringin hydrate, zingerone were purchased from Alfa Aesar (Heysham, Lancs, England). Eugenol was purchased from TCI-EP (Tokyo, Japan). Guaiacol, isoeugenol, propylparaben, and vanillin were purchased from TCI America (Portland, OR). L-Ascorbic acid was purchased from Sigma-Aldrich (St. Louis, MO). *L*-phenylephrine hydrochloride was purchased from MP Biomedicals, LLC. (Solon, Ohio). 1-Naphthyl sulfate potassium salt was purchased from Research Organics (Cleveland, OH). Pterostilbene was purchased from ChromaDex (Irvine, CA). Resveratrol was purchased from Beta Pharma, Inc. (New Haven, CT).

Acetic acid, glacial was purchased from Fisher Scientific (Fair Lawn, NJ). Methanol was purchased from Avantor Performance Materials, Inc. (Center Valley, PA).

High glucose Dulbecco's modified Eagle's medium (DMEM) and non-essential amino acids solution (100X) were purchased from HyClone, Laboratories, Inc., Thermo Scientific (South Logan, Utah).

3.2.2 Apparatus

An Alltima C18 column (250 × 4.6 mm, 5 μm) was purchased from Grace Davison Discovery Sciences (Deerfield, IL).

A Hypersil phenyl column (150 × 2 mm, 3 μm) was purchased from Meta Chem Technologies, Inc. (Torrance, CA).

Savant refrigerated vapor trap was purchased from Thermo Scientific (Waltham, MA).

The chromatographic experiments were conducted by HPLC systems including Waters 2695 separation module, Waters 2487 dual λ absorbance detector, and Waters 2475 multi λ FLU detector (Waters Corporation, Milford, MA).

3.2.3 Screening of Potential Inhibitors

Potential inhibitors were selected by two major criteria: structural characteristics and potential for oral consumption. All potential inhibitors have phenolic groups like PE. The structures of potential inhibitors are shown in **Figure 3.1**. They are from FDA's "GRAS" list, EAFUS, or dietary supplements. Among them curcumin, guaiacol, isoeugenol, methylparaben, naringin, propylparaben, pterostilbene, quercetin, resveratrol, vanillin, and zingerone are substrates of SULTs, which were reported in literature as shown in **Table 3.2**. The SULT activity can usually be inhibited by substrates or their analogues. Since these compounds are substrates of SULTs, they are consumed, and the products are released from the enzyme. It is highly likely for them to be reversible inhibitors for SULTs, since mechanism-based inhibition has not been observed with these dietary compounds in the literature. Curcumin was shown to inhibit acetaminophen sulfation in LS180 cells and human liver cytosol with IC_{50} of $2.6 \pm 0.4 \mu\text{M}$ and $5.9 \pm 0.4 \mu\text{M}$, respectively [80]. Quercetin inhibited sulfation of several compounds such as 4-nitrophenol, dopamine, salbutamol, minoxidil and acetaminophen in duodenum and liver cytosol

[81]. The IC_{50} for quercetin inhibition of 4-nitrophenol sulfation in liver cytosol was 0.10 ± 0.03 μ M. The type of inhibition on partially purified SULT1A1 was noncompetitive inhibition with the dissociation constant for an inhibitor of enzyme (K_i) of 0.1 μ M [82]. Methylparaben and propylparaben were found to inhibit estradiol sulfation [83]. Naringin significantly inhibited human recombinant SULT1A3 but not SULT1A1 [84]. Vanillin strongly inhibited the activity of SULT1A3 [85]. Vanillin inhibited 17α -ethinyloestradiol sulfation in human liver cytosol with IC_{50} of 1.3 μ M. The type of inhibition with vanillin was noncompetitive inhibition [85].

The chemical and PK properties of potential inhibitors are shown in **Table 3.1** and **Table 3.2**, respectively. This list of potential inhibitors does not have any amines, which could be typical MAO substrates. The molecular weights are calculated with the 1997 IUPAC atomic weights. The values of logD, molar solubility, logP, and pKa are predicted by Advanced Chemistry Development/Labs softwares. These predicted values are determined based on the database of accurate experimental values of a large amount of compounds. Most phenolic dietary compounds are unionized at the physiological pH, like intestinal pH and plasma pH, except naringin and quercetin. Most phenolic dietary compounds probably cross the cell membrane by passive diffusion based on their chemical properties. It is less possible for these phenolic dietary compounds to interact with the transporters responsible for PE uptake and inhibit PE uptake. As seen in the tables, potential inhibitors are small molecules, most of which are substrates for SULTs. In **Table 3.2**, the fraction of the oral dose absorbed (F_a) for most potential inhibitors were determined by the percentage of the dose recovered in urine in animals or humans in the literature. According to the available data, potential inhibitors have moderate to high F_a . The data of F_{oral} for potential inhibitors are limited and predictions were not performed. The enzymes responsible for metabolism of these phenolic compounds are also listed in **Table 3.2**.

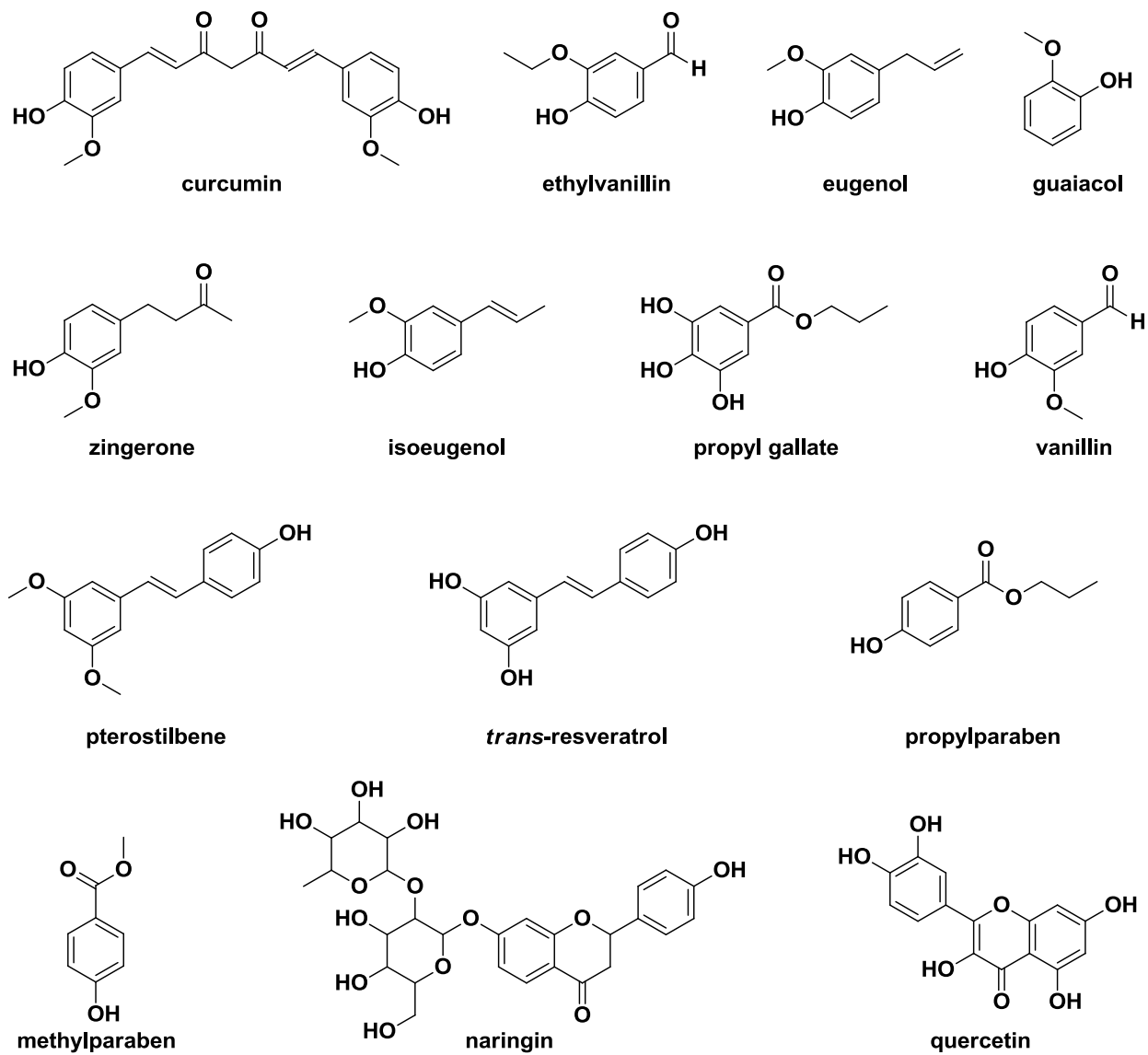


Figure 3.1. Structures of Potential SULT Inhibitors Selected from FDA’s “GRAS” List, EAFUS, or Dietary Compounds

Table 3.1. Chemical Properties of Potential Inhibitors [8]

Compound	logD (25 °C, pH 7)	Solubility (25 °C, pH 7)	logP (25 °C)	Molecular Weight	pKa (25 °C)	
Curcumin	3.02	1.4E-4 mol/L	3.071 ±0.444	368.38	Most acidic	8.11 ±0.46
Ethylvanillin	1.67	0.011 mol/L	1.718 ±0.272	166.17	Most acidic	7.91 ±0.18
Eugenol	2.40	0.011 mol/L	2.403 ±0.236	164.20	Most acidic	10.29 ±0.18
Guaiacol	1.34	0.086 mol/L	1.341 ±0.220	124.14	Most acidic	9.97 ±0.10
Isoeugenol	3.08	7.3E-3 mol/L	3.081 ±0.248	164.20	Most acidic	10.10 ±0.31
Methylparaben	1.86	0.037 mol/L	1.882 ±0.224	152.15	Most acidic	8.31 ±0.13
Naringin	-0.42	1.9E-4 mol/L	-0.198 ±0.791	580.53	Most acidic	7.17 ±0.40
Propyl gallate	1.72	0.037 mol/L	1.779 ±0.331	212.20	Most acidic	7.94 ±0.25
Propylparaben	2.88	6.5E-3 mol/L	2.901 ±0.224	180.20	Most acidic	8.23 ±0.15
Pterostilbene	4.06	2.7E-4 mol/L	4.056 ±0.261	256.30	Most acidic	9.96 ±0.26
Quercetin	1.08	6.3E-3 mol/L	1.989 ±1.075	302.24	Most acidic	6.31 ±0.40
<i>Trans</i> -resveratrol	3.02	9.4E-5 mol/L	3.024 ±0.267	228.24	Most acidic	9.22 ±0.10
Vanillin	1.14	0.028 mol/L	1.208 ±0.272	152.15	Most acidic	7.78 ±0.18
Zingerone	1.17	0.024 mol/L	1.168 ±0.237	194.23	Most acidic	10.03 ±0.20

Table 3.2. Pharmacokinetic Properties of Potential Inhibitors

Compound	F _{oral}	F _a	Metabolite	Metabolizing Enzyme	Dose Range
Curcumin		60%* [86]	glucuronide, sulfate [87-89], tetrahydrocurcumin [89], hexahydrocurcumin, hexahydrocurcuminol [88, 89]	SULT1A1, SULT1A3, alcohol dehydrogenase [89]	0 - 1 mg/kg body weight/day [90], not toxic in humans at 8 g/day oral dose for 3 months [91], 4 g, 6 g, 8 g [91], 450 - 800 mg (dietary supplement)
Ethylvanillin			3-ethoxy-4-hydroxybenzoic acid, 3-ethoxy-4-hydroxymandelic acid [92]		0.143 mg [92]
Eugenol		95% [93]	conjugates of eugenol, 4-hydroxy-3-methoxyphenyl-propane, cir- and trans-isoeugenol, 3-(4-hydroxy-3-methoxyphenyl)-propylene-1,2-oxide, 3-(4-hydroxy-3-methoxyphenyl)-propane-1,2-diol, 3-(4-hydroxy-3-methoxy-phenyl)-propionic acid [93]		
Guaiacol		45% [94]	glucuronide, sulfate [94]		54 mg [94, 95]
Isoeugenol		85%* [96]	glucuronide*, sulfate* [96]		
Methylparaben			glucuronide, sulfate [97]	UGT1A1, UGT1A6, UGT1A7, UGT1A8, UGT1A9, UGT1A10, UGT2B4, UGT2B7, UGT2B15, UGT2B17 [97]	≤ 0.1% in food [98]
Naringin			naringenin (human intestinal bacteria) [99], naringenin glucuronide, naringenin sulfate		16.2 mg/kg [100]
Propyl gallate		79%* [101]	4-methoxygallic acid, pyrogallol, 2-methoxypropylgallol, gallic acid, pyrogallol glucuronide, 4-methoxygallic acid glucuronide, 2-methoxypropylgallol glucuronide* [101]		≤ 0.02% of the fat or oil content [98]
Propylparaben		96%*	p-hydroxybenzoic acid [102],	carboxylesterase [102]	≤ 0.1% in food [98]

		[102]	glucuronides, sulfate, hippuric acid of p-hydroxybenzoic acid* [103]		
Pterostilbene	12.5%* [104], 80%* [105]		glucuronide* [105, 106], sulfate* [105]		50 - 250 mg (dietary supplement)
Quercetin		36 - 53% [107] 65 - 81% [108]	3-glucuronide, 3'-sulfate [109-111], 3'-methylquercetin-3-glucuronide [111]	catechol-O-methyltransferase [112]	8 mg, 20 mg, 50 mg [113], 100 mg (i.v.) [114], 100 - 1575 mg (i.v.) [115], 500 mg (dietary supplement)
<i>Trans</i> -resveratrol		71% [116]	3-glucuronide, 4'-glucuronide [117, 118], 3-sulfate [119, 120], 4'-sulfate, 3,4'-disulfate [120]	SULT1A1, SULT1A2, SULT1A3, SULT1E1 [120], UGT1A1, UGT1A6, UGT1A7, UGT1A9, UGT1A10 [118]	25 mg, 50 mg, 100 mg, 150 mg [121], 0.5 g, 1.0 g, 2.5 g, 5.0 g [119], 100 - 700 mg (dietary supplement)
Vanillin		94%* [122]	vanillin, vanillyl alcohol, vanillic acid, vanilloylglycine, catechol, 4-methylcatechol, guaiacol, 4-methylguaiacol, protocatechuic acid (free and conjugated forms)* [122], sulfate [85, 123]	SULT1A3 [85, 123]	
Zingerone		95%* [124]	glucuronide*, sulfate* [124]		10 mg (dietary supplement)

F_a: fraction of the oral dose absorbed; F_{oral}: oral bioavailability; UGT: uridine 5'-diphospho-glucuronosyltransferase; SULT: sulfotransferase. The asterisk indicates the data are from animal studies.

3.2.4 LS180 Cell Culture

LS180 cells were grown in DMEM with high glucose (4.5 g/L), 10% FBS, and 1% non-essential amino acid at 37 °C with 5% CO₂. The cells were fed every other day. They grew horizontally, and never reach 100% confluence if seeded at a low density. The cell culture medium was continuously increased from 12 to 25 mL in 75 cm² flask to keep pace with increasing metabolic demands of the growing cells.

When LS180 cells were sub-cultured, old medium was removed and the 75 cm² flask was filled with 5 mL fresh medium. Since trypsin changes the cell type, it was not used for cell sub-culture. Instead, cells were gently scraped by a cell scraper. In order to disperse the cells, cells were passed through a 23G ×1 needle for 6 times and dispensed to a new flask. Cells were sub-cultured in 6-7 days with a dilution of 1:10. Cell passage number was between 42 and 60. A new vial of LS180 cells was recovered from the liquid nitrogen about every 3 months.

3.2.5 Characterization of the Sulfation Activity in LS180 Cells

1-Naphthol has a molecular weight of 144.17. The calculated logP is 2.724 ± 0.189 at 25 °C, indicating it is a lipophilic compound, and pKa is 9.4 [8]. It is unionized at physiological pH. 1-Naphthol is a substrate for SULT1A1, SULT1A3, SULT1B1, and SULT1E1, which are the four major SULT isoforms in the intestine [67, 68]. SULT1A3 activity is much higher than SULT1A1 activity when determined at concentrations of 10 and 100 μM 1-naphthol with 13 μM PAP³⁵S and 200 ng recombinant protein [123]. The sulfate of 1-naphthol is commercially available from Research Organics (Cleveland, OH). Therefore 1-naphthol was used to characterize the sulfation activity in LS180 cells.

LS180 cells were seeded at the concentration of 1.9×10^5 cells/mL in the 12-well plate. The experiment was carried out on the 4th day after plating cells. For the linearity study for

incubation time, cells were equilibrated with 0.5 mL 10 mM HEPES in Hank's balanced salt solution (HBSS) (pH 7.4) for 20 min and then incubated with 1-naphthol (10 μ M) in the incubation media for 0 - 2 hrs. After incubation, 0.5 mL 10 mM HEPES in HBSS was removed and stored at -80 °C until analysis. The metabolic reactions were quenched by placing the 12-well plate on ice and quickly rinsing the wells with 1 mL cold (-20 °C) methanolic solution (60% methanol and 40% 70 mM HEPES (pH 5.5)). The cell extraction of metabolites was carried out with 1 mL methanol. Cells were scraped and collected in centrifuge tubes. The suspension was mixed for 2 - 3 min and centrifuged at 13000 rpm for 5 min. 800 μ L supernatant was collected. Each well in the plate was washed with 1 mL methanol twice. The washing solution was collected with the supernatant and dried in the vacuum concentrator. The residue was re-suspended in 35 μ L buffer matrix (50% methanol and 50% (5% triethylamine in water adjusted to pH 3.0 with acetic acid)).

1-naphthol and its sulfate in HBSS buffer containing 10 mM HEPES and cell lysates from metabolism studies in LS180 cells were analyzed by an HPLC method with an Alltima C18 column (250 \times 4.6 mm, 5 μ m) at 40 °C with isocratic elution (50% methanol and 50% (5% triethylamine in water adjusted to pH 3.0 with acetic acid)) at the flow rate of 0.75 mL, and detected by UV at wavelength of 283 nm. The standard curves for 1-naphthol and its sulfate were linear ($r^2 > 0.99$) in the concentration range of 0.15 - 50 μ M. The experiments were repeated three times.

3.2.6 HPLC Method for Phenylephrine

PE samples in DMEM containing 1% non-essential amino acid and cell lysates from metabolism studies in LS180 cells were analyzed by an HPLC method with a phenyl column (150 \times 3.2 mm, 5 μ m, 55 °C) at the flow rate of 0.75 mL (20% methanol and 80% 1% acetic acid

in water) and detected by FLU (excitation 270 nm, emission 305 nm). The standard curves for PE in both extracellular buffer and cell lysate were linear from 0.15 to 5000 μM with $r^2 > 0.99$. Difference from nominal (DFN) at low (0.3 μM), medium (30 μM), and high (100 μM) concentration in extracellular buffer was -3.6%, 0.0%, and 0.0%, respectively. Relative standard deviation (RSD) at low (0.3 μM), medium (30 μM), and high (100 μM) concentration in extracellular buffer was 13.8%, 1.5%, and 0.1%, respectively. DFN at low (0.3 μM), medium (30 μM), and high (100 μM) concentration in cell lysate was 4.2%, 3.8%, and -2.6%, respectively. RSD at low (0.3 μM), medium (30 μM), and high (100 μM) concentration in cell lysate was 6.9%, 5.8%, and 4.6%, respectively.

3.2.7 Linearity of Incubation Time and Concentration-dependent Study

LS180 cells were seeded at a concentration of 1.9×10^5 cells/mL in the 12-well plate. The experiment was carried out on the 4th day after plating the cells. In order to optimize the incubation time, cells were incubated with 0.5 mL DMEM containing 1% non-essential amino acid (pH 7.4) with PE (50 μM) from 0 to 40 hrs at 37 °C with 5% CO₂. For the concentration-dependent study, the cells were incubated with 0.5 mL DMEM containing 1% non-essential amino acid (pH 7.4) with PE covering a wide range of concentrations (1 - 3525 μM) for 18 hrs (from the incubation time optimization study) at 37 °C with 5% CO₂. After incubation, DMEM with 1% non-essential amino acid was removed and stored at -80 °C until analysis. The metabolic reactions were quenched by placing the 12-well plate on ice and quickly rinsing the wells with 1 mL cold (-20 °C) methanolic solution (60% methanol and 40% 70 mM HEPES (pH 5.5)) to avoid non-specific binding. The cell extraction of metabolites was carried out with 1 mL methanol. Cells were scraped and collected in centrifuge tubes. The suspension was vortexed for 2 - 3 min and centrifuged at 13000 rpm for 5 min. 800 μL supernatant was collected. Each well

in the plate was washed with 1 mL methanol twice. The washing solution was collected with the supernatant and dried in the vacuum concentrator. The residue was re-suspended in 35 μ L water. All the samples were analyzed by the HPLC method described above. The experiments were repeated three times.

3.2.8 Optimized Inhibition Assay

According to the preliminary studies, PE concentration for inhibition study was determined as 50 μ M, which was within the range of analytical sensitivity, as well as within the range of GI concentrations following an oral dose. This concentration had little to do with plasma concentrations, since we focused on inhibiting pre-systemic rather than systemic metabolism of PE. The incubation time was set from 14 hrs to 19 hrs, which was within the linear range of incubation time. For the inhibition study, cells were incubated with 0.5 mL DMEM containing 1% non-essential amino acid (pH 7.4) with PE (50 μ M) \pm inhibitor (100 μ M) for 14 hrs to 19 hrs at 37 $^{\circ}$ C with 5% CO₂. Ascorbic acid (when present) was added at a concentration of 1000 μ M. For the combination of curcumin, pterostilbene, resveratrol, and zingerone, four compounds were all at the concentration of 50 μ M. After incubation, the extracellular buffer was collected. The cell lysate experiments and analysis with the HPLC method were exactly the same as described above. The experiments were repeated three times.

3.2.9 Data Description and Statistical Analysis

The data were processed with GraphPad Prism 5. Linear regression was used to determine the linear range of incubation time for the remaining 1-naphthol and sulfate formation in LS180 cell model. Linear regression was also used to determine the linear range of incubation time for the fraction of the remaining PE. The statistically significant differences between the control group (PE incubated with LS180 cells in absence of phenolic dietary compounds) and the treated

groups (PE incubated with LS180 cells in presence of phenolic dietary compounds or combinations) were determined by one-way ANOVA followed by Dunnett's *post hoc* test ($p < 0.05$). The extent of PE disappearance in the control was considered 100%. The extent of PE disappearance in the treated group with phenolic dietary compounds or the combinations was calculated by the amount of PE disappearance in the treated group divided by the amount of PE disappearance in the control. The extent of PE disappearance was expressed as % of the control. Standard error of the mean was calculated by the formula as follows:

$$\frac{\sqrt{CV_{\text{control}}^2 + CV_{\text{treated}}^2}}{\sqrt{n}}$$

CV_{control} was the coefficient of variation of the control group. CV_{treated} was the coefficient of variation of the treated group. n was the number of observations, which was 3 in this case.

3.3 RESULTS

When 1-naphthol (10 μM) was incubated with LS180 cells for 0, 0.5, 1, and 2 hrs, it was efficiently sulfated in LS180 cells during short incubation time (shown in **Figure 3.2**). It was linear at least up to 2 hrs incubation in linear regression analysis with $r^2 = 0.9688$ for the remaining 1-naphthol (**A**) and $r^2 = 0.9958$ for 1-naphthol sulfate formation (**B**). The mass balance at 0.5, 1, and 2 hrs was $90 \pm 1\%$, $101 \pm 1\%$, and $121 \pm 2\%$ (mean \pm SD), respectively.

The fraction of the remaining PE decreased with time over 40 hrs when incubated with LS180 cells at the concentration of 50 μM (shown in **Figure 3.3**). The linear range for incubation time was from 0 to 24 hrs with $r^2 = 0.9579$.

Figure 3.4 shows PE disappearance over a range of concentrations. It seems PE did not saturate the metabolism in LS180 cell model even at a very high concentration (3525 μM). This may be due to the involvement of rate-limiting transport kinetics of PE in LS180 cell system.

The transporters responsible for uptake of PE may become saturated before the enzymes. Alternatively, it may reflect multiple metabolizing enzymes playing a role, from high affinity at low doses to lower affinity at higher doses. During the incubation time, the enzymes appeared to consume PE without saturation.

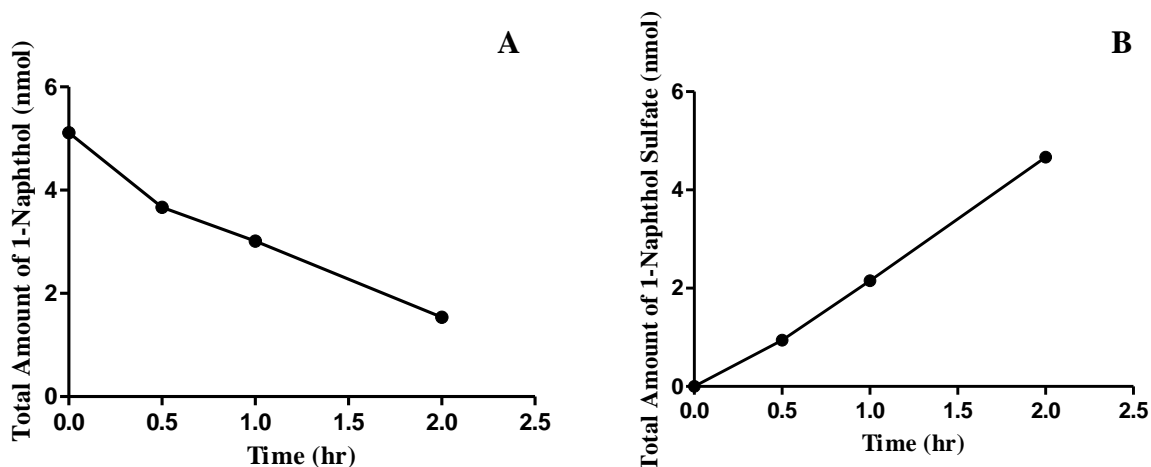


Figure 3.2. Remaining 1-Naphthol and 1-Naphthol Sulfate Formation over 2 hrs in LS180 Cells

The total amount of 1-naphthol decreased with time when incubated with LS180 cells (in 12-well plates 4 days after plating) over 2 hrs at an initial concentration of 10 μ M (A). The formation of 1-naphthol sulfate increased with time over 2 hrs (B). The values are expressed as mean \pm SD (n = 3) in these figures. The error bar is invisible. Both the remaining 1-naphthol and 1-naphthol sulfate formation were linear at least up to 2 hrs incubation.

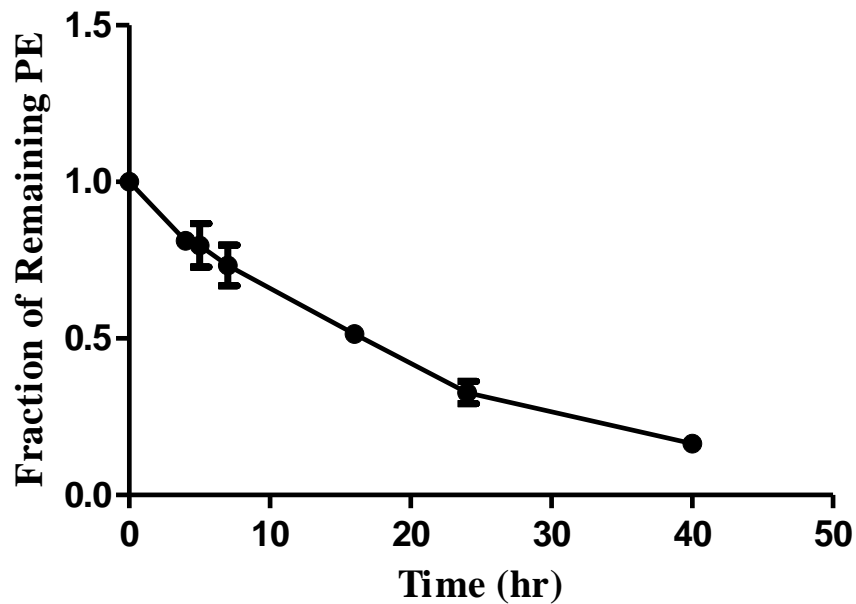


Figure 3.3. Fraction of Remaining Phenylephrine over 40 hrs in LS180 Cells

The fraction of the remaining PE decreased with time when incubated with LS180 cells (in 12-well plates 4 days after plating) over 40 hrs at an initial concentration of 50 μ M. The values are expressed as mean \pm SD ($n = 3$) in this figure. The linear range for incubation time was from 0 to 24 hrs.

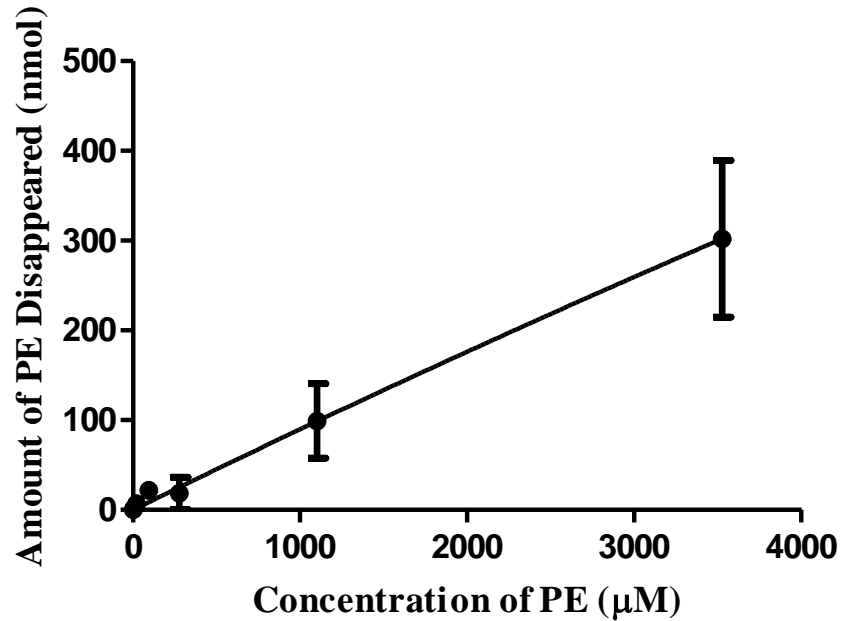


Figure 3.4. Phenylephrine Disappearance over a Broad Range of Concentrations in LS180 Cells

PE was incubated with LS180 cells (in 12-well plates 4 days after plating) covering a wide range of concentrations (1 - 3525 µM) for 18 hrs. The values are expressed as mean \pm SD (n = 3) in this figure. PE did not saturate the metabolism in LS180 cells even at the highest concentration (3525 µM) in this experiment.

As **Table 3.3** and **Table 3.4** show, co-incubation for 14 - 19 hrs with some phenolic dietary compounds or combinations of phenolic dietary compounds significantly decreased the extent of PE disappearance. The extent of disappearance of PE (control = 503 ± 127 pmol/hr, mean \pm SD) was significantly ($p < 0.05$) decreased by curcumin, guaiacol, isoeugenol, pterostilbene, resveratrol, zingerone, and the combinations of eugenol + propylparaben, propylparaben + vanillin, eugenol + propylparaben + vanillin + ascorbic acid, eugenol + vanillin, and pterostilbene + zingerone. The combinations of curcumin + resveratrol and curcumin + pterostilbene + resveratrol + zingerone almost completely inhibited PE disappearance.

When eugenol, propylparaben, or vanillin was used alone, the extent of PE disappearance was 53.8%, 90.2%, and 133% of the control, respectively, which were not significantly different from the control. However, the combinations of eugenol + propylparaben, propylparaben + vanillin, eugenol + vanillin decreased the extent of PE disappearance to 42.6%, 37.0%, and 57.5%, respectively. These combinations significantly decreased the extent of PE disappearance as compared to the control. This suggests synergy when eugenol, propylparaben, or vanillin was used with other compounds.

From these experiments it is known that these phenolic dietary compounds can inhibit PE disappearance in LS180 cell model. The calculated logP values of the phenolic dietary compounds are around 2 - 3 for almost all the phenolic dietary compounds except naringin. Also PE was stable in the DMEM buffer during the incubation time. Therefore, the inhibition of disappearance of PE in LS180 cells is probably due to the inhibition of PE metabolism.

Table 3.3. Effects of Phenolic Dietary Compounds on Phenylephrine Disappearance

Compound	Extent of PE Disappearance (as % of control)	SEM
Propylparaben	53.8%	43.5%
Vanillin	90.2%	24.4%
Propyl gallate	114%	28%
*Curcumin	24.5%	14.0%
*Zingerone	52.4%	14.6%
Methylparaben	75.9%	14.0%
Ethylvanillin	76.5%	11.0%
*Resveratrol	14.2%	28.0%
Quercetin	48.7%	9.2%
Naringin	75.7%	8.3%
Eugenol	133%	30%
*Guaiacol	51.3%	8.0%
*Pterostilbene	70.6%	4.2%
*Isoeugenol	73.9%	4.3%

The asterisk indicates significant difference between the control and the treated group with phenolic dietary compounds. The extent of PE disappearance in the control was considered 100%. The extent of PE disappearance in the treated group (as % of the control) was calculated by the amount of PE disappearance in the treated group divided by the amount of PE disappearance in the control. SEM was calculated by the formula discussed in the method section.

Table 3.4. Effects of Combinations of Phenolic Dietary Compounds on Phenylephrine Disappearance

Compound	Extent of PE Disappearance (as % of control)	SEM
Propylparaben + Ascorbic acid	56.4%	45.0%
*Eugenol + Propylparaben + Vanillin + Ascorbic acid	31.1%	10.9%
*Propylparaben + Vanillin	37.0%	11.2%
*Eugenol + Propylparaben	42.6%	8.4%
*Eugenol + Vanillin	57.5%	20.6%
*Curcumin + Resveratrol	0.0%	-
*Curcumin + Pterostilbene + Resveratrol + Zingerone	0.0%	-
*Pterostilbene + Zingerone	36.5%	7.0%

The asterisk indicates significant difference between the control and the treated group with the combinations of phenolic dietary compounds. The extent of PE disappearance in the control was considered 100%. The extent of PE disappearance in the treated group (as % of the control) was calculated by the amount of PE disappearance in the treated group divided by the amount of PE disappearance in the control. SEM was calculated by the formula discussed in the method section.

3.4 DISCUSSION AND CONCLUSIONS

There are many human intestinal *in vitro* models available to screen potential sulfation inhibitors, such as recombinant enzymes, cytosol, S9 fraction, and cells. Among them, intact cell systems are preferred over subcellular fractions, because as excipients in the formulation, phenolic dietary compounds, are desired to not only inhibit the sulfation of PE, but also to be able to cross the intestinal cell membrane, preferably by passive diffusion, to reach the enzymes and achieve the desired inhibition. *In situ* human intestinal perfusion, Ussing chamber, intestinal slice, primary cells have advantages as intact systems. But they are seldom used due to complicated technologies, limited availability, or short-time viability [125]. Cell lines are convenient methods to be used to investigate drug metabolism. It has been reported that acetaminophen sulfation does not occur in Caco-2 cells grown in a flask, probably due to the incomplete cell differentiation [126]. Cell differentiation is necessary for Caco-2 cells to express all the SULTs [127]. Caco-2 cells need long-term culture (21 - 24 days) to fully achieve cell differentiation, which is the limitation of this cell line.

In this study, LS180 cells were used as a tool to investigate the sulfation inhibition of phenolic dietary compounds. LS180 cell is a human colon adenocarcinoma epithelial cell line. The sulfation activity in LS180 cells has been reported with acetaminophen as the substrate. When acetaminophen is incubated with intact LS180 cells, the formation of acetaminophen sulfate is observed [80]. SULT1A1, SULT1A3/4, SULT1E1, and SULT2A1 are responsible for acetaminophen sulfation [128, 129]. SULT 1A1*2 and SULT1A2*2 polymorphisms have been found in LS180 cell line. These polymorphisms may cause decreased enzyme activities in LS180 cells [130]. The expression of SULT1A3 in LS180 cells is unclear in the literature. However, our

studies show LS180 cells had SULT1A3-like activity in that they sulfated 1-naphthol and PE, which are two known SULT1A3 substrates [51, 123].

According to the characterization of drug metabolism enzymes in LS180 cells, UGT 1A1, UGT 1A6, and UGT2B15 are expressed at the messenger ribonucleic acid (mRNA) level in this cell line [125]. The protein expression level of these enzymes in LS180 cells have not been investigated in the literature. However, acetaminophen glucuronidation have been demonstrated in LS180 cells consistent with UGT activities in this cell line [80]. Sulfation is a major metabolic pathway for PE pre-systemic metabolism. Glucuronidation is a minor metabolic pathway for PE pre-systemic metabolism. In our study, the disappearance of PE was measured, which could be due to non-SULT metabolism (i.e., UGTs). This is one of the limitations in this study.

MAO and aldehyde dehydrogenase (ALDH) expression or activities have not been reported in LS180 cells. 3-Hydroxymandelic acid, the final metabolite from monoamine oxidation pathway of PE metabolism (**Figure 1.2**), was not observed when PE was incubated with LS180 cells. This could be due to the lack of either MAO or ALDH in this cell line.

Another limitation for LS180 cells is that it is a human colon adenocarcinoma cell line, which cannot exactly represent small intestine, where most drug absorption occurs. The enzyme activities in cell lines are usually lower than small intestine [130].

Although PE metabolism in LS180 cells was tested over a broad range of concentrations, PE did not saturate the metabolism even at 3525 μM , which is probably due to the involvement of transport kinetics of PE in LS180 cell model. According to the physicochemical properties of PE, PE is a highly hydrophilic small molecule and ionized at the physiological pH. The uptake of PE into cells is probably mediated by active transporters. According to the renal clearance of PE, PE undergoes net tubular secretion in kidney (shown in **Table 1.2**). PE also has large volume of

distribution at steady state (shown in **Table 1.2**). These support the involvement of drug transporters for PE. However the transporters responsible for the uptake of PE are not clear in the literature. These transporters could be saturated before the enzymes, especially if the expression level of these transporters in LS180 cells is very low. There is no direct literature evidence showing that the uptake of PE into cells is mediated by transporters. But several compounds with structure similarities as PE have been found to be taken up into cells by transporters. Using human jejunal perfusion, the uptake of levodopa into intestine is found to be mediated by active transporters for large neutral amino acids [131]. The amino acid, L-leucine, significantly decreased the uptake of levodopa in the intestine, which could be as the result of competing for the transporters with levodopa [131]. In Caco-2 cell model, phenylalanine has been proved to transport across both the apical side and basolateral side by transporters [132]. The uptake transporters found in LS180 cells at mRNA level are organic cation transporter3, organic anion transporter2, and novel organic cation transporter2 [125]. But none of the uptake transporters have been studied and reported at the protein expression level. 1-Naphthol underwent fast metabolism in LS180 cells as compared to PE. 1-Naphthol crosses the cell membrane by passive diffusion mechanism [133]. Slow PE metabolism in LS180 cells could be also due to the low expression of the transporters for PE uptake on LS180 cell membrane.

An intact system, like LS180 cells, could be used as a model to screen the potential inhibitors for PE sulfation, but it is not suitable for studying the enzyme kinetics with PE. Subcellular fractions like intestinal and hepatic cytosol can be used to investigate the kinetics for PE sulfation and inhibition of PE sulfation with dietary inhibitors.

When eugenol, propylparaben, or vanillin was used alone, the extent of PE disappearance was not significantly different from the control. However, the combinations of eugenol +

propylparaben, propylparaben + vanillin, eugenol + vanillin significantly decreased the extent of PE disappearance as compared to the control. This suggests synergism when eugenol, propylparaben, or vanillin was used with other compounds. The synergistic effect is probably due to the concentration-dependent metabolism, which is observed in both Phase I and Phase II metabolism. The metabolism of 4-methoxybiphenyl in rat hepatocytes has a different pattern, dependent on the concentration of 4-methoxybiphenyl. 4-Methoxybiphenyl is converted to 4-hydroxybiphenyl and further metabolized to its sulfate and glucuronide. Below 25 μM , the percentage of each metabolite formed remains the same. Above 25 μM , the percentage of sulfate decreases proportionally with the concentration. 4-Hydroxybiphenyl and its glucuronide increase proportionally with the concentration [134]. This is because SULTs have higher affinity than UGTs [51]. At low concentration, such substrates are metabolized by SULTs. But at high concentration of substrates, SULTs are saturated and UGTs play a major role in conjugation of the substrates. This is very common in substrates for both SULTs and UGTs. Since PE is also a substrate for both SULTs and UGTs, this could occur in PE metabolism. According to the clinical studies for PE, four metabolites are detected in urine after oral administration of 24.6 mg PE over 8 hrs, which are 30% 3-hydroxymandelic acid, 6% 3-hydroxyphenylglycol sulfate, 47% PE sulfate, and 12% PE glucuronide [20]. In this study, much more PE sulfate is formed than PE glucuronide probably due to its relatively low dose level of PE. If the dose of PE is increased, the metabolism pattern may change, and glucuronidation may become major metabolic pathway for PE. Another example found in the literature is that phenolic compounds harmol and phenol shift from sulfation to glucuronidation when increasing their intravenous dose in an *in vivo* rat study [135]. In rat hepatocytes, the observation is the same as an *in vivo* study in rat [135]. A similar

shift from sulfation to glucuronidation is also observed in acetaminophen when increasing the dose level in a rat *in vivo* model [136].

In the presence of certain inhibitors, some metabolic pathways may be inhibited and other metabolic pathways or enzyme isoforms, which are not affected by the inhibitors, may contribute more to the metabolism of the substrates. For example when inhibitors for harmol sulfation are applied with harmol in a liver perfusion model, the sulfation of harmol decreases to 10% of the control, the total clearance is not changed for harmol and glucuronidation increases to play a major role for harmol metabolism in liver [137]. Eugenol, propylparaben, and vanillin may block PE metabolic pathway mediated by different enzymes or enzyme isoforms. When applying only eugenol, propylparaben, or vanillin, PE may go to the other metabolic pathways that are not blocked by the compound. But when applying the combinations, all the pathways for PE metabolism were blocked. Therefore, the significant decline in the disappearance of PE was observed with the combinations of eugenol + propylparaben, propylparaben + vanillin, eugenol + vanillin.

CHAPTER 4

CHEMICAL SYNTHESIS AND CHARACTERIZATION OF *R*-(-)-PHENYLEPHRINE SULFATE AND *R*-(-)-ETILEFRINE SULFATE

4.1 INTRODUCTION

Sulfation is a very important reaction in Phase II metabolism, which often occurs in some phenols, but has also been seen in some alcohols, amines, and thiols [51]. Many endogenous substances and xenobiotics or their Phase I metabolites are substrates of SULTs in cytosols, which catalyze the transfer of the sulfonate group from the cofactor PAPS to hydroxyl, amino, or thiol groups [51]. In most of the cases, the sulfate formed in the biotransformation is less active but more water-soluble, which facilitates excretion [51].

There are three enzymatic assays for sulfation and its inhibition studies: PAPS generation assay, preformed PAPS assay, and radiometric assay. The PAPS generation assay includes the two-step PAPS synthesis and the following sulfoconjugation. The first step of PAPS synthesis is that under the catalysis of adenosine-5'-triphosphate (ATP) sulfurylase, inorganic sulfate reacts with ATP to generate adenosine 5'-phosphosulfate (APS) and pyrophosphate. In the second step, PAPS is synthesized and the by-product adenosine diphosphate is formed by the reaction between APS and ATP with APS kinase as the catalyst. Magnesium ion is required in both reactions [59]. The enzymatic synthesis of PAPS in the body is a rapid process [59]. With PAPS as the donor of the sulfonate group, sulfation reaction gives the formation of sulfate by SULTs.

The PAPS generation assay is commonly used to identify or produce a large amount of the sulfate product for SULT substrates in old studies [138, 139]. Currently it is seldom used to conduct the enzyme kinetic studies for sulfation because it has multiple-step reactions and it seems difficult to optimize all the factors involved in the whole process. Wong *et al.* investigated the effects of pH, ATP/Mg²⁺ ratio, and their concentrations on the PAPS generation assay. They found the optimal condition for adrenaline sulfation is ATP and Mg²⁺ in the concentration range of 4 - 6 mM with the ratio of 1 at pH 9 [140]. It is unknown whether the same assay condition is suitable for other substrates. They also obtained the same K_m value for adrenaline in both the PAPS generation assay and the preformed PAPS assay [140].

The radiometric sulfation assay measures the formation of sulfate in an indirect way. The substrates for SULTs are incubated with radio-labeled cofactor [³⁵S]PAPS in the enzymatic reaction, which is terminated by adding barium acetate/hydroxide and zinc sulphate to precipitate excess [³⁵S]PAPS and protein [141]. The supernatant is taken to a scintillation vial after centrifugation. The radioactivity determined by the scintillation counting indicates the sulfate formation in the reaction [142-144]. Although the radiometric sulfation assay has been widely applied in the kinetic studies for sulfation and its inhibition, there are some disadvantages with it. The precipitation of excess [³⁵S]PAPS could be incomplete. This assay is not as selective and specific as the one directly detecting the product of sulfate.

The preformed PAPS assay with a validated analytical method is preferred over the other two assays in order to quantitate the sulfate products directly. It is necessary to synthesize the sulfate of the substrates as the reference standard for this assay. Compared to biosynthesis, chemical synthesis seems to be a more scalable strategy, which is usually used to obtain the sulfate.

There is no available information for the synthesis of PE/ET sulfate in the literature. But a large number of chemical synthesis methods for sulfate have been reported, which is very helpful for addressing the problem of PE/ET sulfate synthesis. Chemical synthesis of sulfate for some simple compounds is a single-step sulfating reaction. The sulfating reagent can be concentrated sulfuric acid, chlorosulfonic acid, sulfur trioxide pyridine complex, or sulfur trioxide triethylamine complex [145-148]. However, PE and ET have other functional groups compared to these compounds, which can be easily sulfated in undesired side reactions. Besides the phenolic group, PE and ET have aliphatic hydroxyl groups that can also react with the sulfating reagent. Since the hydroxyl groups of PE/ET compete for sulfation, a protecting group strategy is required to solve this problem. Protecting group strategy is a traditional method applied in chemical synthesis, which inserts two additional steps: introduction and removal of the protecting group [149]. The protecting group should be able to provide selective protection on the target functional group. It should also be compatible with the following reactions and finally can be removed without affecting other functional groups.

According to the literature, there are two ways to protect the secondary hydroxyl group in PE/ET. One is oxidizing the secondary hydroxyl group to the ketone by Jones Oxidation with chromium trioxide in aqueous sulfuric acid and acetone [150]. The removal step is carried out by reducing agent such as sodium borohydride to convert the ketone to the secondary hydroxyl group [146]. Arakawa *et al.* synthesized norepinephrine and epinephrine sulfate by the similar method using starting materials noradrenaline and adrenaline instead of norepinephrine and epinephrine for the sulfating reaction. The ketone is eventually reduced to the hydroxyl group to get the racemic products of norepinephrine and epinephrine sulfates [146]. The design of the synthetic route for PE/ET sulfate with this method is shown in **Figure 4.1**. The first step is Jones

Oxidation with chromium trioxide in aqueous sulfuric acid and acetone to oxidize the secondary hydroxyl group in PE/ET to the ketone at room temperature. This oxidation does not affect the phenolic group in PE/ET. The second reaction is sulfating at the phenolic group with sulfur trioxide pyridine complex in the solvent of pyridine at 60 °C, followed by the reduction with sodium borohydride in ethanol at ambient temperature. The final product is the racemic mixture. A chiral column is required for further isolation and purification to gain *R*-(-)-PE/ET sulfate, which is the disadvantage of this method. The advantage of this synthetic route is that all the reactions are classic and facile.

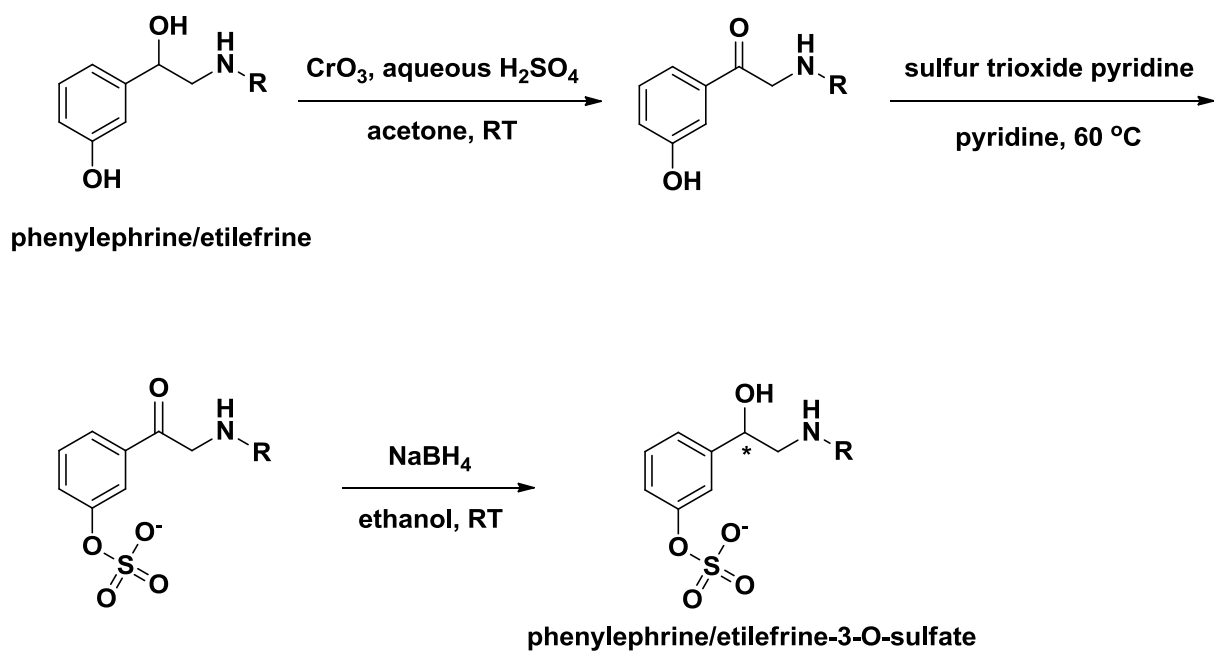


Figure 4.1. Synthetic Route for Phenylephrine/Etilefrine Sulfate by Protecting the Secondary Hydroxyl Group with Jones Oxidation

PE: R = CH₃; ET: R = C₂H₅. RT: room temperature. This figure shows the potential route for PE/ET sulfate synthesis with the protecting group strategy. The asterisk indicates the chiral center. The final product is a racemic mixture.

The other protecting group method is esterification of the aliphatic hydroxyl group in PE/ET with the use of trifluoroacetic anhydride. The reaction may also occur at the secondary amine group in PE/ET to form the amide. But trifluoroacetic anhydride does not stably esterify the phenolic group, which ensures the success in the protecting group strategy. This has been demonstrated in the synthesis of 2,2,2-trifluoro-*N*-(3-hydroxy-4-methoxybenzyl)-*N*-(4-hydroxyphenethyl)acetamide from 5-((4-hydroxyphenethylamino)methyl)-2-methoxyphenol in the supplementary material [151]. Although the mole ratio of trifluoroacetic anhydride to the reactant is around 4:1, there is no *O*-acylation at the phenolic group during the reaction [151]. The synthetic route for PE/ET sulfate with this protecting group method is shown in **Figure 4.2**. After protecting the secondary hydroxyl group, the sulfating reaction at the phenolic group is carried out by adding sulfur trioxide pyridine complex and stirring at 60 °C in pyridine. The protecting group is removed by hydrolysis with aqueous potassium bicarbonate at 30 °C. The pH of the potassium bicarbonate solution (100 mg/mL) is about 8.5. In this pH condition, trifluoroacetate ester is easily hydrolyzed [152]. The amide can also undergo hydrolysis in the basic pH range. This pH value does not favor the hydrolysis of sulfate. Sulfate hydrolysis is promoted dramatically in the acidic pH range (pH < 4) [153]. Sulfate is not very sensitive to mild alkalinity. The alkaline condition (pH > 10) only leads to very weak sulfate hydrolysis [153]. If the initial compound PE/ET is *R*-form, using this method can obtain the final product as *R*-(-)-PE/ET sulfate without isolation of the racemic mixture by chiral column, which is the advantage of this method as compared to the first method described above.

Therefore this synthetic route in **Figure 4.2** was selected to synthesize *R*-(-)-PE/ET sulfate in our lab.

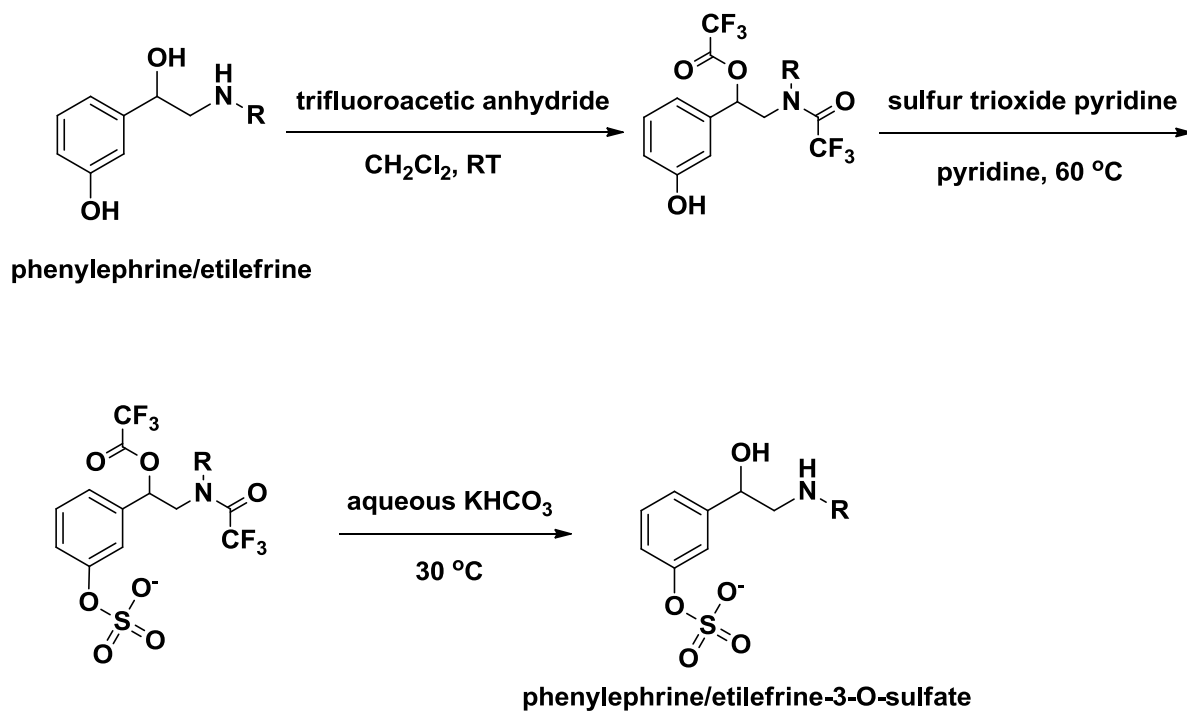


Figure 4.2. Synthetic Route for Phenylephrine/Etilefrine Sulfate by Protecting the Secondary Hydroxyl Group with Esterification

PE: R = CH₃; ET: R = C₂H₅. RT: room temperature. The figure shows the potential route for PE/ET sulfate synthesis with the protecting group strategy.

4.2 MATERIALS AND METHODS

4.2.1 Chemicals and Reagents

L-phenylephrine (base) was purchased from AK Scientific, Inc. (Mountain View, CA). ET hydrochloride was purchased from Frontier Scientific Services (Newark, NJ). Sulfur trioxide pyridine complex, tech. (48.8 - 50.3% active SO₃) was purchased from Acros Organics (Fair Lawn, NJ). Trifluoroacetic anhydride was purchased from Oakwood Chemical (West Columbia, SC).

Acetonitrile, dichloromethane, and methanol were purchased from Avantor Performance Materials, Inc. (Center Valley, PA). Ammonium acetate, dimethyl sulfoxide, potassium bicarbonate, sodium hydroxide, and triethylamine were purchased from Fisher Scientific (Fair Lawn, NJ). Ethyl acetate was purchased from Mallinckrodt Baker, Inc. (Phillipsburg, NJ). Hexane, hydrochloric acid, and pyridine were purchased from EMD Chemicals Inc. (Gibbstown, NJ). Isopropyl alcohol was purchased from Avantor Performance Materials, Inc. (Phillipsburg, NJ). Trifluoroacetic acid was purchased from Alfa Aesar (Ward Hill, MA).

4.2.2. Apparatus

pH indicator paper was purchased from EMD Chemicals Inc. (Gibbstown, NJ). Silica gel TLC plates were purchased from Analtech, Inc. (Newark, DE). Silica gel flash columns, strong cation-exchange flash columns, and semi-preparative HILIC column (250 × 10 mm, 5 μm) were purchased from Bonna-Agela Technologies (Wilmington, DE). Varian Microsorb-MV 100-3 C18 column (100 × 4.6 mm, 3 μm) was purchased from Agilent Technologies (Santa Clara, CA).

Savant refrigerated vapor trap was purchased from Thermo Scientific (Waltham, MA).

The lyophilizer was purchased from Labconco (Kansas City, MO).

The semi-preparative HPLC system included Waters 600 controller, Waters 717 plus autosampler (Waters Corporation, Milford, MA), PerkinElmer Series 200 vacuum degasser (PerkinElmer, Waltham, MA), Eppendorf column heater, remote Eppendorf TC-50 (Eppendorf, Hamburg, Germany), Shimadzu SPD-6A UV spectrophotometric detector (Shimadzu, Kyoto, Japan), Waters 474 scanning FLU detector (Waters Corporation, Milford, MA), PeakSimple chromatography data system SRI Model 302, and PeakSimple 2000 chromatography integration software (SRI Instruments, Torrance, CA).

The chromatographic experiments were conducted by the HPLC systems including Waters 2695 separation module, Waters 2487 dual λ absorbance detector, and Waters 2475 multi λ FLU detector (Waters Corporation, Milford, MA).

API4000 Q TRAP MS (Applied Biosystems Sciex, Concord, Canada) with turbo electrospray ion (ESI) source was utilized in negative ion mode for characterizing PE and ET sulfate. Analyst software Version 1.5 was used for data collection and processing.

NMR 400 MHz spectrometer was purchased from Bruker (Billerica, MA).

4.2.3 Reaction I

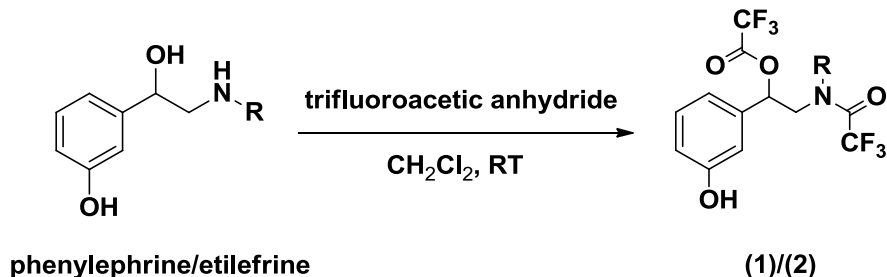


Figure 4.3. Reaction I for Synthesis of Trifluoro-acetic acid 1-(3-hydroxy-phenyl)-2-[methyl-(2,2,2-trifluoro-acetyl)-amino]-ethyl ester/Trifluoro-acetic acid 2-[ethyl-(2,2,2-trifluoro-acetyl)-amino]-1-(3-hydroxy-phenyl)-ethyl ester

PE: R = CH₃; ET: R = C₂H₅; Trifluoro-acetic acid 1-(3-hydroxy-phenyl)-2-[methyl-(2,2,2-trifluoro-acetyl)-amino]-ethyl ester (1): R = CH₃; Trifluoro-acetic acid 2-[ethyl-(2,2,2-trifluoro-acetyl)-amino]-1-(3-hydroxy-phenyl)-ethyl ester (2): R = C₂H₅. RT: room temperature.

The reaction for synthesis of PE/ET trifluoroacetic acid derivatives is shown in **Figure 4.3**. Trifluoroacetic anhydride (835 μ L, 5.98 mmol) was added to a suspension of PE base (100 mg, 0.598 mmol) in anhydrous methylene chloride (2 mL). For ET hydrochloride (100 mg, 0.46 mmol), trifluoroacetic anhydride (642 μ L, 4.60 mmol) was added to conduct the reaction. The mole ratio of trifluoroacetic anhydride to PE/ET was 10:1. The reaction mixture was stirred at room temperature and monitored by silica gel TLC. PE/ET could be identified by silica gel TLC plate with the mobile phase composed of 15% methanol, 42.5% ethyl acetate, and 42.5% hexane. The formation of PE/ET trifluoroacetic acid derivatives could also be detected by silica gel TLC plate with the mobile phase composed of 30% ethyl acetate and 70% hexane. Two PE/ET trifluoroacetic acid derivatives were observed by this method. According to their molecular weight confirmed by MS, they were PE/ET with protecting groups on both the hydroxyl and amine groups (1)/(2) (**Figure 4.3**) and by-products shown in **Figure 4.4**, which could be PE/ET

with protection on either the hydroxyl group (3)/(4) or the amine group (5)/(6). After 24 hrs PE/ET was completely consumed and the reaction was quenched by slowly adding methanol (1 mL) under stirring at room temperature. The solvent was dried under reduced pressure. The viscous residue was dissolved in ethyl acetate (1 mL). Most of the by-products in ethyl acetate were removed by extraction with 0.1 M hydrochloric acid (2 mL) into the aqueous layer three times. This indicated it was much more likely that the by-product was PE/ET with protection on the hydroxyl group (3)/(4). The organic layer with most (1)/(2) dissolved in it was evaporated under reduced pressure. Further purification was conducted by silica gel flash column chromatography with a step-wise gradient method (0 - 15% ethyl acetate in hexane) to yield (1)/(2) with a little amount of (3)/(4) or (5)/(6).

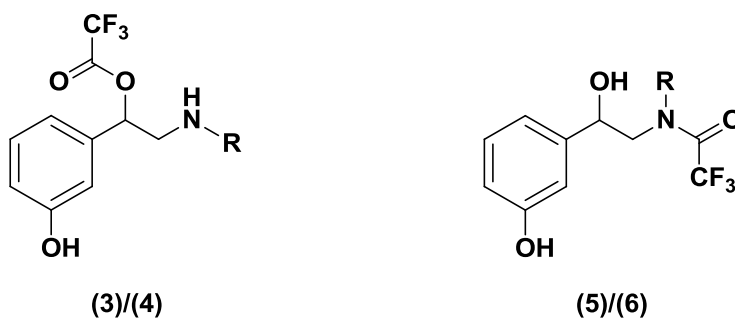


Figure 4.4. Potential By-products from Reaction I

Trifluoro-acetic acid 1-(3-hydroxy-phenyl)-2-methylamino-ethyl ester (3): R = CH₃; Trifluoro-acetic acid 2-ethylamino-1-(3-hydroxy-phenyl)-ethyl ester (4): R = C₂H₅; 2,2,2-Trifluoro-*N*-[2-hydroxy-2-(3-hydroxy-phenyl)-ethyl]-*N*-methyl-acetamide (5): R = CH₃; *N*-Ethyl-2,2,2-trifluoro-*N*-[2-hydroxy-2-(3-hydroxy-phenyl)-ethyl]-acetamide (6): R = C₂H₅.

4.2.4 Reaction II

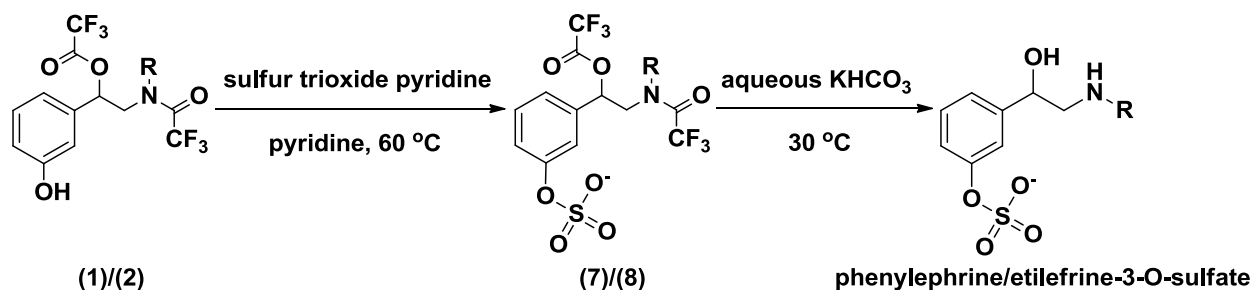


Figure 4.5. Reaction II for Synthesis of Phenylephrine/Etilefrine Sulfate

PE: R = CH₃; ET: R = C₂H₅; Trifluoro-acetic acid 1-(3-hydroxy-phenyl)-2-[methyl-(2,2,2-trifluoro-acetyl)-amino]-ethyl ester (1): R = CH₃; Trifluoro-acetic acid 2-[ethyl-(2,2,2-trifluoro-acetyl)-amino]-1-(3-hydroxy-phenyl)-ethyl ester (2): R = C₂H₅; 3-(2-(2,2,2-Trifluoro-*N*-methylacetamido)-1-(2,2,2-trifluoroacetoxy)ethyl)phenyl sulfate (7): R = CH₃; 3-(2-(*N*-Ethyl-2,2,2-trifluoroacetamido)-1-(2,2,2-trifluoroacetoxy)ethyl)phenyl sulfate (8): R = C₂H₅.

The reaction for synthesis of PE/ET sulfate is shown in **Figure 4.5**. The products (1)/(2) from Reaction I were dissolved in anhydrous pyridine (2 mL). Sulfur trioxide pyridine complex (0.3 g) was added to start the reaction. Under anhydrous condition the reaction mixture was stirred at 60 °C with reflux for 3 hrs. The pyridine solvent was immediately dried under reduced pressure after the reaction. Potassium bicarbonate solution (100 mg/mL) was slowly added to the remaining white solid until it was completely dissolved and no bubbles appeared. The pH value was checked with the pH indicator paper and adjusted to 8.5 with potassium bicarbonate solution (100 mg/mL). The reaction was stirred at 30 °C for 3 hrs and then the pH was adjusted to 7.0 with 0.1 M hydrochloric acid. The solution was dried down under reduced pressure. PE/ET sulfate was extracted by methanol three times and the solvent was evaporated under reduced pressure. The resulting solid was dissolved in water and loaded to a strong cation-exchange flash column (NH₄⁺ form) to remove PE/ET. The further isolation and purification was accomplished

by a semi-preparative HILIC column (250 × 10 mm, 5 μm) with isocratic elution in a mobile phase composed of 3.5 g ammonium acetate, 48 mL water, 86 mL methanol, 95 mL acetonitrile, 770 mL isopropyl alcohol. The fraction of the product PE/ET sulfate was collected and dried down in the vacuum. The solid was then dissolved in water and the solution was evaporated by lyophilization to remove the volatile salts ammonium acetate and yield the final product as yellow solid in the salt form.

4.2.5 Identification and Characterization of PE/ET Sulfate

Both the proton and carbon NMR were performed with the solvent of methanol-d to identify the structures of the synthesized PE/ET sulfate. The molecular weight of PE/ET sulfate was determined by the MS. The HPLC method was used to test the purity of PE/ET sulfate with a C18 column (100 × 4.6 mm, 3 μm, 40 °C) at the flow rate of 1 mL/min by the isocratic elution (5% acetonitrile, 95% (6.5 mM triethylamine and 13 mM trifluoroacetic acid in water)) and UV detection at the wavelength of 254 nm.

4.2.6 Chemical Hydrolysis of PE/ET Sulfate

The standard compounds of PE/ET sulfate are not available and the chemical synthesis has never been reported in the literature. PE/ET sulfate has both cation and anion within the same molecule in a broad pH range. The intramolecular ionic bond could form in PE/ET sulfate. PE/ET sulfate molecule could form the salt with ammonium acetate in the mobile phase as well. Due to the complexity of PE/ET sulfate existing forms (intramolecular salt and ammonium salt), the molecular weight of PE/ET sulfate was uncertain and it was difficult to determine the molar concentration of PE/ET sulfate. Since PE/ET reference compounds are commercially available, acid-based hydrolysis of PE/ET sulfate was applied to determine its molar concentration by comparing the disappearance of PE/ET sulfate with the formation of PE/ET. PE/ET sulfate in

dimethyl sulfoxide (DMSO) was diluted by 1:500 with 1 M hydrochloric acid and incubated at 37 °C for 0 hr and 3 hrs. PE/ET in 1 M hydrochloric acid at the concentration of 20 μM was also incubated at 37 °C for 0 hr and 3 hrs to test their stability in the acidic solution. After incubation, 50 μL of 2 M sodium hydroxide was added to 100 μL of 1 M hydrochloric acid with PE/ET or PE/ET sulfate in it. The solution was mixed well by vortex and injected into the HPLC for analysis.

PE/ET and its sulfate were analyzed with a C18 column (100 × 4.6 mm, 3 μm, 40 °C) at the flow rate of 1 mL/min with the gradient elution. The mobile phase A was 6.5 mM triethylamine and 13 mM trifluoroacetic acid in water and B was acetonitrile. A was kept at 100% from 0 to 2 min and then B was steadily increased to 50% from 2 to 6 min. PE sulfate and PE were eluted at 2.9 and 3.5 min, respectively. ET sulfate and ET were eluted at 4.8 and 5.0 min, respectively. After the elution of the sulfate and the parent compound, B was reduced to 0% from 6 to 8 min and maintained until 10 min. PE/ET and its sulfate were detected by FLU with excitation wavelength at 270 nm and emission wavelength at 305 nm. The standard curve for PE/ET in the solution was linear from 0.03 to 30 μM with $r^2 > 0.99$.

During the incubation, the disappearance of PE/ET sulfate was equal to the formation of PE/ET in the unit of mole. The equation used to calculate the original concentration of PE/ET sulfate in the solution is shown as follows. Thus the concentration of PE/ET sulfate in the stock solution was 500 times the original concentration of PE/ET sulfate in the solution.

$$\frac{\text{PE/ET sulfate original mole concentration in solution}}{\text{the height of PE/ET sulfate peak at 0 hr}} = \frac{\text{the increased PE/ET mole concentration after 3hrs}}{\text{the height of PE/ET sulfate peak at 0 hr} - \text{the height of PE/ET sulfate peak after 3 hrs}}$$

4.3 RESULTS

PE sulfate salt yielded 12%.

For PE sulfate, the proton NMR spectrum is shown in **Figure 4.6**.

$^1\text{H-NMR}$ (400 MHz, MeOD): δ 2.71 (3H, s, $-\text{CH}_3$), 3.13 (2H, m, $-\text{CH}_2-$), 4.93 (1H, m, $-\text{CH-}$), 7.23 (2H, m, $-\text{CH=}$), 7.35 (1H, m, $-\text{CH=}$), 7.38 (1H, m, $-\text{CH=}$).

The carbon NMR spectrum of PE sulfate is shown in **Figure 4.7**.

$^{13}\text{C-NMR}$ (100 MHz, MeOD): δ 33.90, 56.71, 69.85, 120.10, 122.48, 123.28, 130.55, 143.62, 154.36.

MS (ESI): m/z $[\text{M-H}]^-$ calculated for $\text{C}_9\text{H}_{12}\text{NO}_5\text{S}$:246.26; found: 245.8.

The HPLC was used to test the apparent purity of the synthesized PE sulfate (shown in **Figure 4.8**). The results from the purity test are listed in **Table 4.1**. The peak for PE sulfate was sharp and symmetric.

Table 4.1. HPLC Purity Test for Phenylephrine Sulfate

Peak	Retention Time (min)	Peak Height	Peak Area ($\mu\text{V}\cdot\text{sec}$)	Area (%)
PE Sulfate	1.73	152658	624053	98.77
Impurity I	2.35	699	4498	0.71
Impurity II	3.79	543	3240	0.51

The acid-based hydrolysis of PE sulfate was conducted to determine the molar concentration of PE sulfate in the stock solution by analyzing the formation of PE during the incubation with the reference compound.

ET sulfate salt yielded 8%.

For ET sulfate, the proton NMR spectrum is shown in **Figure 4.9**.

$^1\text{H-NMR}$ (400 MHz, MeOD): δ 1.31 (3H, t, $J = 7.32$ MHz, $-\text{CH}_3$), 3.09 (4H, m, $-\text{CH}_2-$), 4.93 (1H, m, $-\text{CH-}$), 7.24 (2H, m, $-\text{CH=}$), 7.35 (1H, m, $-\text{CH=}$), 7.39 (1H, m, $-\text{CH=}$).

The carbon NMR spectrum of ET sulfate is shown in **Figure 4.10**.

^{13}C -NMR (100 MHz, MeOD): δ 30.65, 44.16, 54.58, 69.96, 120.12, 122.57, 123.22, 130.58, 143.58, 154.38.

MS (ESI): m/z $[\text{M-H}]^-$ calculated for $\text{C}_{10}\text{H}_{14}\text{NO}_5\text{S}$: 260.29; found: 259.2.

The HPLC was used to test the apparent purity of the synthesized ET sulfate (shown in **Figure 4.11**). The results from the purity test are listed in **Table 4.2**. The peak for ET sulfate was sharp and symmetric.

Table 4.2. HPLC Purity Test for Etilefrine Sulfate

Peak	Retention Time (min)	Peak Height	Peak Area ($\mu\text{V}\cdot\text{sec}$)	Area (%)
ET Sulfate	2.22	250677	1179719	99.94
Impurity	5.64	152	673	0.06

The acid-based hydrolysis of ET sulfate was conducted to determine the molar concentration of ET sulfate in the stock solution by analyzing the formation of ET during the incubation with the reference compound.

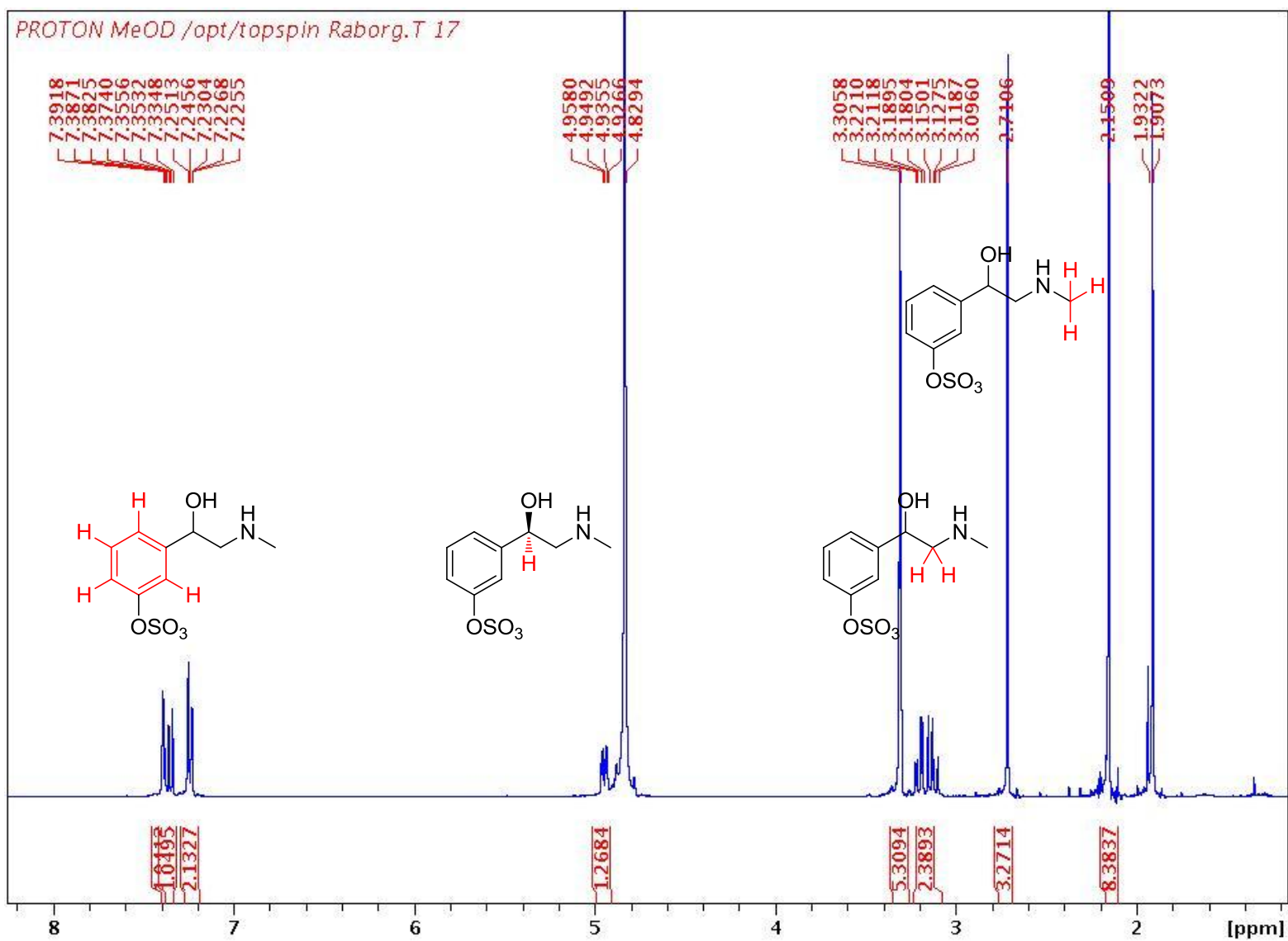


Figure 4.6. ¹H-NMR Spectrum for Phenylephrine Sulfate

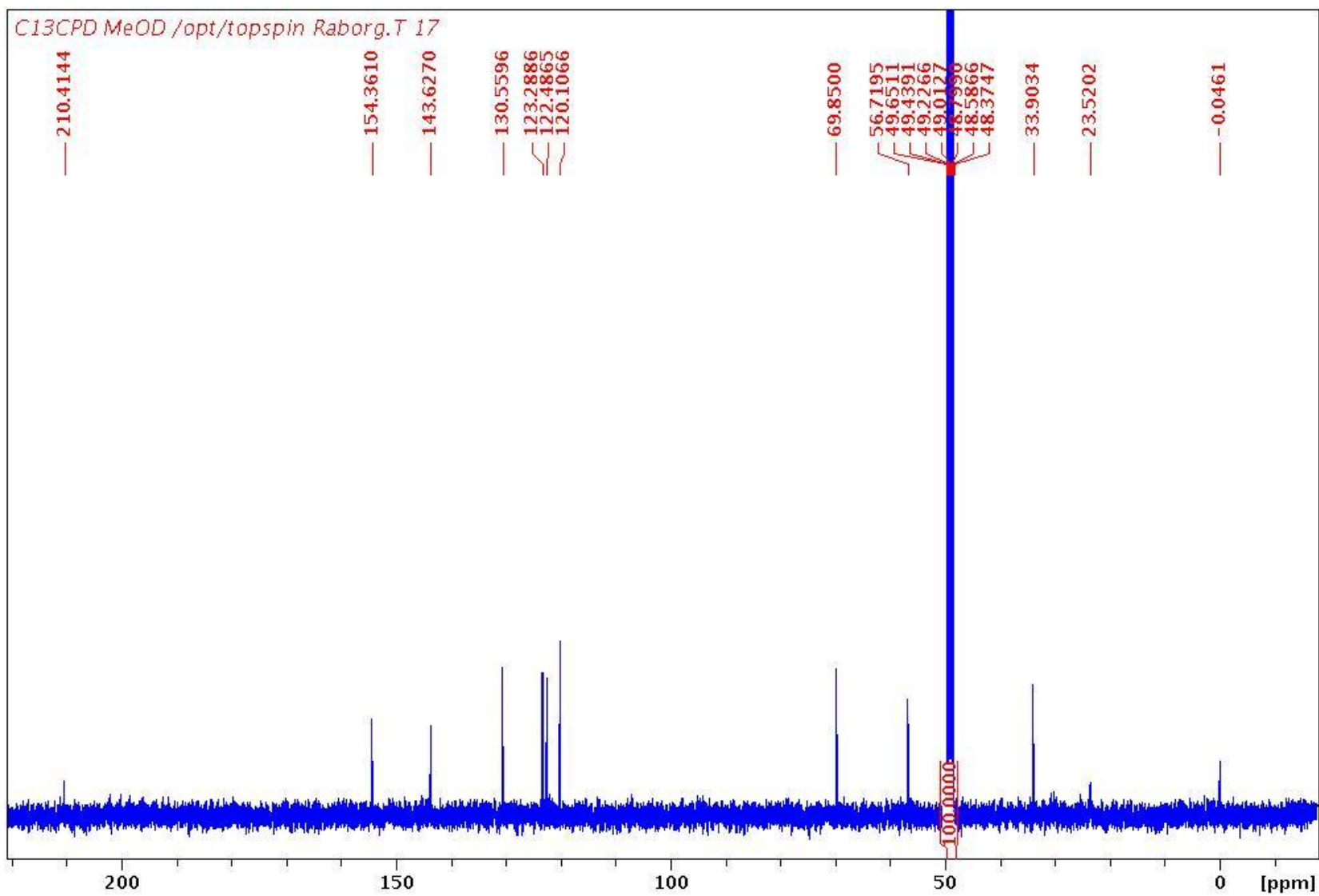


Figure 4.7. ^{13}C -NMR Spectrum for Phenylephrine Sulfate

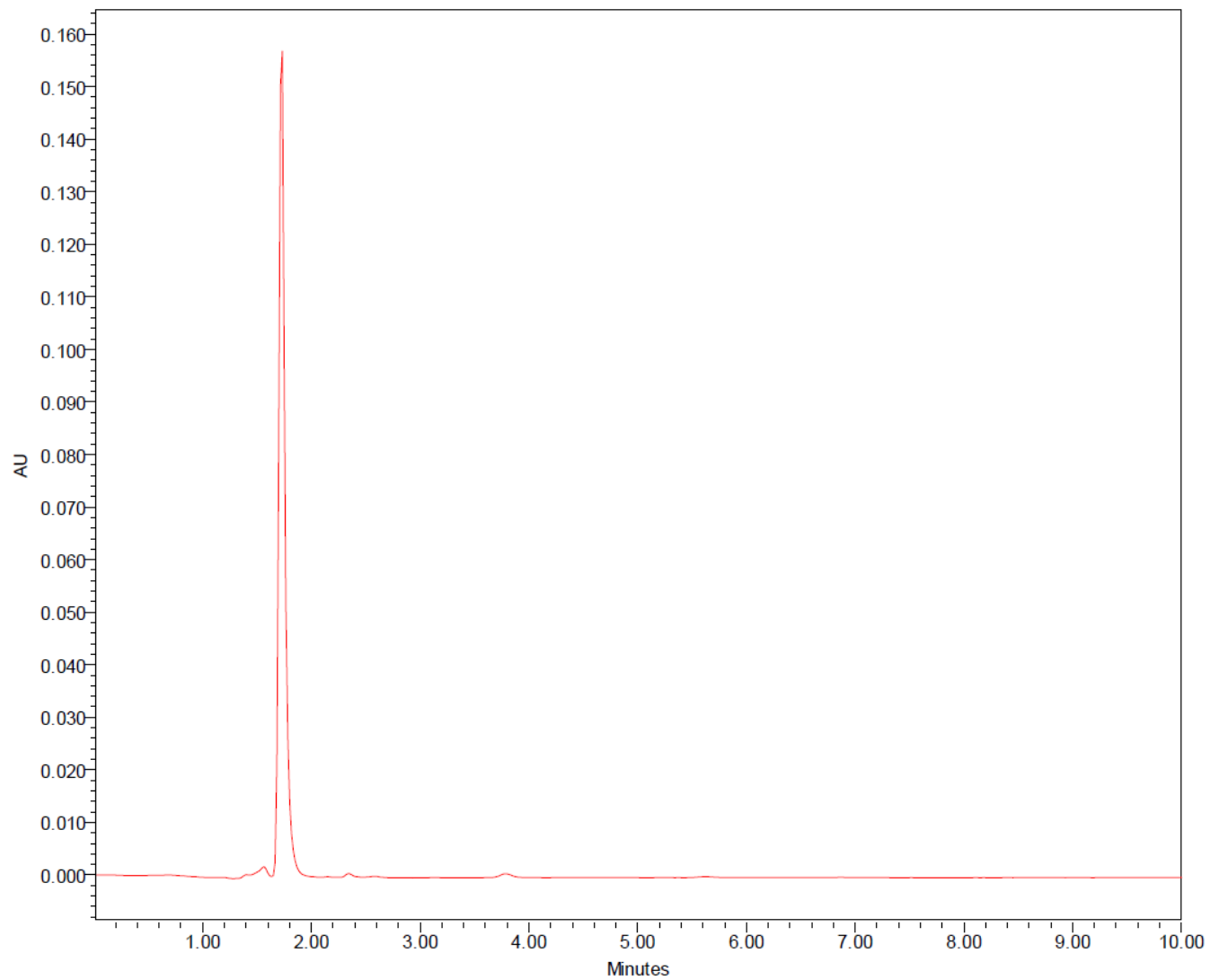


Figure 4.8. HPLC Purity Test for Phenylephrine Sulfate

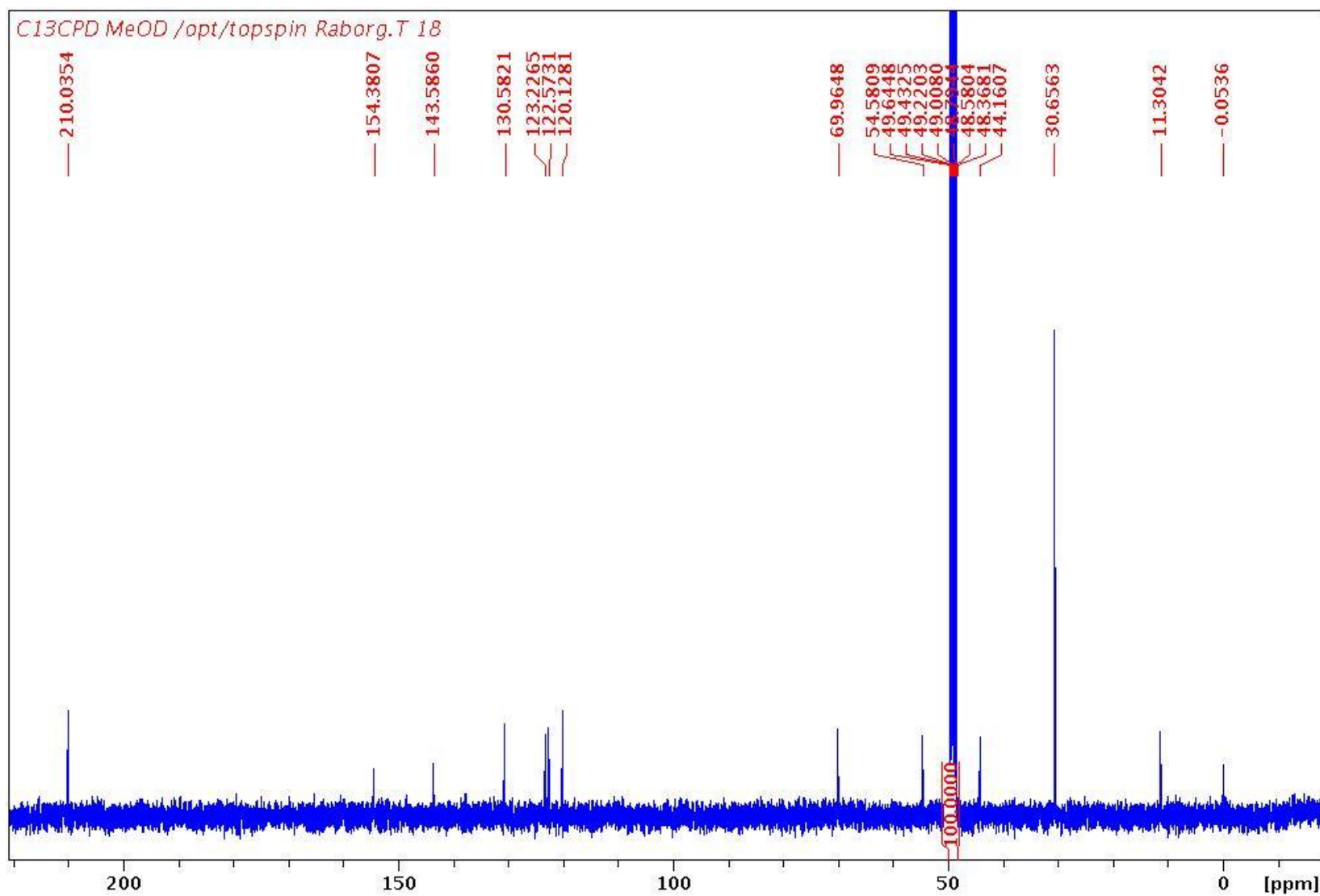


Figure 4.10. ^{13}C -NMR Spectrum for Etilefrine Sulfate

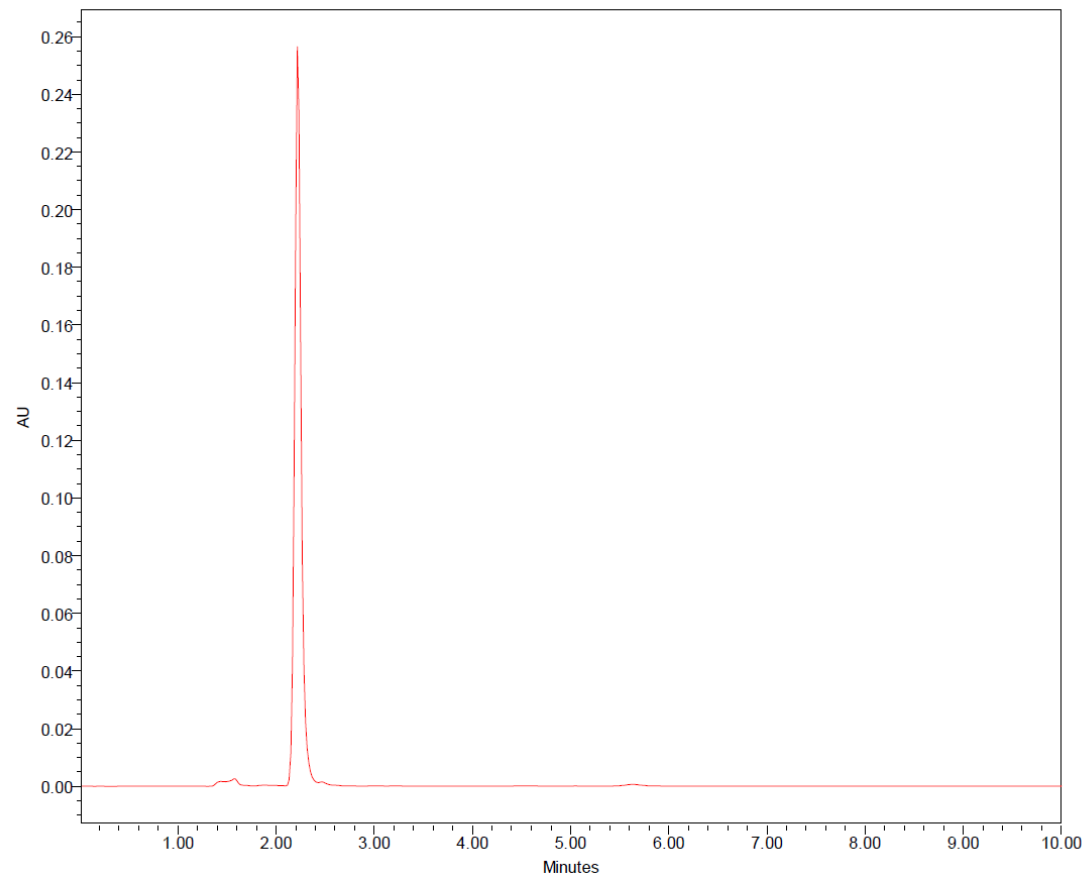


Figure 4.11. HPLC Purity Test for Etilefrine Sulfate

4.4 DISCUSSION AND CONCLUSIONS

In Reaction I, since trifluoroacetic anhydride can easily react with water to produce trifluoroacetic acid, it was very important to maintain the anhydrous condition throughout the entire reaction.

Although excess trifluoroacetic anhydride was added leading to the mole ratio of trifluoroacetic anhydride to PE/ET equal to 10:1, PE/ET with protection on either the hydroxyl group (3)/(4) or the amine group (5)/(6) was still detected after reaction. Reaction I and the following purification yielded PE and ET with protection on both the hydroxyl and amine groups (1)/(2) 76 mg and 109 mg, respectively, containing a trace amount of (3)/(4) or (5)/(6).

When Reaction I was conducted in the ice bath under the condition that the mole ratio of trifluoroacetic anhydride to PE was 1:1, both PE with two protecting groups and PE with only one protecting group could be identified by silica gel TLC. This demonstrates the products formed from the reaction were not dependent on the mole ratio of trifluoroacetic anhydride to PE/ET.

When the protecting group was introduced for ET sulfate synthesis, pyridine was first used as the solvent for the reaction. Because ET was in the salt form as ET hydrochloride, it was considered that excess pyridine can react with ET hydrochloride to form pyridine hydrochloride. Therefore although ET hydrochloride salts were added to the reaction, they behaved like ET base in the solvent of pyridine. However, this method failed several times. When trifluoroacetic anhydride was added to initiate the reaction, a large amount of fume can be observed. The reason was not clear. Instead of pyridine, methylene chloride was used as the solvent and the reaction was accomplished. Two compounds (ET with two protecting groups and ET with only one protecting group) were detected from this reaction, which was the same observation from the

first-step reaction for PE sulfate synthesis. The products from Reaction I were not dependent on the form of PE/ET.

In Reaction II, it was necessary to use the fresh reagent sulfur trioxide pyridine complex to ensure the anhydrous condition. This reagent is very easy to degrade in moist air. It should be stored in the vacuum desiccator and should not be kept for a long time. Otherwise the poor quality of the reagent can definitely affect the reaction. Anhydrous pyridine was preferred as the solvent for the reaction.

The intermediate was not purified after the sulfating reaction with sulfur trioxide pyridine complex. Potassium bicarbonate solution was added and the hydrolysis reaction was carried out immediately at 30 °C. The reason for not purifying the intermediate was that PE/ET sulfate was generated promptly when adding potassium bicarbonate solution, which was detected by LC-MS/MS. In order to obtain higher yield, the purification of the intermediate after the sulfating reaction was eliminated.

The last step for the synthesis was removal of the protecting group. It was first conducted by base-catalyzed hydrolysis with sodium bicarbonate (100 mg/mL). The reaction was very slow and not complete at room temperature or 30 °C. When changing the base to potassium bicarbonate (100 mg/mL), the reaction was still very slow and incomplete at room temperature. When the temperature was increased to 30 °C, the reaction can be finished in 3 hrs. Also at this pH and temperature, the sulfate group did not hydrolyze. When the pH was increased to 13 (0.1 M NaOH), the hydrolysis of the sulfate group was rapid.

The most difficult part of the synthesis was the isolation and purification of PE/ET sulfate after Reaction II. The silica gel flash column was tried to purify the compound with gradient elution. Even when the composition of the mobile phase was increased to 50% methanol in

methylene chloride, PE/ET sulfate was not eluted. This was probably because the final product PE/ET sulfate is a very polar and ionized compound, which may stick to the silica gel column. Since PE/ET sulfate has strongly anionic sulfate group, amine flash column was used as weak anion exchange column to isolate the compound. The amine column was conditioned with 10 column volume of methanol and then washed with 20 column volume of 5% acetic acid. PE/ET sulfate was dissolved in water and loaded into the flash column system. A step-wise gradient elution was applied with 0 to 100% 1 M NaH₂PO₄ (pH 4.6) in water. PE/ET sulfate was not eluted even at the highest ionic strength (100% 1 M NaH₂PO₄). This could be due to the binding of positive charged secondary amine group of PE/ET sulfate to the counter-ion on the amino-propyl bonded phase of the amine column. Even if PE/ET sulfate can be eluted, the products would contain a large amount of salts after the purification with amine column. It is necessary to desalt the products with a C18 flash column, on which PE/ET sulfate usually does not have any retention. This could also cause a problem for purification. HILIC flash column with isocratic elution (3.5 g ammonium acetate, 48 mL water, 86 mL methanol, 95 mL acetonitrile, 770 mL isopropyl alcohol) was tried but could not retain PE/ET sulfate on it owing to the large pore size of the flash column. HILIC TLC was also tried for the isolation and purification. But it could not achieve good separation for PE/ET and PE/ET sulfate as a result of ionic bond. Finally, semi-preparative HILIC column was tested and considered to be the best way to purify PE/ET sulfate. Since the mobile phase contained ammonium acetate, lyophilization was applied to remove the volatile salts.

The peaks in the ¹H-NMR and ¹³C-NMR spectra were consistent with the structure of PE/ET sulfate. The measured molecular weight by MS was very close to the calculated molecular weight of PE/ET sulfate. These results supported the successful synthesis of PE/ET sulfate.

In conclusion, PE and ET sulfate were chemically synthesized and purified in amounts greater (about 10 mg) than what can feasibly be synthesized by biosynthesis (< 1 mg). Their structures were verified by $^1\text{H-NMR}$, $^{13}\text{C-NMR}$, and MS.

CHAPTER 5

LC-MS/MS METHOD DEVELOPMENT FOR SIMULTANEOUS QUANTITATION OF PHENYLEPHRINE AND ITS METABOLITES

5.1 INTRODUCTION

PE and its metabolites (PE sulfate and 3-hydroxymandelic acid) are small molecules with molecular weight of 167.21, 246.26, and 168.15, respectively. According to the structure of PE, it has two ionizable groups: the secondary amine group and the phenolic group. The calculated pKa values of the secondary amine group and the phenolic group are 9.2 and 9.8, respectively [8]. PE is ionized with the positive charge on the secondary amine group in the recommended pH range of 2 to 8 for most silica-based columns. Besides the cationic secondary amine group, the metabolite PE sulfate has a sulfate group with the pKa value less than 1, which is highly anionic in most mobile phase conditions. Another major PE metabolite 3-hydroxymandelic acid has a carboxyl group with the estimated pKa value of 3.4, which could be neutral or negatively charged within the pH range of most columns. Like the parent compound PE, the phenolic group of 3-hydroxymandelic acid is uncharged in most liquid chromatography conditions. The calculated logP values for PE and 3-hydroxymandelic acid are 0.117 ± 0.269 and 0.291 ± 0.328 , respectively [8].

Since PE and its metabolites are charged and extremely hydrophilic compounds, liquid-liquid extraction for the sample preparation may not work. SPE is applied for extraction of PE from

human plasma/serum samples when the assays are developed to quantitatively analyze PE. The cartridges used in these studies are phenyl, WCX, and C18 phases [21-23, 29]. The WCX cartridge is not appropriate for PE sulfate and 3-hydroxymandelic acid because of the negative charge in these compounds. Since PE sulfate has much lower lipophilicity than PE, phenyl and C18 cartridges may not be suitable for it. The online sample clean-up with column switching technique could be a good option but has never been used for PE analysis in the literature. This method needs a proper column which has retention for both PE and its metabolites.

Due to their small molecular weight, ionized state, and low lipophilicity, PE and its metabolites have minimal retention on reversed-phase C18 columns. Most HPLC assays for PE developed with C18 or C8 columns use ion-pairing methods to achieve better retention [22, 23, 30-33, 36, 37, 40]. Some columns specially designed for polar compounds are selected to facilitate the assay development for PE, such as CN, PEG, PFP, and HILIC columns [25-30]. Serotonin, dopamine, and their sulfates can also be analyzed by LC-MS/MS with PFP column, which ensures both enough retention and good separation [154, 155]. PGC column has been utilized for analysis of compounds with similar structures and chemical properties as PE, which may have the potential for the analysis of PE and its metabolites. An LC-MS/MS method is used to analyze the catecholamines in brain tissue by PGC column [156]. L-dopa and its metabolites are cleaned, separated and determined by column switching strategy with two PGC columns [157]. Other columns such as amide C16 column, phenyl column, and SCX column are also applied to quantitate compounds like PE [158-160]. Since PE is cation and the metabolites (PE sulfate and 3-hydroxymandelic acid) are anions in most mobile phase, PE and the metabolites should be detected under positive and negative mode in MS, respectively. Therefore, separation

is required for PE and its metabolites to ensure ionization under positive/negative mode when developing an LC-MS/MS method.

For detection of PE, FLU, EC, UV, and MS detectors are commonly used [21-40]. UV detector usually has relatively high LLOQ values for PE [26, 27]. PE analysis in simple matrix like different pharmaceutical formulations is often performed with UV detection. The best LLOQ for PE by UV detector is 15.3 ng/mL in extraction of sachets reported by Olmo *et al.* [28]. PE has very strong FLU signal (excitation 270 nm, emission 305 nm), so analytical methods for PE with FLU detection could achieve good sensitivity. The LLOQ in human serum samples by FLU detector is 5 ng/mL reported by Yamaguchi *et al.* [37]. PE is ionized in a broad pH range, which favors the EC detector. The EC detector can reach the LLOQ of 0.35 ng/mL in serum matrix reported by Vuma *et al.* [22]. The LC-MS/MS method for analyzing PE parent drug in human plasma has an LLOQ of 0.05 ng/mL, which is the best LLOQ value in the literature so far [24]. Comparing all the available analytical methods in the literature, LC-MS/MS can achieve the best LLOQ even in the complicated matrix like plasma. The low concentration of PE sulfate could not be detected by UV or FLU detectors. EC detection is unstable and less commonly available. The LC-MS/MS method for quantitatively analyzing PE and its metabolites (PE sulfate and 3-hydroxymandelic acid) is not available in the literature. Therefore, it is necessary to develop an LC-MS/MS method to analyze the parent drug PE and its metabolites in the enzymatic reaction to facilitate the enzyme kinetic study of PE sulfation in intestinal and hepatic cytosol as well as the inhibition study with phenolic dietary compounds.

5.2 MATERIALS AND METHODS

5.2.1 Chemicals and Reagents

ET hydrochloride was purchased from Frontier Scientific Services (Newark, NJ). Homovanillic acid was purchased from Sigma-Aldrich (St. Louis, MO). 3-Hydroxymandelic acid was purchased from PFALTZ & BAUER, Inc. (Waterbury, CT). PE hydrochloride was purchased from MP Biomedicals, LLC. (Solon, Ohio).

Acetonitrile was purchased from Avantor Performance Materials, Inc. (Center Valley, PA). Formic acid was purchased from Fisher Scientific (Fair Lawn, NJ).

5.2.2 Apparatus

Pursuit 3 PFP column (50 × 2.0 mm, 3 μm) was purchased from Agilent Technologies (Fort Worth, Texas). Pinnacle CN column (50 × 2.1 mm, 5 μm) was purchased from Restek (Bellefonte, PA).

The chromatographic experiments were conducted by two HPLC systems including Shimadzu HPLC system with controller SCL-10Avp, delivery pumps LC 10ADvp, solvent degasser DGU14A (Shimadzu, Kyoto, Japan) and Acquity UPLC system (Waters Corporation, Milford, MA). The column switching technique was achieved by a 10-port Cheminert switching valve and a microelectric actuator (Valco Instruments Co. Inc., Houston, TX).

API4000 Q TRAP MS (Applied Biosystems Sciex, Concord, Canada) with turbo ESI source was utilized in negative ion mode for determining the concentrations of PE metabolites and positive ion mode for determining the concentration of PE by mode transition within the same run. Analyst software, Version 1.5 was used for data collection and processing.

5.2.3 Application of the Preliminary LC-MS/MS Method

The preliminary LC-MS/MS method was applied to detect the formation of PE sulfate in inhibition study with LS180 cell model, which has been discussed in Chapter 3. Briefly, LS180 cells were incubated with 0.5 mL DMEM containing 1% non-essential amino acid (pH 7.4) with PE (50 μ M) /inhibitor (100 μ M) for 18.5 hrs at 37 °C with 5% CO₂. For the combination of curcumin, pterostilbene, resveratrol, and zingerone, four compounds were all at the concentration of 50 μ M. After incubation, the extracellular buffer was collected. The cell extraction of metabolites was carried out with 1 mL methanol. Cells were scraped and collected in centrifuge tubes. The suspension was vortexed for 2 - 3 min and centrifuged at 13000 rpm for 5 min at room temperature. Supernatant (800 μ L) was collected. Each well in the plate was washed with 1 mL methanol twice. The washing solution was collected with the supernatant and dried in vacuum concentrator. The residue was re-suspended in 35 μ L water. The samples from the extracellular buffer and cell lysate were analyzed by the preliminary LC-MS/MS method.

5.2.4 LC-MS/MS Method Development

The preliminary LC-MS/MS method could detect PE metabolites (PE sulfate and 3-hydroxymandelic acid) but not the parent compound (PE). An LC-MS/MS method for simultaneous analysis of PE and its metabolites (PE sulfate and 3-hydroxymandelic acid) with internal standard was developed later by column switching technique (shown in **Figure 5.1**). The PFP column (60 °C) was used as a loading column to desalt the samples followed by the separation on a CN column (40 °C) with gradient elution, which allowed ionization of PE metabolites and PE under negative/positive ion mode. The internal standards (I.S.) were homovanillic acid and ET for negative and positive ion mode, respectively, with structures shown in **Figure 5.2**. The volume of the samples injected by Waters Acquity UPLC system was

25 μ L. In the first 0.5 min, the mobile phase (0.4 mL/min, 0.1% formic acid in water) was delivered by the loading pump through the loading column and directly went to the waste to remove the salts in the samples (solid line in **Figure 5.1**). After 0.5 min, the analytical column was connected to the loading column by the 10-port cheminert switching valve and microelectric actuator. The eluting pump in the Shimadzu HPLC system delivered the mobile phase (0.5 mL/min, A: 0.1% formic acid in water, B: 0.1% formic acid in acetonitrile) through the loading column followed by the analytical column and finally went to the API4000 Q TRAP MS for determination of PE metabolites and PE (dash line in **Figure 5.1**). The gradient curve for elution is shown in **Figure 5.3** with the description of the method in **Table 5.1**. The mobile phase B was 0% at the beginning and increased to 30% at 1 min, which was maintained until 2.2 min. The mobile phase B was then increased to 90% from 2.2 min to 3.5 min and maintained at 90% until 5 min. From 5 min to 5.1 min, the mobile phase B was decreased to 0% and maintained until 8 min.

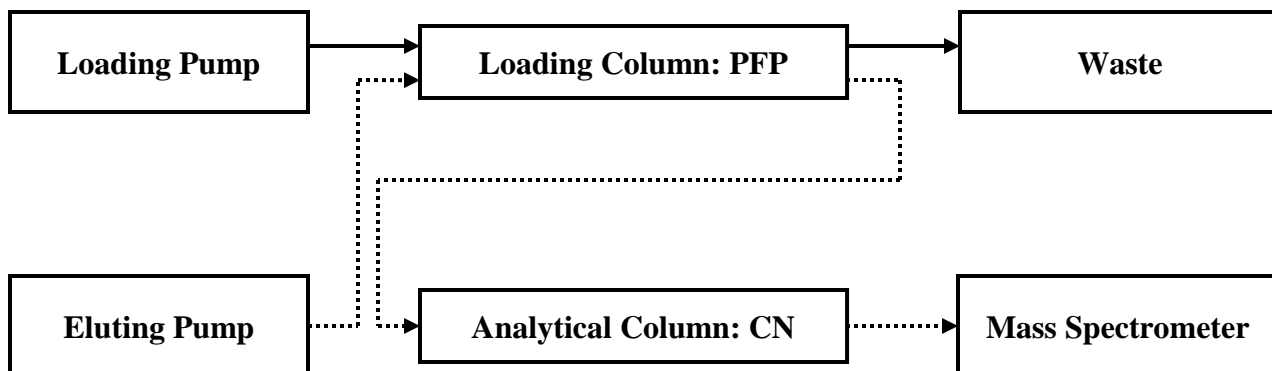


Figure 5.1. Column Switching Technique for LC-MS/MS Method

PFP: pentafluorophenyl column; CN: cyano column. In the first 0.5 min, the mobile phase was delivered by the loading pump through the loading column and directly went to the waste (solid line). After 0.5 min, the eluting pump delivered the mobile phase through the loading column followed by the analytical column and finally went to the MS (dash line).

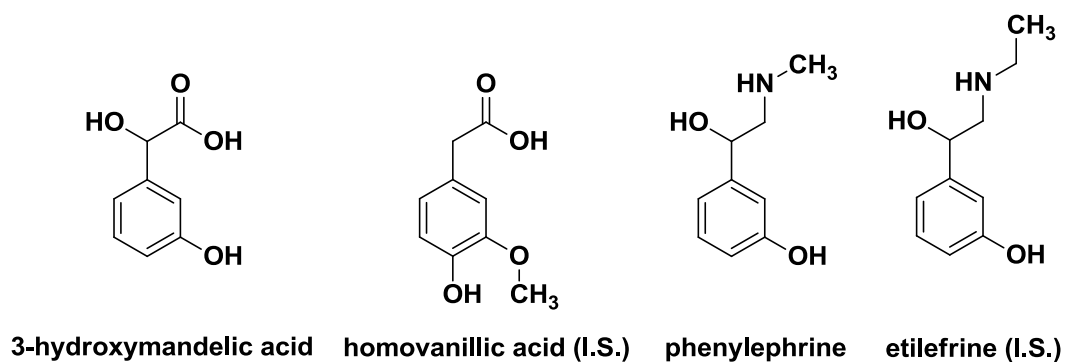


Figure 5.2. Structures of Internal Standards for 3-Hydroxymandelic Acid and Phenylephrine

Homovanillic acid is the internal standard for 3-hydroxymandelic acid. ET is the internal standard for PE.

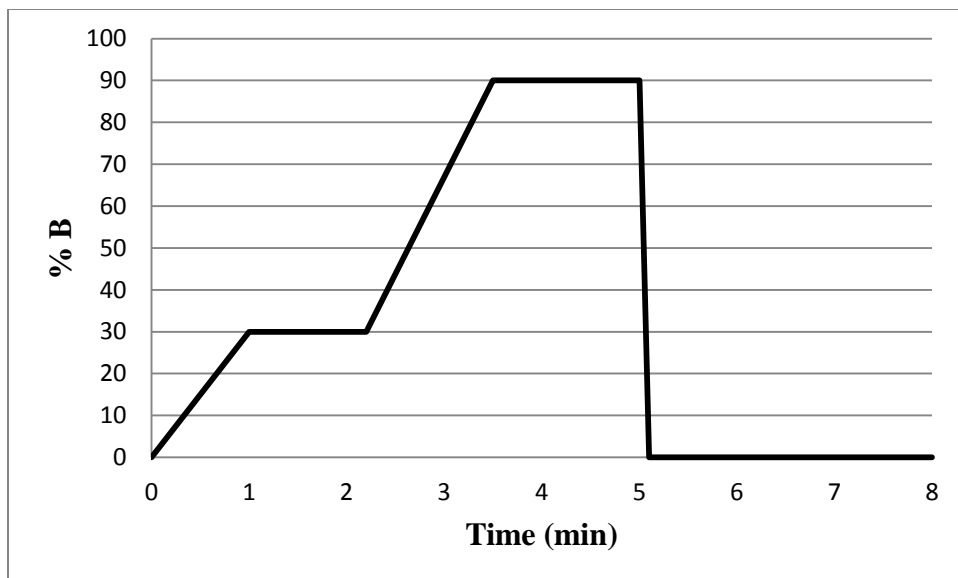


Figure 5.3. Gradient Curve for LC Method

This curve shows the gradient elution based on the percentage of mobile phase B (0.1% formic acid in acetonitrile).

Table 5.1. Gradient Elution for LC Method

Time (min)	A: 0.1% Formic Acid in Water (%)	B: 0.1% Formic Acid in Acetonitrile (%)
0.0	100	0
1.0	70	30
2.2	70	30
3.5	10	90
5.0	10	90
5.1	100	0
8.0	100	0

The API4000 Q TRAP MS was used for determination of PE metabolites and the parent compound. The ion source temperature was set at 450 °C. The ion transfer voltage was set to 4500 V. The curtain gas, ion source gas 1, and ion source gas 2 were 20, 50, 23, respectively, in arbitrary unit. Tuning was carried out to determine the multiple reaction monitoring (MRM) transitions for PE and its metabolites as well as their internal standards, which are listed in **Table 5.2**. The MS parameters were individually optimized for each analyte including declustering potential (DP), entrance potential (EP), collision energy (CE) and collision cell exit potential (CXP), which are listed in **Table 5.3**. After PE metabolites (PE sulfate and 3-hydroxymandelic acid) and internal standard (homovanillic acid) were eluted under the detection by the negative ion mode, the transition was made to the positive ion mode to facilitate the detection of PE and its internal standard. The retention time for PE metabolites and PE is listed in **Table 5.2**. The representative chromatography of PE metabolites and PE as well as their internal standards dissolved in mobile phase are shown in **Figure 5.4** (negative ion mode) and **Figure 5.5** (positive ion mode).

Table 5.2. MRM Transitions for PE Metabolites, PE and their Internal Standards

Analyte	Retention Time (min)	MRM Transitions (Parent ion → Product ions)
PE sulfate	1.39	246.0 → 166.0, 121.0, 93.0
3-Hydroxymandelic acid	1.49	166.9 → 121.0, 93.2
Homovanillic acid (I.S.)	1.90	181.0 → 137.0, 122.0
PE	2.41	168.0 → 150.2, 135.0
ET (I.S.)	2.64	182.0 → 135.2, 109.1

MRM: multiple reaction monitoring.

Table 5.3. Optimized Mass Spectrometer Parameters

Analyte	DP (V)	EP (V)	CE (V)	CXP (V)
PE sulfate	-123	-10	-45	-10
3-Hydroxymandelic acid	-123	-10	-45	-10
Homovanillic acid (I.S.)	-53	-10	-22	-10
PE	123	10	26	10
ET (I.S.)	123	10	33	10

DP: declustering potential; EP: entrance potential; CE: collision energy; CXP: collision cell exit potential.

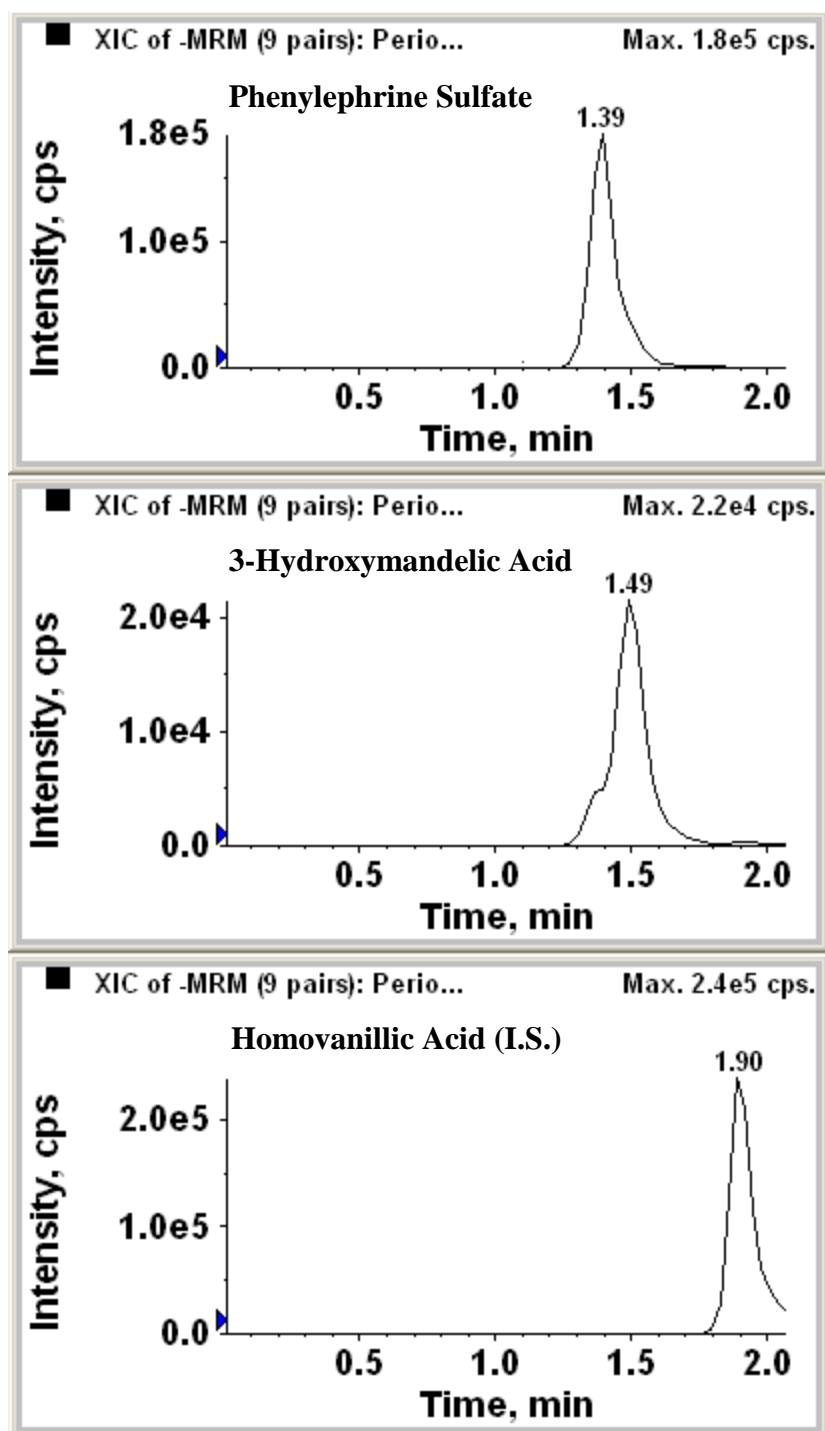


Figure 5.4. Representative Chromatograph of Phenylephrine Sulfate, 3-Hydroxymandelic Acid, and Homovanillic Acid (I.S.) in Negative Ion Mode

The peaks and retention time are shown in this figure for PE metabolites (PE sulfate and 3-hydroxymandelic acid) and internal standard (homovanillic acid) under negative ion mode.

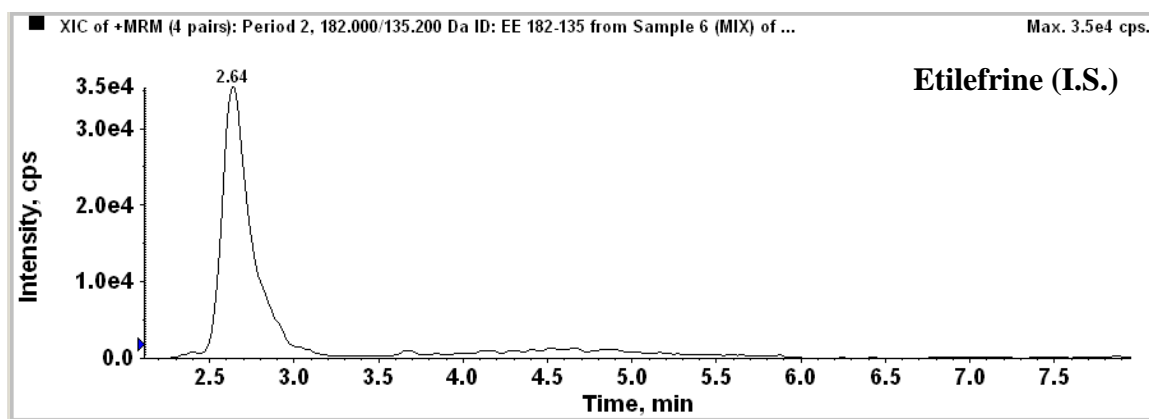
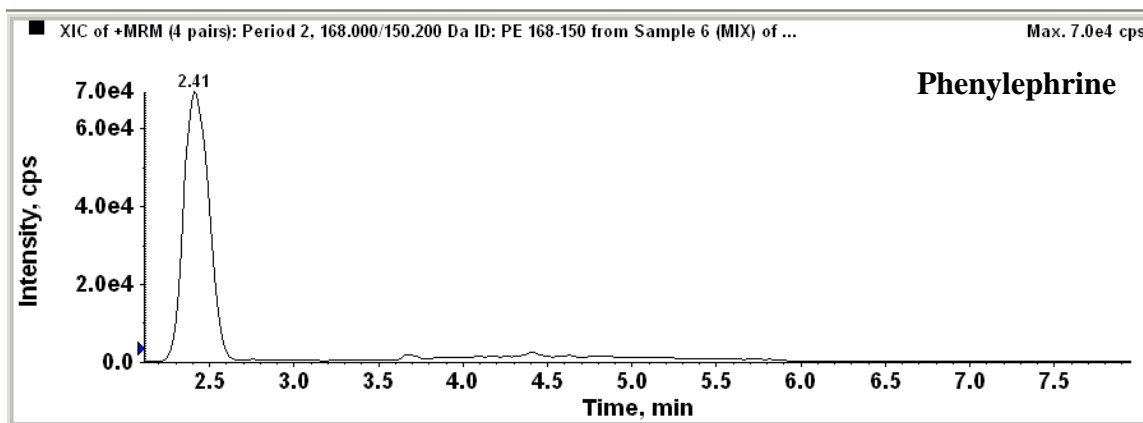


Figure 5.5. Representative Chromatograph of Phenylephrine and Etilefrine (I.S.) in Positive Ion Mode

The peaks and retention time are shown in this figure for PE and its internal standard (ET) under positive ion mode.

5.3 RESULTS AND DISCUSSION

From the preliminary LC-MS/MS data of the study in LS180 cell model, the formation of 3-hydroxymandelic acid was not detected but sulfation of PE was readily apparent when PE was incubated with LS180 cells. The phenolic dietary compounds showing inhibitory effects on disappearance of PE probably inhibited the sulfation of PE in LS180 cells. PE sulfate formation was inhibited by $67.0 \pm 4.2\%$ (mean \pm SEM, as % of control) with guaiacol and by $71.7 \pm 2.6\%$ with pterostilbene + zingerone. The combinations of curcumin + resveratrol and curcumin + pterostilbene + resveratrol + zingerone inhibited $\geq 99\%$ of PE sulfate formation (shown in **Table 5.4**). These results were consistent with those from analysis of the disappearance of PE in LS180 cells (shown in **Table 5.5**).

Table 5.4. Inhibition of Phenylephrine Sulfate Formation with Dietary Compounds in LS180 Cells

Compound	Inhibition of PE Sulfate Formation (as % of control)	SEM
*Guaiacol	67.0%	4.2%
*Curcumin + Resveratrol	99.9%	-
*Pterostilbene + Zingerone	71.7%	2.6%
*Curcumin + Pterostilbene + Resveratrol + Zingerone	99.3%	-

Table 5.5. Comparison of Phenylephrine Disappearance and Sulfate Formation with Dietary Compounds in LS180 Cells

Compound	Extent of PE Disappearance (as % of control)	PE Sulfate Formation (as % of control)
*Guaiacol	51.3%	33.0%
*Curcumin + Resveratrol	0.0%	0.0795%
*Pterostilbene + Zingerone	36.5%	28.3%
*Curcumin + Pterostilbene + Resveratrol + Zingerone	0.0%	0.688%

The LC-MS/MS method for determination of PE has been reported in the literature as well as some methods for determination of compounds with structural similarity to PE and their metabolites [154-160]. It was the first time that an LC-MS/MS method was developed for simultaneously quantitating PE and its metabolites (PE sulfate and 3-hydroxymandelic acid). Many difficulties occurred during this method development, including sample preparation, column selection, and mobile phase modification, as described below.

Sample preparation for analysis of PE and its metabolites was more complicated than for analysis of PE alone. Solid-phase extraction (Waters Oasis WCX cartridge) was successfully utilized to clean the plasma samples for analysis of PE alone. The solid phase is in a mixed mode with both weak cation-exchanger and reversed-phase resin. The carboxylic-acid-cation-exchanger bound to the reversed phase selectively retains basic compounds. In addition, the reversed-phase interaction also helps with the retention. The procedure of the extraction was uncomplicated. The cartridge was conditioned with 3 mL methanol followed by 3 mL water. The plasma, spiked with PE, was loaded into the cartridge. The cartridge was washed with 3 mL water. Finally, PE was eluted by 500 μ L 2% trifluoroacetic acid in methanol and water (80 : 20) three times. The recovery yield was 91% and 87% for 100 ng/mL and 10 ng/mL PE in plasma, respectively. The phenyl cartridges were also tested for PE plasma samples, which could not retain PE. Obviously the WCX cartridge is not suitable for the extraction of PE sulfate and 3-hydroxymandelic acid due to their anionic nature. For simultaneous detection of PE and its metabolites, in the same run, solid-phase extraction may not work. Liquid-liquid extraction is not a good option for ionized hydrophilic compounds.

In this study, on-line clean up was used for sample preparation. The challenge was the selection of the loading column that would have retention for all the analytes. Many types of

columns were tested to see whether they can retain PE and its metabolites. Most reversed-phase columns such as C18, C8, phenyl columns had almost no retention for PE sulfate. The peak shape of PE on HILIC column was very broad with a peak width of about 1 min. Hypercarb column also gave very broad peaks. According to the literature, Hypercarb column in long-term use has the potential of oxidizing analytes, which is another disadvantage of this type of column [161]. The graphite material of the column can be oxidized by an oxidizer in mobile phase. The oxidized column then causes the oxidation of analytes [161]. PE as an analyte may be easily oxidized by the column. The normal-phase silica column was also tried and showed no retention for PE sulfate and 3-hydroxymandelic acid with 5% water in organic solvent, which was probably due to dissolution of silica in the presence of water. PFP was eventually selected as the loading column after many trials on other columns because of the good retention on this column.

As the analytical column, good separation for PE and its metabolites was required to ensure the detection of PE under positive ion mode and PE metabolites under negative ion mode. Among all the columns tested in this study, the CN column had the best separation for PE and its metabolites, which was applied as the analytical column.

For the HPLC method of PE, 6.5 mM triethylamine and 13 mM trifluoroacetic acid were used as the mobile phase modifier in aqueous phase. Trifluoroacetic acid can act as an ion-pairing agent at its high concentration, which can improve PE retention. Triethylamine as an additive can fix the tailing problem of PE on the column. The reason for the peak tailing could be that metals like sodium and potassium bound to silanol, exchange with ionized basic analytes at low pH. Excess triethylamine in the mobile phase could replace the metals instead of basic analytes. Therefore, triethylamine can reduce the peak tailing [162]. Triethylamine and trifluoroacetic acid can lead to ion suppression in MS. Therefore, they could not be used as the

mobile phase modifier in LC-MS/MS method. Instead, the volatile formic acid was used in the mobile phase for the LC-MS/MS method. As seen in **Figure 5.4** and **Figure 5.5**, the peaks for PE and its metabolites were relatively sharp and symmetrical.

A preliminary LC-MS/MS assay was developed, overcoming significant challenges of low retention, low resolution, and differing ionic detection modes for three compounds including PE (cationic), 3-hydroxymandelic acid (anionic), and PE sulfate (zwitterionic). Further studies on factors such as matrix effect, LLOQ, accuracy, precision, recovery, stability are necessary for the complete LC-MS/MS method validation.

CHAPTER 6

THE EFFECT OF POTENTIAL INHIBITORS ON MONOAMINE OXIDASE A/B ACTIVITY

6.1 INTRODUCTION

The drug-drug interactions between many oral sympathomimetic amines and MAO inhibitors have been well studied in the literature. The most common adverse effect is high blood pressure. Other adverse effects include headache, chest pain, cardiac arrhythmias, circulation insufficiency, etc [15]. The mechanism of the interaction is that MAO inhibitors inhibit pre-systemic and systemic metabolism of some sympathomimetic amines, which are substrates for MAO, resulting in the elevated level of these sympathomimetic amines in circulation [15].

Sympathomimetic amines can be divided into two types: direct and indirect acting amines. Indirect acting sympathomimetic amines stimulate the release of noradrenaline from the storage in the sympathetic nerve terminals to interact with postsynaptic adrenergic receptors. MAO inhibitors can increase the level of noradrenaline stored in the nerve terminals. These effects from sympathomimetic amines and MAO inhibitors cause the adverse interaction [15, 163]. Direct acting sympathomimetic amines bind directly to adrenergic receptors. Elimination of these direct acting sympathomimetics from interacting with adrenergic receptors occurs via metabolism by MAO and catechol-O-methyl transferase, and reuptake into presynaptic neurons.

Therefore, MAO inhibitors can affect indirectly acting sympathomimetic amines more than directly acting sympathomimetic amines such as PE [163].

Hypertensive crises were observed when phenylpropanolamine (50 mg) was orally administered to subject who had been treated with MAO inhibitor tranylcypromine (30 mg) for 20 - 30 days [164]. A woman who was on phenelzine (15 mg) for three months suffered severe headache and had dramatic rise in blood pressure after she took oral phenylpropanolamine (32 mg) [165]. A similar adverse effect occurred in a man on MAO inhibitor therapy when taking an appetite suppressant containing phenylpropanolamine [166]. An increase in blood pressure was observed when oral ephedrine was given to healthy subjects during the treatment with tranylcypromine as compared to that before the treatment [167].

The interaction between PE and MAO inhibitors has been reported in the literature. When PE (45 mg) was administered orally to human subjects together with the MAO inhibitor phenelzine or tranylcypromine, blood pressure was quickly and dramatically elevated, compared to the baseline. As a result, an α -adrenergic receptor blocking drug, phentolamine, had to be given intravenously to reverse hypertension [167].

Besides drug-drug interactions, certain food that contains substrates of MAO or MAO inhibitors may also cause the adverse effects with the interaction of oral sympathomimetic amines. The mechanism is similar as described above for the interaction of sympathomimetic amines and MAO inhibitors. The hypertensive effect has been reported with the food-drug interaction of pargyline and broad beans containing dopa [168]. The interaction between MAO inhibitors and tyramine in cheese and yeast causes severe hypertensive crises which has been found in many patients [169].

Some phenolic dietary compounds are not substrates for MAO, but they have inhibitory effects on MAO, such as curcumin, eugenol, piperine, quercetin, and resveratrol [170-175]. Curcumin inhibits both MAO-A and MAO-B in mouse brain after p.o. administration [170]. Piperine and paeonol are reversible inhibitors for both MAO-A and MAO-B in rat brain. The mode of inhibition with piperine on MAO-A and MAO-B is mixed and competitive inhibition, giving K_i values of 35.8 μM and 79.9 μM , respectively [172]. Paeonol has K_i values of 51.1 μM and 38.2 μM on MAO-A and MAO-B with non-competitive and competitive inhibition, respectively [172]. Emodin shows mixed mode inhibition on MAO-B with K_i value of 15.1 μM in rat brain [172]. Quercetin inhibits MAO-A activity in mouse brain [173, 174]. Resveratrol is a potent inhibitor of MAO-A in rat brain with IC_{50} and K_i of 2 μM and 2.5 μM , respectively [175]. Eugenol can competitively inhibit both human recombinant MAO-A and MAO-B with K_i of 26 μM and 211 μM [171]. These phenolic compounds all lack amine groups and therefore MAO inhibition is unexpected and not immediately explained.

The co-administration of sympathomimetic amines with MAO inhibitors may have severe or even fatal adverse effects. Some phenolic dietary compounds have been proven to be inhibitors of MAO-A, MAO-B or both of them. It is necessary to evaluate the inhibitory effects of the potential inhibitors for PE sulfation screened from LS180 cell model on MAO-A and MAO-B. However, the oxidative deamination of PE is followed by oxidation mediated by ALDH, resulting in formation of 3-hydroxymandelic acid as the terminal product of the two sequential enzymatic reactions. The intermediate after the first oxidative deamination reaction is not commercially available, which restricts the investigation of the inhibitory effects of phenolic dietary compounds on oxidative deamination of PE. Instead, the typical substrate of MAO-A and MAO-B, kynuramine, was used to test if these phenolic compounds can inhibit MAO-A or

MAO-B because the metabolite of kynuramine (3-(2-aminophenyl)-3-oxo-propionaldehyde) rapidly and spontaneously rearranges (by the Schiff base reaction) to the commercially available 4-hydroxyquinoline (shown in **Figure 6.1**), which has strong FLU for sensitive detection [14].

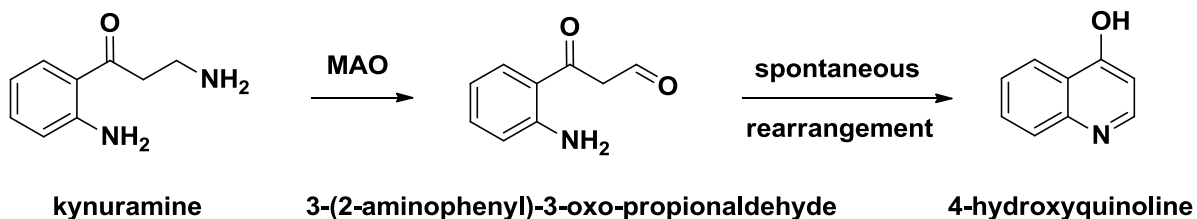


Figure 6.1. Kynuramine Converted to 4-Hydroxyquinoline via 3-(2-Aminophenyl)-3-oxo-propionaldehyde

6.2 MATERIALS AND METHODS

6.2.1 Chemicals and Reagents

Curcumin (mixture of curcumin, demethoxycurcumin and bisdemethoxycurcumin) was purchased from Acros Organics (New Jersey, USA). Guaiacol and isoeugenol were purchased from TCI America (Portland, OR). 4-Hydroxyquinoline and zingerone were purchased from Alfa Aesar (Heysham, Lancs, England). Kynuramine dihydrobromide was purchased from Sigma-Aldrich (St. Louis, MO). Pterostilbene was purchased from ChromaDex (Irvine, CA). Resveratrol was purchased from Beta Pharma, Inc. (New Haven, CT).

Acetonitrile was purchased from Avantor Performance Materials, Inc. (Center Valley, PA). Dimethyl sulfoxide, perchloric acid (70%), sodium hydroxide, and triethylamine were purchased from Fisher Scientific (Fair Lawn, NJ). Potassium phosphate monobasic was purchased from Sigma (St. Louis, MO). Potassium phosphate dibasic was purchased from J.T.Baker (Phillipsburg, NJ). Trifluoroacetic acid was purchased from Alfa Aesar (Ward Hill, MA).

Human recombinant MAO-A, MAO-B and the control were purchased from BD Biosciences (San Jose, CA).

6.2.2 Apparatus

The chromatographic experiments were conducted by HPLC systems including Waters 2695 separation module, Waters 2487 dual λ absorbance detector, and Waters 2475 multi λ FLU detector (Waters Corporation, Milford, MA).

6.2.3 HPLC Method for Kynuramine and 4-Hydroxyquinoline

6.2.3.1 Chromatographic Conditions and Detection

The HPLC method was developed to simultaneously detect and quantify kynuramine and 4-hydroxyquinoline to monitor the enzymatic reaction of human recombinant MAO-A/B. A C18 column (100 \times 4.6 mm, 3 μ m, 30 $^{\circ}$ C) was used to separate kynuramine and 4-hydroxyquinoline at a flow rate of 1 mL/min. The gradient elution was applied with 6.5 mM triethylamine and 13 mM trifluoroacetic acid in water as mobile phase A and acetonitrile as mobile phase B (shown in **Table 6.1**). Kynuramine was detected by UV at 364 nm, and 4-hydroxyquinoline was detected by FLU (excitation 316 nm, emission 357 nm).

Table 6.1. Gradient Elution for Kynuramine and 4-Hydroxyquinoline

Time (min)	Mobile Phase A (%)	Mobile Phase B (%)
0	90	10
1	90	10
5	50	50
7	90	10
8	90	10

In the inhibition studies with phenolic dietary compounds, the HPLC method had to be modified to separate the phenolic compounds from kynuramine and 4-hydroxyquinoline to avoid interference, due to their FLU. When doing inhibition studies with guaiacol, the gradient method

was modified as follows: 10% B in A was maintained for 1 min and then the mobile phase B was increased to 50% in 4 min. After kynuramine and 4-hydroxyquinoline were eluted successfully, the mobile phase B was decreased to the original 10% in 2 min and maintained for 5 min. When doing inhibition studies with isoeugenol, pterostilbene, and zingerone, the gradient method was modified as follows: 10% B in A was maintained for 1 min and then the mobile phase B was increased to 50% in 4 min. The mobile phase B was further increased to 90% in 2 min and maintained for 2 min. After all the compounds were eluted successfully, the mobile phase B was decreased to the original 10% in 2 min and maintained for 4 min. The HPLC method modification did not change the retention time and the peak shape of kynuramine and 4-hydroxyquinoline. It helped the elution of the phenolic dietary compounds after kynuramine and 4-hydroxyquinoline to avoid interference in the following runs. The extension in run time was not expected to affect validation parameters.

6.2.3.2 Stock Solution Preparation

The reference standards of kynuramine and 4-hydroxyquinoline were dissolved in DMSO to obtain stock solution with a concentration of 50 mM and 200 mM, respectively. Further stock solutions were prepared by diluting the stock solution with DMSO. All the stock solutions were stored at -80 °C and protected from the light.

6.2.3.3 Preparation of Standard Curves and Quality Controls

The matrix solution was made by mixing MAO (0.01 mg/mL) in potassium phosphate buffer (100 mM, pH 7.4), 2 N NaOH, and 70% perchloric acid in the ratio of 8:3:1. Standard curves were prepared freshly by spiking the stock solutions in the prepared matrix solution with a concentration range of 2.00 - 1.00×10^3 μ M for kynuramine and 0.050 - 30 μ M for 4-hydroxyquinoline, which covered the concentrations in the samples.

The quality controls were prepared freshly by spiking the stock solutions in the prepared matrix solution with LLOQ (2.00 μM for kynuramine and 0.050 μM for 4-hydroxyquinoline), low quality control (10.0 μM for kynuramine and 0.25 μM for 4-hydroxyquinoline), medium quality control (300 μM for kynuramine and 7.5 μM for 4-hydroxyquinoline), high quality control (600 μM for kynuramine and 15 μM for 4-hydroxyquinoline).

6.2.3.4 Sample Preparation

For standards curves and quality controls, samples were vortexed and centrifuged for 5 min at $10,000 \times g$. The supernatant was taken and transferred to an autosampler vial. The volume injected into the HPLC was 100 μL .

For samples after the enzymatic reaction, 2 N NaOH (75 μL) was added into the reaction mixture and followed by 70% perchloric acid (25 μL) to stop the reaction as well as precipitate the protein. Then the samples were vortexed and centrifuged for 5 min at $10,000 \times g$. The supernatant was taken and transferred to an autosampler vial. The volume injected into the HPLC was 100 μL .

6.2.3.5 Method Validation

The linearity of standard curves was determined by GraphPad Prism 5 using a simple linear model without y-intercept or first-order polynomial (straight line). r^2 was obtained from the fitting and was required to be larger than 0.99.

The LLOQ was determined with the criterion that the signal to noise ratio was 10:1 when compared to blank samples from matrix.

For determination of intra-assay accuracy and precision, the quality control samples at LLOQ, low, medium, and high concentrations were assayed six times within the same run.

For determination of inter-assay accuracy and precision, the quality control samples at LLOQ, low, medium, and high concentrations were assayed six times in three separate runs.

The recoveries were determined as follows: the quality control samples at LLOQ, low, medium, and high concentrations were compared with the samples spiked at the same final concentrations after sample preparation. Each concentration was assayed three times.

For sample processing stability, the quality control samples at LLOQ, low, medium, and high concentrations were prepared and kept in the autosampler at 4 °C for 40 hrs and then injected into the HPLC for analysis. Each concentration was assayed six times. The criterion for stability was the detected concentrations of the quality control samples should be less than 15% change of the nominal spiked concentrations for low, medium, and high concentrations. For LLOQ, the detected concentration of the quality control sample should be less than 20% change of the nominal spiked concentrations.

6.2.4 Preliminary Studies

Time-dependent and MAO concentration-dependent studies were conducted to optimize the enzyme kinetic assay for kynuramine with MAO-A and MAO-B. Briefly, kynuramine (11.11 μM) in 180 μL potassium phosphate buffer (100 mM, pH 7.4) was made from the stock solution in DMSO and pre-warmed for 5 min before initiation of the enzymatic reaction. The DMSO concentration in the final reaction buffer was less 0.5%. After pre-incubation, MAO-A/B (0.1 mg/mL) in 20 μL potassium phosphate buffer (100 mM, pH 7.4) was added and mixed with the kynuramine solution to initiate the reaction. The final concentration of kynuramine and MAO-A/B was 10 μM and 0.01 mg/mL in 200 μL reaction solution for the time-dependent study. The enzymatic reaction was stopped by 2 N NaOH (75 μL) followed with 70% perchloric acid (25 μL) at incubation times of 10, 20, 30, 40, and 60 min. The samples were vortexed and

centrifuged for 5 min at $10000 \times g$. The supernatant was taken and injected to the HPLC with the method discussed above. For assessment of protein concentration-dependence, the same concentration of kynuramine ($11.11 \mu\text{M}$) was prepared in $180 \mu\text{L}$ potassium phosphate buffer (100 mM , $\text{pH } 7.4$) and pre-warmed for 5 min. Various MAO concentrations (0.03 , 0.1 , 0.3 mg/mL) in $20 \mu\text{L}$ potassium phosphate buffer (100 mM , $\text{pH } 7.4$) were added and the total protein concentration was kept constant at 0.3 mg/mL by standardizing with the MAO control. The incubation time was 15 min, which was selected based on the results from the time-dependent study that are discussed below in the result section. The experiments were conducted six times.

6.2.5 Optimized Enzyme Kinetic Assay and K_m Determination

The optimized incubation time and MAO concentration were selected in the linear range from the time-dependent and MAO concentration-dependent studies, as shown below. The final concentration of MAO in the reaction solution was 0.01 mg/mL . The incubation time was 15 min. In the optimized condition, the concentration-dependent study for kynuramine metabolism with MAO-A/B was carried out at the final concentrations of 2 , 5 , 10 , 25 , 50 , 100 , 250 , $500 \mu\text{M}$. The procedure of the assay was exactly the same as described above. The experiments were conducted three times in triplicate. GraphPad Prism 5 was applied to fit a Michaelis-Menten model to the data to obtain the K_m value.

6.2.6 Inhibition Screening and IC_{50} Determination

According to the K_m value determined in the experiment described above, the final concentration of kynuramine was set at $10 \mu\text{M}$ for the inhibition assay, which was less than the K_m values for MAO-A and MAO-B. The incubation time was 15 min and MAO concentration was 0.01 mg/mL . For the inhibition screening with phenolic dietary compounds, the concentrations of the compounds were determined by comparing their solubility ($25 \text{ }^\circ\text{C}$, $\text{pH } 7$)

and maximum single dose concentration, which are listed in **Table 6.2**. If the concentration calculated from the maximum single dose in 250 mL water (recommended by FDA) is larger than the solubility of the compound, the solubility would be used to test the inhibitory effects on MAO-A/B. These concentrations mimicking the maximal GI concentrations are the possible maximum concentrations of these phenolic compounds to interact with MAO. Due to the low oral bioavailability of these compounds, the systemic concentrations of these compounds would be much lower than the maximal GI concentrations, resulting in less inhibitory effects on MAO. The concentration used to screen the inhibitors of MAO-A/B for curcumin, guaiacol, isoeugenol, pterostilbene, resveratrol, and zingerone was 140, 435, 110, 270, 94, and 51 μM , respectively. The experiments were conducted six times. The data were processed with GraphPad Prism 5. Significant differences between control and treated group were determined by a one-way ANOVA followed by Dunnett's *post hoc* test ($p < 0.05$). If the compounds at these concentrations significantly decrease the formation of 4-hydroxyquinoline, further studies would be accomplished to determine their IC_{50} for the inhibition of MAO-A/B.

The condition of the IC_{50} study was incubation of kynuramine (10 μM) and a broad concentration range of inhibitors with MAO-A/B (0.01 mg/mL) for 15 min. For MAO-A, the concentration range is listed as follows and shown in **Figure 6.10**: curcumin 0.0001 - 100 μM , guaiacol 0.1 - 1800 μM , isoeugenol 0.0001 - 100 μM , pterostilbene 0.001 - 250 μM , resveratrol 0.001 - 90 μM , and zingerone 0.0001 - 400 μM . For MAO-B, the concentration range is listed as follows and shown in **Figure 6.11**: curcumin 0.001 - 100 μM , guaiacol 0.001 - 2400 μM , isoeugenol 0.001 - 1000 μM , pterostilbene 0.00001 - 100 μM , and resveratrol 0.01 - 90 μM . The procedure was exactly the same as described above. The experiments were conducted six times.

GraphPad Prism 5 was applied to fit the data to obtain IC₅₀ values by using the concentration-response equation as follows:

$$\frac{v_i}{v_0} = \frac{1}{1 + 10^{((\text{Log}[I] - \text{LogIC}_{50}) \times \text{Hill Coefficient})}}$$

This equation includes the Hill coefficient as the parameter and could help to characterize the inhibition.

If the 95% confidence interval of the Hill coefficient did include 1, the concentration-response equation with the Hill coefficient fixed at 1 was used to fit the data again by the following equation:

$$\frac{v_i}{v_0} = \frac{1}{1 + 10^{(\text{Log}[I] - \text{LogIC}_{50})}}$$

Table 6.2. Solubility and Maximum Single Dose of Phenolic Dietary Compounds

Phenolic Dietary Compound	Solubility (μM, 25 °C, pH 7)	Maximum Single Dose (mg)	Maximum Single Dose Concentration (μM)	Relevant GI Concentration (μM)
Curcumin	1.4E2	140	1520	140
Guaiacol	8.6E4	54	1740	1740
Isoeugenol	7.3E3	18	438	438
Pterostilbene	2.7E2	250	3902	270
Resveratrol	94	83	1455	94
Zingerone	2.4 E4	10	206	206

The calculated solubility values for phenolic dietary compounds are obtained from SciFinder [8]. The maximum single dose for guaiacol is from published papers [94, 95]. Maximum single doses for other phenolic dietary compounds are from FDA's GRAS list, EAFUS, U.S. Federal Regulations, or Fenaroli's handbook of flavor ingredients [98, 176-178].

6.3 RESULTS

6.3.1 HPLC Method Validation

The standard curves for kynuramine were linear from 2.00 to 1.00×10^3 μM with $r^2 > 0.99$.

The standard curves for 4-hydroxyquinoline were linear from 0.050 to 30 μM with $r^2 > 0.99$.

The LLOQ for kynuramine and 4-hydroxyquinoline were 2.00 μM and 0.050 μM , respectively.

The intra-assay accuracy and precision for kynuramine and 4-hydroxyquinoline are listed in **Table 6.3** and **Table 6.4**. The DFN and RSD for LLOQ were within 20%. The DFN and RSD for other quality control concentrations were within 15%.

Table 6.3. Intra-assay Accuracy and Precision for Kynuramine

Kynuramine Concentration (μM)	N	Mean	DFN	RSD
2.00	6	2.01	0.6%	4.1%
10.0	6	10.0	0.0%	0.2%
300	6	304	1.4%	0.2%
600	6	605	0.9%	0.1%

Table 6.4. Intra-assay Accuracy and Precision for 4-Hydroxyquinoline

4-Hydroxyquinoline Concentration (μM)	N	Mean	DFN	RSD
0.050	6	0.058	15.9%	5.0%
0.25	6	0.25	1.1%	0.2%
7.5	6	7.3	-2.1%	0.3%
15	6	14	-3.8%	0.2%

The inter-assay accuracy and precision for kynuramine and 4-hydroxyquinoline are listed in **Table 6.5** and **Table 6.6**. The DFN and RSD for LLOQ were within 20%. The DFN and RSD for other quality control concentrations were within 15%.

Table 6.5. Inter-assay Accuracy and Precision for Kynuramine

Kynuramine Concentration (µM)	N	Day 1	Day 2	Day 3	Mean	DFN	RSD
2.00	6	2.01	2.01	2.00	2.01	0.5%	0.2%
10.0	6	10.0	10.0	10.0	10.0	-0.1%	0.3%
300	6	304	304	305	305	1.5%	0.2%
600	6	605	601	606	604	0.7%	0.5%

Table 6.6. Inter-assay Accuracy and Precision for 4-Hydroxyquinoline

4-Hydroxyquinoline Concentration (µM)	N	Day 1	Day 2	Day 3	Mean	DFN	RSD
0.050	6	0.058	0.058	0.060	0.059	17.2%	1.8%
0.25	6	0.25	0.25	0.26	0.25	1.5%	1.6%
7.5	6	7.3	7.3	7.5	7.4	-1.6%	1.5%
15	6	14	14	15	15	-3.5%	1.9%

The average recoveries for kynuramine at LLOQ, low, medium, and high concentrations were 98.0%, 99.1%, 100.8%, and 100.2%, respectively.

The average recoveries for 4-hydroxyquinoline at LLOQ, low, medium, and high concentrations were 101.8%, 99.8%, 101.1%, and 100.2%, respectively.

The stability tests for kynuramine and 4-hydroxyquinoline in the autosampler at 4 °C for 40 hrs are listed in **Table 6.7** and **Table 6.8**. The DFN and RSD for LLOQ were within 20%. The DFN and RSD for other quality control concentrations were within 15%.

Table 6.7. Sample Processing Stability for Kynuramine

Kynuramine Concentration (µM)	N	Mean	DFN	RSD
2.00	6	1.96	-1.8%	4.5%
10.0	6	10.0	0.1%	0.2%
300	6	305	1.7%	0.1%
600	6	607	1.1%	0.1%

Table 6.8. Sample Processing Stability for 4-Hydroxyquinoline

4-Hydroxyquinoline Concentration (μM)	N	Mean	DFN	RSD
0.050	6	0.059	18.3%	5.2%
0.25	6	0.26	2.2%	0.4%
7.5	6	7.4	-0.9%	0.4%
15	6	15	-2.5%	0.2%

6.3.2 Preliminary Studies

The time-dependent study for oxidative deamination of kynuramine with MAO-A is shown in **Figure 6.2**. Kynuramine (10 μM) was incubated with MAO-A (0.01 mg/mL) in 200 μL potassium phosphate buffer (100 mM, pH 7.4) for 10, 20, 30, 40, and 60 min. The formation of 4-hydroxyquinoline was analyzed after the enzymatic reaction. A simple linear model without y-intercept was used to fit the data with GraphPad Prism 5. The formation of 4-hydroxyquinoline was linear over 60 min with the rate of 3.28 ± 0.09 nmol/mg/min (mean \pm SEM) and $r^2 = 0.9887$. According to the results from this study, the incubation time was selected as 15 min for the following enzymatic assay.

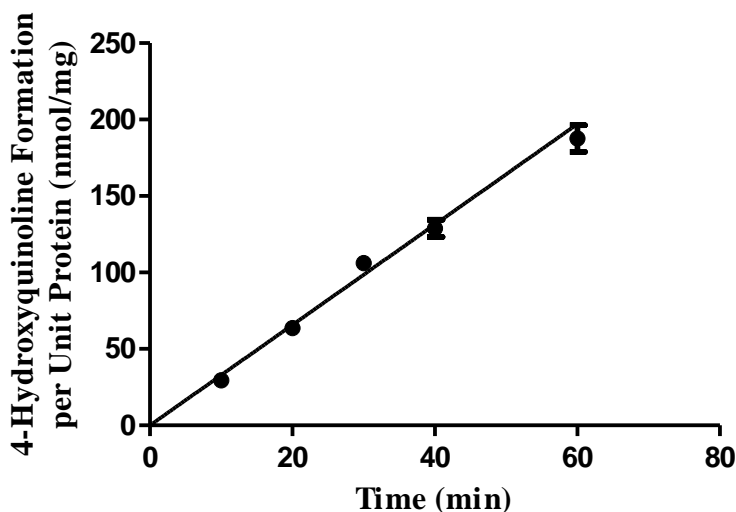


Figure 6.2. Time Dependence for Oxidative Deamination of Kynuramine with MAO-A

Kynuramine (10 μM) was incubated with MAO-A (0.01 mg/mL) for 10, 20, 30, 40, and 60 min. A simple linear model without y-intercept was used to fit the data with GraphPad Prism 5. The formation of 4-hydroxyquinoline per unit protein (expressed as mean \pm SD ($n = 6$) in this figure) was linear over 60 min with the rate of 3.28 ± 0.09 nmol/mg/min (mean \pm SEM) and $r^2 = 0.9887$.

The time-dependent study for oxidative deamination of kynuramine with MAO-B is shown in **Figure 6.3**. Kynuramine (10 μM) was incubated with MAO-B (0.01 mg/mL) in 200 μL potassium phosphate buffer (100 mM, pH 7.4) for 10, 20, 30, 40, and 60 min. The formation of 4-hydroxyquinoline was analyzed after the enzymatic reaction. A simple linear model without y-intercept was used to fit the data with GraphPad Prism 5. The formation of 4-hydroxyquinoline was linear over 60 min with the rate of 2.70 ± 0.07 nmol/mg/min (mean \pm SEM) and $r^2 = 0.9841$. According to the results from this study, the incubation time was selected as 15 min for the following enzymatic assay.

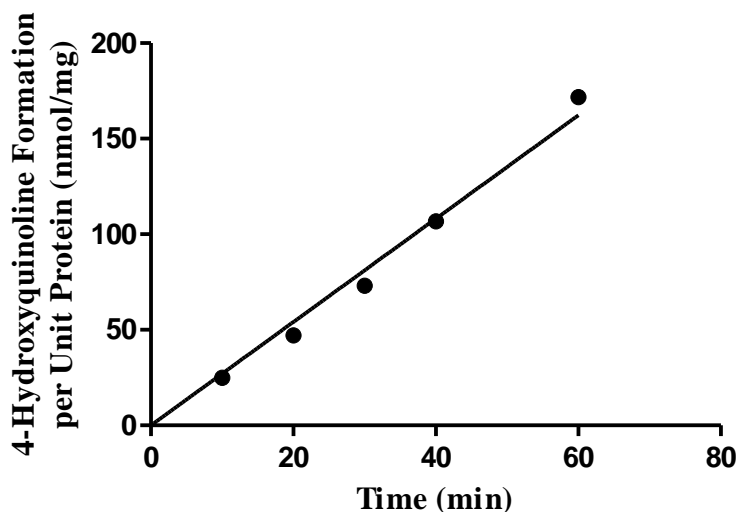


Figure 6.3. Time Dependence for Oxidative Deamination of Kynuramine with MAO-B

Kynuramine (10 μM) was incubated with MAO-B (0.01 mg/mL) for 10, 20, 30, 40, and 60 min. A simple linear model without y-intercept was used to fit the data with GraphPad Prism 5. The formation of 4-hydroxyquinoline per unit protein (expressed as mean \pm SD ($n = 6$) in this figure) was linear over 60 min with the rate of 2.70 ± 0.07 nmol/mg/min (mean \pm SEM) and $r^2 = 0.9841$. The error bar is invisible.

The MAO concentration-dependent study for oxidative deamination of kynuramine with MAO-A is shown in **Figure 6.4**. Kynuramine (10 μM) was incubated with MAO-A (0.003, 0.01, 0.03 mg/mL) in 200 μL potassium phosphate buffer (100 mM, pH 7.4) for 15 min. The total protein concentration was kept constant at 0.03 mg/mL by compensating with the MAO control. The formation of 4-hydroxyquinoline was analyzed after the enzymatic reaction and showed linearity over 0.03 mg/mL MAO-A with the rate of 3.06 ± 0.03 nmol/mg/min (mean \pm SEM) and $r^2 = 0.9970$. According to the results from this study, the MAO-A concentration was selected as 0.01 mg/mL for the following enzymatic assay.

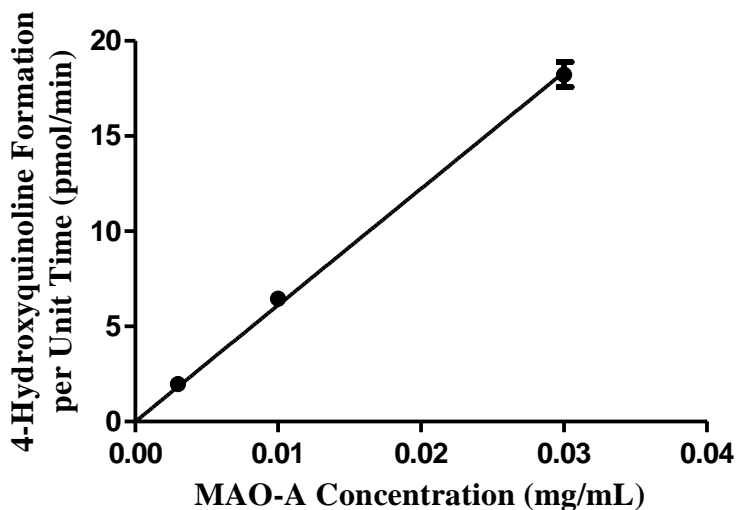


Figure 6.4. MAO Concentration Dependence for Oxidative Deamination of Kynuramine with MAO-A

Kynuramine (10 μ M) was incubated with various concentrations of MAO-A (0.003, 0.01, 0.03 mg/mL). A simple linear model without y-intercept was used to fit the data with GraphPad Prism 5. The formation of 4-hydroxyquinoline per unit time (expressed as mean \pm SD (n = 6) in this figure) was linear over 0.03 mg/mL MAO-A with the rate of 3.06 ± 0.03 nmol/mg/min (mean \pm SEM) and $r^2 = 0.9970$.

The MAO concentration-dependent study for oxidative deamination of kynuramine with MAO-B is shown in **Figure 6.5**. Kynuramine (10 μ M) was incubated with MAO-B (0.003, 0.01, 0.03 mg/mL) in 200 μ L potassium phosphate buffer (100 mM, pH 7.4) for 15 min. The total protein concentration was kept constant at 0.03 mg/mL by compensating with the MAO control. The formation of 4-hydroxyquinoline was analyzed after the enzymatic reaction and showed linearity over 0.03 mg/mL MAO-B with the rate of 3.66 ± 0.08 nmol/mg/min (mean \pm SEM) and $r^2 = 0.9942$. According to the results from this study, the MAO-B concentration was selected as 0.01 mg/mL for the following enzymatic assay.

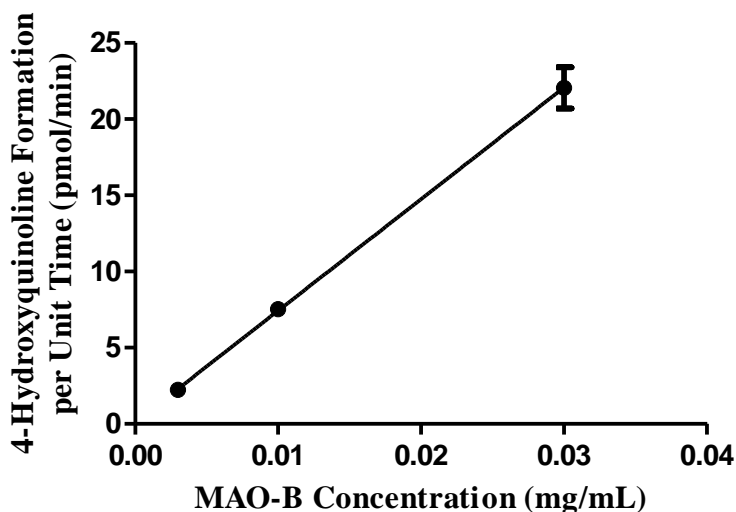


Figure 6.5. MAO Concentration Dependence for Oxidative Deamination of Kynuramine with MAO-B

Kynuramine (10 μM) was incubated with various concentrations of MAO-B (0.003, 0.01, 0.03 mg/mL). First-order polynomial (straight line) was used to fit the data with GraphPad Prism 5. The formation of 4-hydroxyquinoline per unit time (expressed as mean \pm SD ($n = 6$) in this figure) was linear over 0.03 mg/mL MAO-B with the rate of 3.66 ± 0.08 nmol/mg/min (mean \pm SEM) and $r^2 = 0.9942$.

6.3.3 Optimized Enzyme Kinetic Assay and K_m Determination

The concentration dependence for oxidative deamination of kynuramine with MAO-A is shown in **Figure 6.6**. Kynuramine (2, 5, 10, 25, 50, 100, 250, and 500 μM) was incubated in 200 μL potassium phosphate buffer (100 mM, pH 7.4) for 15 min with MAO-A (0.01 mg/mL). The Michaelis-Menten model was used to fit the data by GraphPad Prism 5. The experiments were conducted 3 times in triplicate. The graph is a single representative experiment. The K_m and V_{max} were 23.1 ± 0.8 μM and 10.2 ± 0.2 nmol/min/mg (mean \pm SEM), respectively. From these data, the concentration of kynuramine was set at 10 μM for the following inhibition study so that kynuramine concentration was $< K_m$.

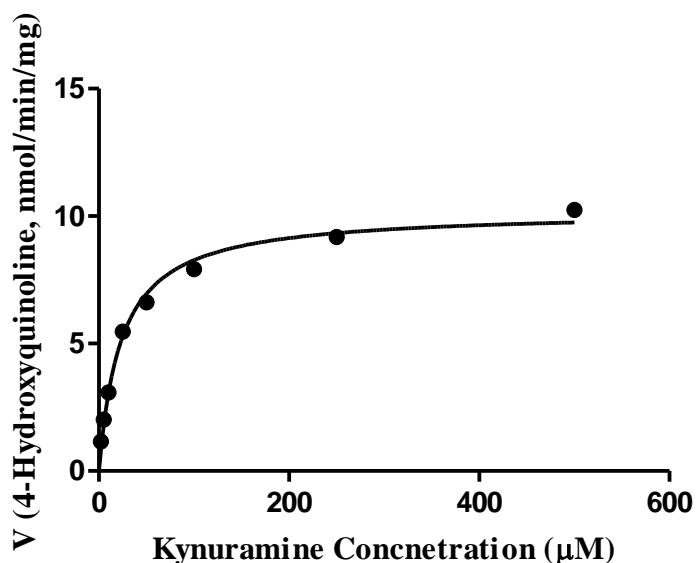


Figure 6.6. Concentration Dependence for Oxidative Deamination of Kynuramine with MAO-A

Kynuramine (2, 5, 10, 25, 50, 100, 250, and 500 μM) was incubated with MAO-A (0.01 mg/mL). The Michaelis-Menten model was used to fit the data by GraphPad Prism 5. The formation of 4-hydroxyquinoline per unit time per unit protein is expressed as mean \pm SD in this figure. The experiments were conducted 3 times in triplicate. The graph is a single representative experiment. The error bar is invisible.

The concentration dependence for oxidative deamination of kynuramine with MAO-B is shown in **Figure 6.7**. Kynuramine (2, 5, 10, 25, 50, 100, 250, and 500 μM) was incubated in 200 μL potassium phosphate buffer (100 mM, pH 7.4) for 15 min with MAO-B (0.01 mg/mL). The Michaelis-Menten model was used to fit the data by GraphPad Prism 5. The experiments were conducted 3 times in triplicate. The graph is a single representative experiment. The K_m and V_{max} were $18.0 \pm 2.3 \mu\text{M}$ and $7.35 \pm 0.69 \text{ nmol/min/mg}$ (mean \pm SEM), respectively. From these data, the concentration of kynuramine was set at 10 μM for the following inhibition study so that kynuramine concentration was $< K_m$.

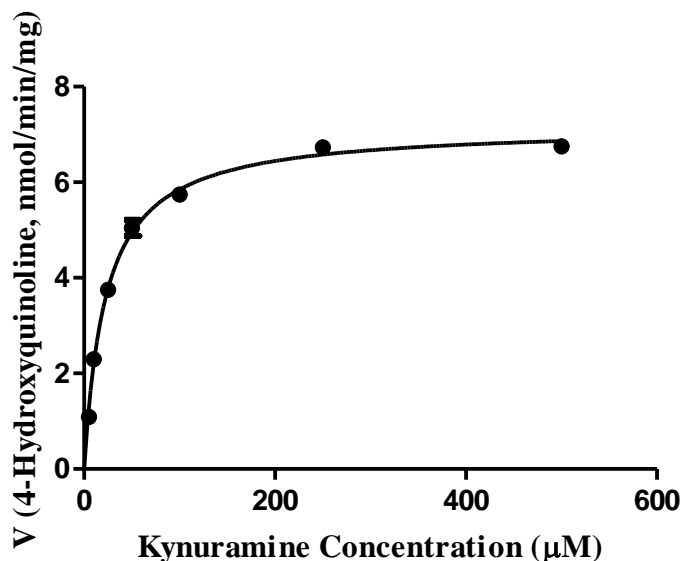


Figure 6.7. Concentration Dependence for Oxidative Deamination of Kynuramine with MAO-B

Kynuramine (2, 5, 10, 25, 50, 100, 250, and 500 μM) was incubated with MAO-B (0.01 mg/mL). The Michaelis-Menten model was used to fit the data by GraphPad Prism 5. The formation of 4-hydroxyquinoline per unit time per unit protein is expressed as mean \pm SD in this figure. The experiments were conducted 3 times in triplicate. The graph is a single representative experiment.

6.3.4 Inhibition Screening and IC_{50} Determination

The inhibition screening for oxidative deamination of kynuramine with MAO-A is shown in **Figure 6.8**. Kynuramine (10 μM) was incubated in 200 μL potassium phosphate buffer (100 mM, pH 7.4) for 15 min with MAO-A (0.01 mg/mL) and one of these phenolic dietary compounds. The control was the incubation with kynuramine but without any dietary compounds. The numbers are expressed as means \pm SD and the significant differences were analyzed between the control (with no inhibitor) and treatments in presence of phenolic dietary compounds using one-way ANOVA analysis followed by Dunnett's *post hoc* test in GraphPad Prism 5. All the phenolic compounds tested in the experiments showed significant inhibition of MAO-A activity

with $p < 0.05$. These MAO-A inhibitors were curcumin, guaiacol, isoeugenol, pterostilbene, resveratrol, and zingerone.

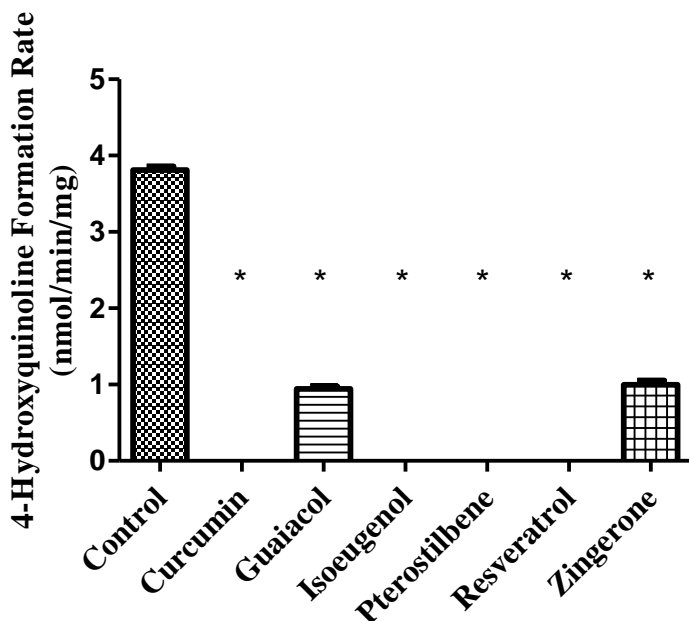


Figure 6.8. Inhibition of MAO-A Activity by Phenolic Dietary Compounds

The inhibition screening for oxidative deamination of kynuramine with MAO-A was conducted with kynuramine (10 μM) incubated with MAO-A (0.01 mg/mL) and one of these phenolic dietary compounds. The control was the incubation with kynuramine but without any dietary compounds. The numbers are expressed as means \pm SD ($n = 6$) and * indicates the significant differences between the control (with no inhibitor) and treatments in presence of phenolic dietary compounds analyzed with one-way ANOVA followed by Dunnett's *post hoc* test in GraphPad Prism 5. Not detected indicates formation of 4-hydroxyquinoline was below LLOQ. The error bar is invisible.

The inhibition screening for oxidative deamination of kynuramine with MAO-B is shown in **Figure 6.9**. Kynuramine (10 μM) was incubated in 200 μL potassium phosphate buffer (100 mM, pH 7.4) for 15 min with MAO-B (0.01 mg/mL) and one of these phenolic dietary compounds. The control was the incubation with kynuramine but without any dietary compounds. The numbers are expressed as means \pm SD and the significant differences were analyzed between the

control (with no inhibitor) and treatments in presence of phenolic dietary compounds using one-way ANOVA analysis followed by Dunnett's *post hoc* test in GraphPad Prism 5. All the phenolic compounds tested in the experiments showed significant inhibition of MAO-B activity with $p < 0.05$. These MAO-B inhibitors were curcumin, guaiacol, isoeugenol, pterostilbene, resveratrol, and zingerone. However, zingerone showed less than 10% inhibition at 51 μM . Therefore, it was not necessary to further investigate IC_{50} for zingerone.

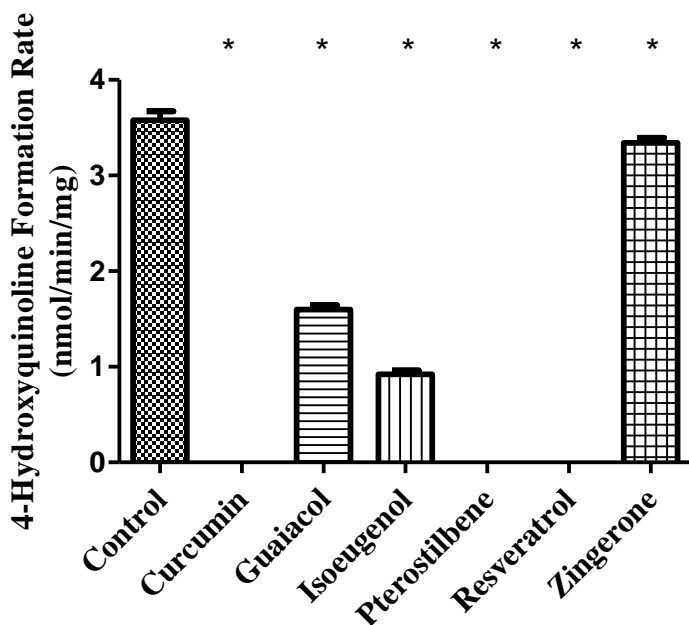


Figure 6.9. Inhibition of MAO-B Activity by Phenolic Dietary Compounds

The inhibition screening for oxidative deamination of kynuramine with MAO-B was conducted with kynuramine (10 μM) incubated with MAO-B (0.01 mg/mL) and one of these phenolic dietary compounds. The control was the incubation with kynuramine but without any dietary compounds. The numbers are expressed as means \pm SD ($n = 6$) and * indicates the significant differences between the control (with no inhibitor) and treatments in presence of phenolic dietary compounds analyzed with one-way ANOVA followed by Dunnett's *post hoc* test in GraphPad Prism 5. Not detected indicates formation of hydroxyquinoline was below LLOQ.

The IC₅₀ curves for the inhibitors of kynuramine oxidative deamination with MAO-A are shown in **Figure 6.10**. MAO-A activity was measured by the formation of 4-hydroxyquinoline during 15 min incubation of kynuramine with MAO-A in presence of inhibitor in a broad range of concentrations (at least 10⁴ fold). The fractional activity is the value of MAO activity (in presence of inhibitor) divided by the control (in absence of inhibitor). The formation of 4-hydroxyquinoline was under LLOD when incubating kynuramine with the negative control for MAO activity. IC₅₀ values and Hill coefficient were determined from non-linear regression with the model described in the method section (shown in **Table 6.9**). The concentration-dependent study for inhibitors determined the IC₅₀ values as follows: 12.9 ± 1.3 μM for curcumin, 131 ± 6 μM for guaiacol, 3.72 ± 0.20 μM for isoeugenol, 13.4 ± 1.5 μM for pterostilbene, 0.313 ± 0.008 μM for resveratrol, 16.3 ± 1.1 μM for zingerone.

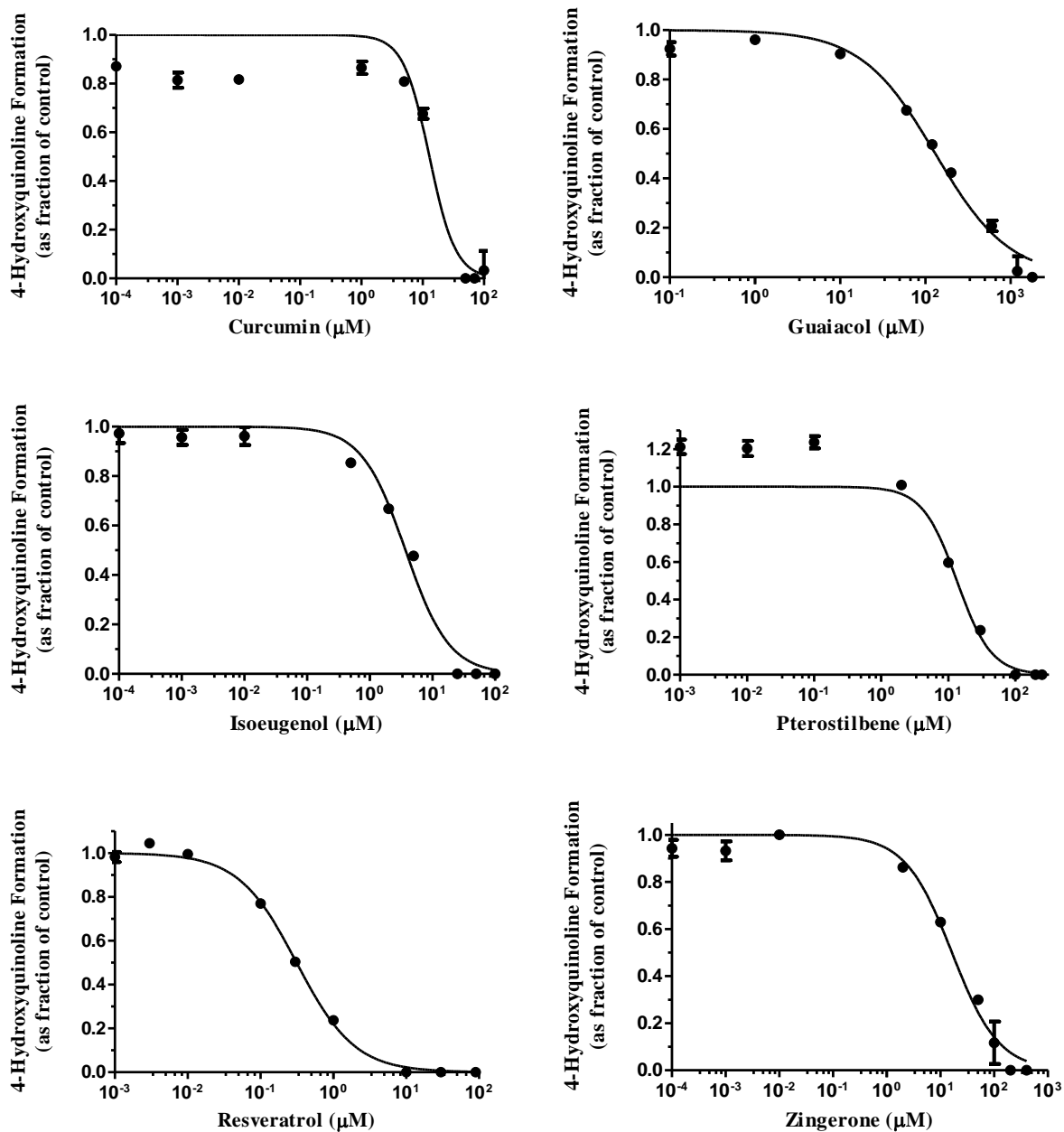


Figure 6.10. Determination of IC_{50} for Curcumin, Guaiacol, Isoeugenol, Pterostilbene, Resveratrol, and Zingerone on MAO-A Activity

MAO-A activity was measured by the formation of 4-hydroxyquinoline with inhibitor in a broad range of concentrations (at least 10^4 fold). The Y axis is expressed as fraction of the control (in absence of inhibitor) and all points on the curves are expressed as mean \pm SD ($n = 6$).

Table 6.9. IC₅₀ and Hill Coefficient for MAO-A Inhibition by Phenolic Compounds

Compound	IC ₅₀ (μM)	SEM	Hill Coefficient	SEM
Curcumin	12.9	1.3	2.0	0.4
Guaiacol	131	6	1.0	
Isoeugenol	3.72	0.20	1.2	0.1
Pterostilbene	13.4	1.5	1.7	0.3
Resveratrol	0.313	0.008	1.1	0.0
Zingerone	16.3	1.1	1.0	

The IC₅₀ curves for the inhibitors of kynuramine oxidative deamination with MAO-B are shown in **Figure 6.11**. MAO-B activity was measured by the formation of 4-hydroxyquinoline during 15 min incubation of kynuramine with MAO-B in presence of inhibitor in a broad range of concentrations (at least 10⁴ fold). The fractional activity is the value of MAO activity (in presence of inhibitor) divided by the control (in absence of inhibitor). The formation of 4-hydroxyquinoline was under LLOD when incubating kynuramine with the negative control for MAO activity. IC₅₀ values and Hill coefficient were determined from non-linear regression with the model described in the method section (shown in **Table 6.10**). The concentration-dependent study for inhibitors determined the IC₅₀ values as follows: 6.30 ± 0.11 μM for curcumin, 322 ± 27 μM for guaiacol, 102 ± 5 μM for isoeugenol, 0.138 ± 0.013 μM for pterostilbene, 15.8 ± 1.3 μM for resveratrol.

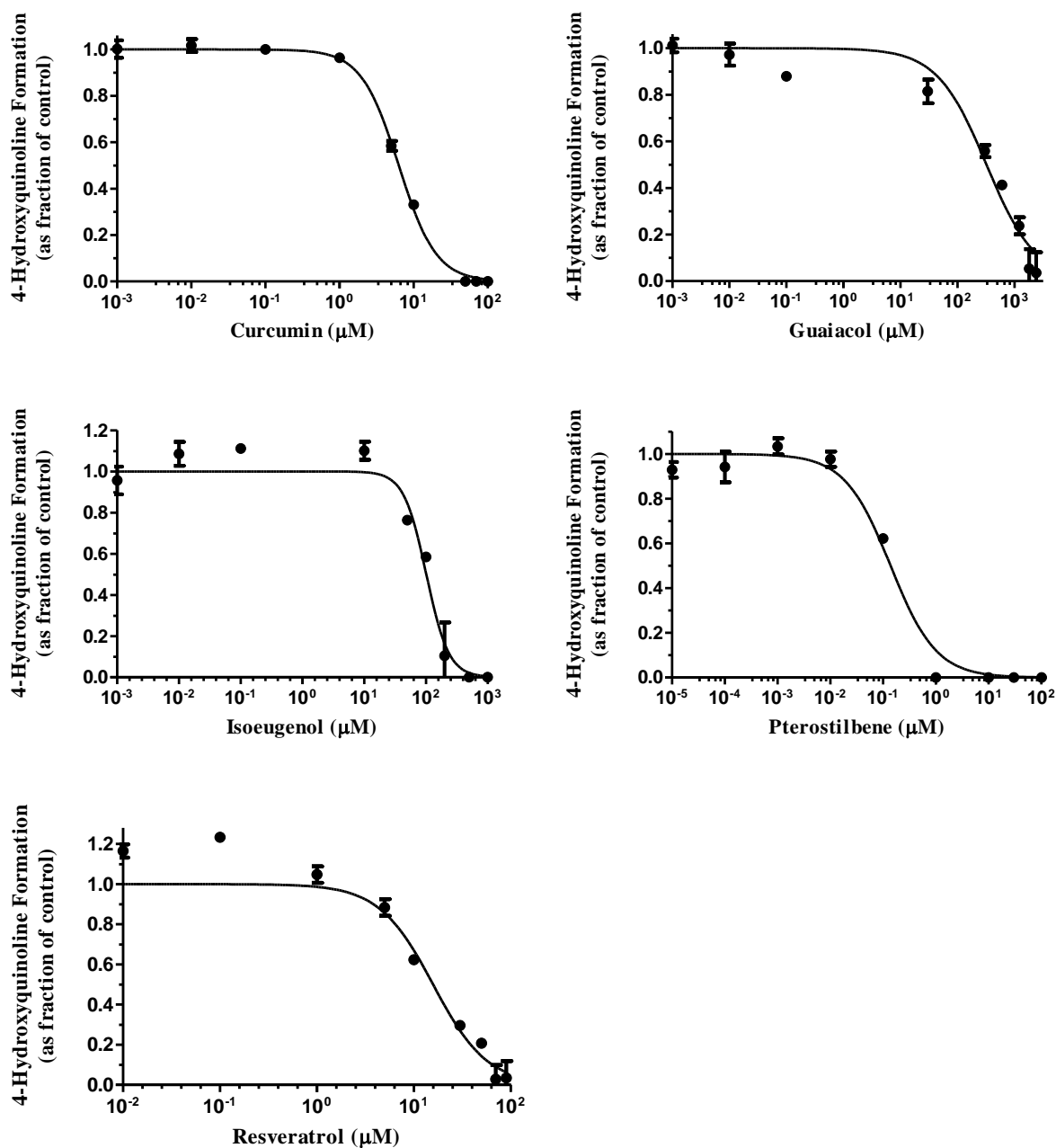


Figure 6.11. Determination of IC_{50} for Curcumin, Guaiacol, Isoeugenol, Pterostilbene, and Resveratrol on MAO-B Activity

MAO-B activity was measured by the formation of 4-hydroxyquinoline with inhibitor in a broad range of concentrations (at least 10^4 fold). The Y axis is expressed as fraction of the control (in absence of inhibitor) and all points on the curves are expressed as mean \pm SD (n = 6).

Table 6.10. IC₅₀ and Hill Coefficient for MAO-B Inhibition by Phenolic Compounds

Compound	IC ₅₀ (μM)	SEM	Hill Coefficient	SEM
Curcumin	6.30	0.11	1.7	0.1
Guaiacol	322	27	1.0	
Isoeugenol	102	5	2.4	0.3
Pterostilbene	0.138	0.013	1.0	
Resveratrol	15.8	1.3	1.6	0.2

6.4 DISCUSSION AND CONCLUSIONS

The analytical assays for kynuramine and its MAO-mediated terminal metabolite, 4-hydroxyquinoline, have been reported in the literature. The quantitative analysis could be simply achieved by fluorometric assay [179]. Other analyses are accomplished by HPLC with UV and FLU detection as well as LC-MS/MS method [180-183]. The phenolic compounds tested in this study have very strong FLU, which may interfere with the FLU signal from 4-hydroxyquinoline if measured in a microplate reader. Therefore, fluorometric microplate assay may not be selective for the detection of 4-hydroxyquinoline and thus the chromatographic separation of 4-hydroxyquinoline and the phenolic compounds were required. Since 4-hydroxyquinoline has very good FLU and kynuramine can be detected by UV detection, HPLC methods with UV and FLU detectors were found to be quite adequate for analysis in *in vitro* enzyme kinetic studies. Herraiz *et al.* developed a reversed-phase HPLC method by gradient elution with 50 mM ammonium phosphate buffer at pH 3 and 20% of this buffer in acetonitrile [180, 181]. The mobile phase contained ammonium phosphate, which is easy to precipitate in the HPLC equipment. In order to avoid the high pressure caused by the precipitation or even damage to the HPLC system, modification of the mobile phase was considered and discussed in the method section.

The HPLC method for quantitative analysis of kynuramine and 4-hydroxyquinoline used 6.5 mM triethylamine and 13 mM trifluoroacetic acid in water as its aqueous phase, which has a pH value around 2. The estimated most basic pKa of kynuramine is 8.4, which makes it form a cation under the pH condition of the mobile phase [8]. The estimated most acidic and most basic pKa of 4-hydroxyquinoline are 4.3 and 11.1, respectively [8]. Hence 4-hydroxyquinoline is also a cation at the mobile phase pH. At high concentration, trifluoroacetic acid can act as an ion-pairing agent for cations, which can improve kynuramine and 4-hydroxyquinoline retention. When using the aqueous mobile phase with trifluoroacetic acid at 0.05%, there was a tailing problem with the peak shape. This can be caused by the ions like sodium and potassium bound to silanol exchanging with ionized basic analytes at low pH. As an additive in the mobile phase, triethylamine can fix the tailing problem on the column. Excess triethylamine in the mobile phase can replace the ions instead of basic analytes. Therefore, triethylamine can reduce the peak tailing [162].

An HPLC method was developed to simultaneously quantitate kynuramine and 4-hydroxyquinoline. The formation of 4-hydroxyquinoline was measured to determine MAO activity. Kynuramine concentration was also measured for the mass balance calculation. The mass balance ranged from 90% to 110% in all the experiments.

For the preliminary study, the formation of 4-hydroxyquinoline was linear over 60 min with the protein concentration range of 0.003 mg/mL – 0.03 mg/mL, which was comparable with the results from the paper published by Herraiz *et al.* in 2006 [180]. The K_m values of kynuramine oxidative deamination by MAO-A and MAO-B were 23 μ M and 18 μ M, respectively, which indicated MAO-A has similar affinity toward kynuramine, compared to MAO-B. In the literature, the K_m values of kynuramine for human MAO-A and MAO-B were reported as 42 μ M and 26

μM [182]. Another study obtained the K_m values of MAO-A and MAO-B with kynuramine as 44.1 and 90.0 μM , respectively [184]. K_m values reported here were similar to the values in the literature, although differences in methods may account for differences in reported K_m values. The concentration of kynuramine for the inhibition study with phenolic compounds was set at 10 μM , which was below the K_m value for both MAO-A and MAO-B.

Theoretically, at extremely low concentration of inhibitors, the fractional enzyme activity should be 1, and at very high concentration of inhibitors, the fractional enzyme activity should be 0. Therefore, the Hill equation with two parameters instead of four parameters (including top and bottom as parameters) was first used to fit the IC_{50} data. The Hill coefficient was not fixed at 1. This equation could also facilitate the investigation of the stoichiometry or allosterism of the interaction between enzyme and the inhibitor. If the 95% confidence interval of the Hill coefficient included 1, then the data would be plotted with one parameter equation with the Hill coefficient fixed at 1. This indicated the stoichiometry of binding of the enzyme and inhibitor was 1-to-1. According to the obtained Hill coefficient, guaiacol and zingerone was 1-to-1 binding with MAO-A. Guaiacol and pterostilbene followed 1-to-1 binding with MAO-B. The Hill coefficient of resveratrol with MAO-A was 1.08, which was very close to 1, but the 95% confidence interval of the Hill coefficient of resveratrol with MAO-A was 1.02 to 1.16, which did not include 1. Curcumin, isoeugenol, pterostilbene had the Hill coefficient larger than 1, suggesting positive cooperativity, multiple active sites, or non-ideal inhibition behavior [185]. Non-ideal inhibition behavior is usually caused by protein denaturants [185]. In our experiment system, DMSO solvent for stock solution is such a protein denaturant. However, the concentration of DMSO in the final solution was less than 0.5% which was far below the concentration 2% as recommended by BD Biosciences, which is thought to cause minimal

inhibitory effects on both MAO-A and MAO-B. So the non-ideal inhibition behavior was unlikely to occur in our studies. Positive cooperativity could be a possible reason. The binding of the inhibitor to one active site on the enzyme may increase the binding affinity of the inhibitor to other active sites [185]. Another possibility is that the complete inhibition of an enzyme can be achieved by binding of more than one molecule of inhibitor to the enzyme [185]. Further study is required to investigate the mechanism of inhibition which leads to the Hill coefficient larger than 1, including possible allosterism.

Among these tested phenolic dietary compounds, the inhibitory effects on MAO-A and MAO-B in animal models were reported in the literature previously [170, 175]. However, the investigation was never conducted with human MAO. In this study, human recombinant MAO-A and MAO-B enzymes were used as models to test these phenolic compounds. Curcumin can inhibit MAO-A and MAO-B in mouse brain after oral administration [170]. We also found out that curcumin was a potent inhibitor for both MAO-A and MAO-B with IC_{50} as 12.9 μM and 6.30 μM , respectively. In this study, resveratrol was the most potent inhibitor for MAO-A with IC_{50} as 0.313 μM . Resveratrol is a potent inhibitor of MAO-A in rat brain with IC_{50} of 2 μM and K_i of 2.5 μM [175].

Compared to the GI concentration converted from the maximum single dose, the IC_{50} values of all phenolic inhibitors on MAO-A and MAO-B are smaller than the maximum concentration in GI tract. The most potent inhibitor for MAO-A was resveratrol followed by isoeugenol, curcumin, pterostilbene, zingerone, and guaiacol in descending order of the inhibition magnitude. The most potent inhibitor for MAO-B was pterostilbene followed by curcumin, resveratrol, isoeugenol, and guaiacol in descending order of the inhibition magnitude.

Phenolic compounds are substrates for neither MAO-A or MAO-B. The mechanism of the inhibition of phenolic compounds on MAO is not clear, but none of them has been reported to have irreversible inhibition on MAO-A or MAO-B [171, 172]. The researchers found that they are reversible inhibitors with various mode of inhibition such as competitive inhibition, non-competitive, or mixed-type inhibition [171, 172].

The mRNA levels of MAO-A and MAO-B are similar in the liver with the ratio of the target mRNA to peptidylprolyl isomerase A mRNA as 0.346 and 0.476, respectively [186]. The ratio of MAO-A mRNA in small intestine is 0.719. The ratio of MAO-B mRNA in small intestine is 0.163. The mRNA expression of MAO-A in small intestine is much higher than MAO-B [186].

According to the literature, these phenolic MAO-A inhibitors all have low bioavailability. Curcumin has poor bioavailability after oral administration in humans even after a high dose of 12 g/day, which leads to low plasma concentration [187]. At the dose 4 g, 6 g, and 8 g, the maximum concentration of curcumin in plasma is 0.51 μM , 0.64 μM , and 1.77 μM , respectively [91]. After gavage administration, the absolute bioavailability of isoeugenol in female and male rats is 19% and 10%, respectively. The low bioavailability of isoeugenol was also observed in mice as 28% for male mice and 31% for female mice after gavage bolus [188]. The peak concentration of resveratrol in human is very low after oral dose [119, 121]. At 25 mg, 50 mg, 100 mg, and 150 mg dose level, the maximum concentration of resveratrol is 1.48 ng/mL, 6.59 ng/mL, 21.4 ng/mL, and 24.8 ng/mL, respectively [121]. At higher dose level of 0.5 g, 1.0 g, 2.5 g, and 5.0 g, the corresponding peak concentration of resveratrol is 72.6 ng/mL, 117.0 ng/mL, 268.0 ng/mL, and 538.8 ng/mL [119]. The oral bioavailability in rats was determined as 12.5% after 10 mg/kg gavage administration by Lin *et al.* [104]. After giving rats 56 or 168 mg/kg/day pterostilbene by gavage for 14 continuous days, the oral bioavailability is 0.8

[105]. The reason why these phenolic compounds have such low bioavailability is that they all undergo extensive pre-systemic metabolism and are converted to their metabolites before going to the systemic circulation [87-89, 96, 105, 106, 117-120].

As described above, in the dose range of 25 mg to 5.0 g, the maximum concentration of resveratrol is in the range 1.48 to 538.8 ng/mL. Considering the plasma protein binding of 91% for resveratrol, the unbound peak concentration is in the range 5.84×10^{-4} to 0.212 μM [189]. With the IC_{50} values of 0.313 and 15.8 μM for MAO-A and MAO-B and assuming competitive inhibition of resveratrol on human MAO-A and MAO-B, the K_i would be 0.218 and 10.2 μM for MAO-A and MAO-B, respectively. Therefore, the drug-drug interaction index for MAO-A and MAO-B with resveratrol is calculated by unbound C_{max}/K_i [190]. The drug-drug interaction index for MAO-A is in the range of 2.7×10^{-3} to 0.97. The drug-drug interaction index for MAO-B is in the range of 5.7×10^{-5} to 0.021. At high dose level of resveratrol (5.0 g), the drug-drug interaction on MAO-A may occur.

Since these phenolic compounds all have relatively low bioavailability, the inhibition occurring after first-pass metabolism is likely to be limited. Most inhibitory effects on MAO-A and MAO-B would be limited to GI tract and liver. This could limit the possible side effects when giving PE and these phenolic MAO inhibitors together.

CHAPTER 7

OVERALL CONCLUSIONS AND FUTURE DIRECTIONS

PE is the most popular nonprescription oral nasal decongestant currently on the market. It has been used for decades and is considered safe [7]. It has pharmacological activity as a selective α_1 -adrenergic receptor agonist [7]. But the oral bioavailability of PE is low and highly variable, due to its extensive first-pass metabolism [19]. The efficacy study conducted for PE shows that an oral dose of 10 mg PE is not significantly different from the placebo based on the effects on nasal airway resistance [3]. The low bioavailability and associated variability of PE probably cause the poor efficacy. Unlike oral bioavailability problems caused by poor solubility that may be solved by modified formulations, low oral bioavailability of PE is due to extensive pre-systemic metabolism. Therefore, if the pre-systemic metabolism can be inhibited, the bioavailability of PE would be expected to increase with reduced variability. According to the clinical studies, the predominant metabolic pathways of PE after oral administration are sulfation and oxidative deamination [20]. Since MAO inhibitors, especially irreversible inhibitors, are found to increase the risk of hypertension when co-administered with sympathomimetic amines, they should not be systemically administered with PE [167]. In order to increase the oral bioavailability and eventually improve the efficacy of PE, this research project aimed to investigate the feasibility of inhibiting the pre-systemic sulfation of PE with some phenolic compounds from FDA's "GRAS" list, EAFUS, or dietary supplements, which are generally considered as safe.

LS180 cell line, which was demonstrated to have sulfation activity by 1-naphthol sulfation, was used as a model to test the inhibitory effects of these phenolic compounds on the sulfation of PE (50 μ M). The phenolic compounds were at the concentration of 100 μ M. Ascorbic acid (when present) was added at a concentration of 1000 μ M. For the combination of curcumin, pterostilbene, resveratrol, and zingerone, four compounds were all at the concentration of 50 μ M. The extent of disappearance of PE was significantly decreased with the following phenolic dietary compounds: curcumin, guaiacol, isoeugenol, pterostilbene, resveratrol, zingerone, and the combinations eugenol + propylparaben, vanillin + propylparaben, eugenol + propylparaben + vanillin + ascorbic acid, eugenol + vanillin, and pterostilbene + zingerone. The combinations of curcumin + resveratrol and curcumin + pterostilbene + resveratrol + zingerone almost completely inhibited PE disappearance.

PE was stable during the incubation time in absence of LS180 cells, suggesting that these inhibitor treatments probably inhibited PE metabolism rather than decreasing the degradation of PE. Based on the LC-MS/MS observation, 3-hydroxymandelic acid, the metabolite from oxidative deamination of PE, was not found when PE was incubated with LS180 cells, indicating either MAO or ALDH is absent in this cell line. Therefore, most likely PE disappearance was mainly due to Phase II metabolism, particularly sulfation.

In order to confirm the inhibition of sulfation activity in LS180 cells by these phenolic dietary compounds, PE sulfate was chemically synthesized by using hydroxyl and amine-protecting group strategy and reacting with sulfur trioxide pyridine complex. The structure of PE sulfate was confirmed by ^1H - and ^{13}C -NMR and MS. LC-MS/MS method with column switching technique was developed to quantitate PE sulfate and the parent drug PE, simultaneously. A PFP column was used as the loading column to desalt the samples followed by the separation on a CN

column with gradient elution, which allows ionization of PE metabolites and PE with negative/positive mode switching.

The formation of PE sulfate in the inhibition study using PE (50 μM) as a substrate in LS180 cells with phenolic dietary compounds or the combinations such as guaiacol, pterostilbene + zingerone, curcumin + resveratrol, curcumin + pterostilbene + resveratrol + zingerone was analyzed by the LC-MS/MS method. The phenolic compounds were at the concentration of 100 μM . For the combination of curcumin, pterostilbene, resveratrol, and zingerone, four compounds were all at the concentration of 50 μM . PE sulfate formation was inhibited by $67.0 \pm 4.2\%$ (mean \pm SEM, as % of control) with guaiacol and by $71.7 \pm 2.6\%$ with pterostilbene + zingerone. The combinations of curcumin + resveratrol and curcumin + pterostilbene + resveratrol + zingerone inhibited $\geq 99\%$ of PE sulfate formation. These results were consistent with those from analysis of the disappearance of PE in LS180 cells, providing stronger evidence that the inhibitor treatment which showed inhibitory effects on disappearance of PE did so by inhibiting the sulfation of PE in LS180 cells.

When eugenol, propylparaben, or vanillin were used alone, the extent of PE disappearance was not significantly different from the control. However, the combinations of eugenol + propylparaben, eugenol + vanillin, propylparaben + vanillin significantly decreased the extent of PE disappearance as compared to the control. This suggested synergism when eugenol, propylparaben, or vanillin was used with other compounds.

The synergistic effect was possibly due to the concentration-dependent metabolism, which has been well demonstrated in the literature [20, 134-137, 191]. The metabolic pattern could be changed dependent on the dose of the parent drug. The contribution of certain enzymes to the metabolism of the drug may change with substrate concentration. Eugenol, propylparaben, and

vanillin may inhibit PE metabolic pathway mediated by different enzymes or enzyme isoforms. When applying only eugenol, propylparaben, or vanillin, PE may switch to the other metabolic pathways that are not inhibited by the compound. But when applying the inhibitor combinations, all these pathways for PE metabolism may have been blocked. Therefore, the significant decline in the disappearance of PE was observed with combinations of eugenol + propylparaben, eugenol + vanillin, propylparaben + vanillin.

In conclusion, several compounds and especially their combinations have shown the inhibitory effects on PE sulfation in LS180 cell model and could be potential compounds for co-administration with PE to improve its oral bioavailability.

Considering the potential safety issue related to MAO inhibition, the drug-drug interaction of sympathomimetic amines and MAO inhibitors may cause hypertension in patients. Thus, it was necessary to test the inhibitory effects of these phenolic compounds on MAO-A/B. Since the immediate metabolite from PE oxidative deamination by MAO is not commercially available, kynuramine was used as a model substrate of MAO-A/B for the inhibition study. The preliminary linearity studies were conducted to optimize the assay condition. The K_m values for human recombinant MAO-A and B were $23.1 \pm 0.8 \mu\text{M}$ and $18.0 \pm 2.3 \mu\text{M}$ (mean \pm SEM), respectively. The inhibition screening for oxidative deamination with MAO-A/B was using kynuramine as substrate at $10 \mu\text{M}$. Significant inhibition was found with curcumin, guaiacol, isoeugenol, pterostilbene, resveratrol, and zingerone on both MAO-A and B at expected relevant GI concentrations.

Further kinetic studies were conducted to determine the IC_{50} values of these inhibitors for MAO-A and MAO-B. The most potent inhibitor for MAO-A was resveratrol ($0.313 \pm 0.008 \mu\text{M}$, mean \pm SEM) followed by isoeugenol ($3.72 \pm 0.20 \mu\text{M}$), curcumin ($12.9 \pm 1.3 \mu\text{M}$), pterostilbene

($13.4 \pm 1.5 \mu\text{M}$), zingerone ($16.3 \pm 1.1 \mu\text{M}$), and guaiacol ($131 \pm 6 \mu\text{M}$). The most potent inhibitor for MAO-B was pterostilbene ($0.138 \pm 0.013 \mu\text{M}$, mean \pm SEM) followed by curcumin ($6.30 \pm 0.11 \mu\text{M}$), resveratrol ($15.8 \pm 1.3 \mu\text{M}$), isoeugenol ($102 \pm 5 \mu\text{M}$), and guaiacol ($322 \pm 27 \mu\text{M}$). The phenolic compounds are substrates for neither MAO-A or MAO-B. The mechanism of the inhibition of phenolic compounds on MAO is not clear, but none of them have been reported to be irreversible inhibitors on MAO-A or MAO-B. The researchers found that they are reversible inhibitors with various mode of inhibition such as competitive, non-competitive, or mixed-type inhibition [171, 172].

Based on the evidence from the literature, these phenolic MAO inhibitors all have low oral bioavailability [104, 105, 119, 121, 187, 188]. Even at very high doses, expected and observed plasma concentrations of these compounds are very low and sometimes could not be detected [119, 121, 187]. The reason why these phenolic compounds have such low bioavailability is that they all undergo extensive pre-systemic metabolism and are mostly converted to their metabolites before reaching the systemic circulation [87-89, 96, 105, 106, 117-120]. Since these phenolic compounds all have relatively low bioavailability, the inhibition that would occur systemically after first-pass metabolism is limited. Most inhibitory effects on MAO-A and MAO-B if any would be on the GI tract and liver. This could limit the possible side effects when giving PE and these phenolic MAO inhibitors together.

So far it is not clear which phenolic dietary compound or combination could be used as excipients with PE to inhibit pre-systemic sulfation of PE without adverse effects (such as systemic MAO inhibition) and to effectively increase the oral bioavailability of PE. Future studies are needed for further investigation. Kinetic studies on sulfation inhibition with phenolic compounds using intestinal and hepatic cytosol are necessary to investigate the IC_{50} values of

these compounds. The use of recombinant SULT isoforms would also be valuable. The mode of inhibition is better to determine for inhibitors on sulfation as well as oxidative deamination.

Ultimately, we anticipate designing a double-blind, randomized, cross-over study in humans and clinically testing a combination approach, which would enable use of each inhibitor at safe and clinically feasible dose, and utilize the potential synergy observed in these studies. The envisioned product would therefore include PE and more than one phenolic dietary inhibitor at established safe doses. The combination of inhibitors would be chosen based upon achievable doses, efficacy to inhibit SULT, lack of MAO inhibition at anticipated peak plasma concentrations, and low oral bioavailability and toxicity of the inhibitor itself. The potential clinical utility of the approach would be evaluated by determining the relative bioavailability of PE.

REFERENCES

1. Empey, D.W. and K.T. Medder, *Nasal decongestants*. *Drugs*, 1981. **21**(6): p. 438-43.
2. Kanfer, I., R. Dowse, and V. Vuma, *Pharmacokinetics of oral decongestants*. *Pharmacotherapy*, 1993. **13**(6 Pt 2): p. 116S-128S; discussion 143S-146S.
3. Hatton, R.C., et al., *Efficacy and safety of oral phenylephrine: systematic review and meta-analysis*. *Ann Pharmacother*, 2007. **41**(3): p. 381-90.
4. Porter, R.S., *The Merck Manual of Diagnosis and Therapy*. 2011: Wiley.
5. Kernan, W.N., et al., *Phenylpropanolamine and the risk of hemorrhagic stroke*. *N Engl J Med*, 2000. **343**(25): p. 1826-32.
6. Meadows, M., *FDA issues public health advisory on phenylpropanolamine in drug products*. *FDA Consum*, 2001. **35**(1): p. 9.
7. Eccles, R., *Substitution of phenylephrine for pseudoephedrine as a nasal decongestant. An illogical way to control methamphetamine abuse*. *Br J Clin Pharmacol*, 2007. **63**(1): p. 10-4.
8. *SciFinder*. 2012, Chemical Abstracts Service.
9. Lin, W.-D., et al., *Enantioselective synthesis of (< i> S</i>)-phenylephrine by whole cells of recombinant< i> Escherichia coli</i> expressing the amino alcohol dehydrogenase gene from< i> Rhodococcus erythropolis</i> BCRC 10909*. *Process Biochemistry*, 2010. **45**(9): p. 1529-1536.
10. Axelrod, J., *O-methylation of epinephrine and other catechols in vitro and in vivo*. *Science*, 1957. **126**(3270): p. 400-401.
11. Brenner, G.M. and C. Stevens, *Pharmacology*. 2009: Elsevier Health Sciences.
12. Hendeles, L., *Selecting a decongestant*. *Pharmacotherapy*, 1993. **13**(6 Pt 2): p. 129S-134S; discussion 143S-146S.
13. Hendeles, L. and R.C. Hatton, *Oral phenylephrine: an ineffective replacement for pseudoephedrine?* *J Allergy Clin Immunol*, 2006. **118**(1): p. 279-80.
14. Keys, A. and A. Violante, *THE CARDIO-CIRCULATORY EFFECTS IN MAN OF NEO-SYNEPHRIN (1- α -hydroxy- β -methylamino-3-hydroxy-ethylbenzene hydrochloride)*. *Journal of Clinical Investigation*, 1942. **21**(1): p. 1.
15. Sjöqvist, F., *Psychotropic drugs (2) interaction between monoamine oxidase (MAO) inhibitors and other substances*. *Proceedings of the Royal Society of Medicine*, 1965. **58**(11 Pt 2): p. 967.
16. Callingham, B.A., *Some aspects of the enzymic inactivation of sympathomimetic amines*. *Blood Vessels*, 1987. **24**(5): p. 240-52.

17. Poctova, M. and B. Kakac, [*Fluorometric determination of the hydrochlorides of norpseudoephedrine, p-hydroxynorephedrine and phenylephrine*]. Cesk Farm, 1980. **29**(6): p. 191-5.
18. Dombrowski, L.J., P.M. Comi, and E.L. Pratt, *GLC determination of phenylephrine hydrochloride in human plasma*. Journal of Pharmaceutical Sciences, 1973. **62**(11): p. 1761-1763.
19. Hengstmann, J.H. and J. Goronzy, *Pharmacokinetics of 3H-phenylephrine in man*. Eur J Clin Pharmacol, 1982. **21**(4): p. 335-41.
20. Ibrahim, K.E., et al., *The mammalian metabolism of R-(-)-m-synephrine*. J Pharm Pharmacol, 1983. **35**(3): p. 144-7.
21. Chien, D.S. and R.D. Schoenwald, *Fluorometric determination of phenylephrine hydrochloride by liquid chromatography in human plasma*. J Pharm Sci, 1985. **74**(5): p. 562-4.
22. Vuma, V. and I. Kanfer, *High-performance liquid chromatographic determination of phenylephrine in human serum with coulometric detection*. J Chromatogr B Biomed Appl, 1996. **678**(2): p. 245-52.
23. Gumbhir, K. and W.D. Mason, *High-performance liquid chromatographic determination of phenylephrine and its conjugates in human plasma using solid-phase extraction and electrochemical detection*. J Pharm Biomed Anal, 1996. **14**(5): p. 623-30.
24. Gao, S., et al., *Evaluation of volatile ion-pair reagents for the liquid chromatography-mass spectrometry analysis of polar compounds and its application to the determination of methadone in human plasma*. J Pharm Biomed Anal, 2006. **40**(3): p. 679-88.
25. Galmier, M.J., et al., *High-performance liquid chromatographic determination of phenylephrine and tropicamide in human aqueous humor*. Biomed Chromatogr, 2000. **14**(3): p. 202-4.
26. Garcia, A., et al., *Poly(ethyleneglycol) column for the determination of acetaminophen, phenylephrine and chlorpheniramine in pharmaceutical formulations*. J Chromatogr B Analyt Technol Biomed Life Sci, 2003. **785**(2): p. 237-43.
27. Marin, A. and C. Barbas, *CE versus HPLC for the dissolution test in a pharmaceutical formulation containing acetaminophen, phenylephrine and chlorpheniramine*. J Pharm Biomed Anal, 2004. **35**(4): p. 769-77.
28. Olmo, B., et al., *New approaches with two cyano columns to the separation of acetaminophen, phenylephrine, chlorpheniramine and related compounds*. J Chromatogr B Analyt Technol Biomed Life Sci, 2005. **817**(2): p. 159-65.
29. Ptacek, P., J. Klima, and J. Macek, *Development and validation of a liquid chromatography-tandem mass spectrometry method for the determination of*

- phenylephrine in human plasma and its application to a pharmacokinetic study.* J Chromatogr B Analyt Technol Biomed Life Sci, 2007. **858**(1-2): p. 263-8.
30. Dousa, M. and P. Gibala, *Fast HPLC method using ion-pair and hydrophilic interaction liquid chromatography for determination of phenylephrine in pharmaceutical formulations.* J AOAC Int, 2010. **93**(5): p. 1436-42.
 31. Ghanekar, A.G. and D. Das Gupta, *Applications of paired ion high-pressure liquid chromatography to catecholamines and phenylephrine.* J Pharm Sci, 1978. **67**(9): p. 1247-50.
 32. Wilson, T.D., M.D. Forde, and A.V. Crain, *Simultaneous liquid chromatographic determination of glutaric acid, phenylephrine, and benzyl alcohol in a prototype nasal spray with application to di- and tricarboxylic acids.* J Pharm Sci, 1985. **74**(3): p. 312-5.
 33. Schieffer, G.W., et al., *Determination of the structure of a synthetic impurity in guaifenesin: modification of a high-performance liquid chromatographic method for phenylephrine hydrochloride, phenylpropanolamine hydrochloride, guaifenesin, and sodium benzoate in dosage forms.* J Pharm Sci, 1984. **73**(12): p. 1856-8.
 34. Das Gupta, V. and K.R. Stewart, *Chemical stabilities of lignocaine hydrochloride and phenylephrine hydrochloride in aqueous solution.* J Clin Hosp Pharm, 1986. **11**(6): p. 449-52.
 35. Martinsson, A., S. Bevegard, and P. Hjemdahl, *Analysis of phenylephrine in plasma: initial data about the concentration-effect relationship.* Eur J Clin Pharmacol, 1986. **30**(4): p. 427-31.
 36. Lau, O.W., et al., *The simultaneous determination of active ingredients in cough-cold mixtures by isocratic reversed-phase ion-pair high-performance liquid chromatography.* J Pharm Biomed Anal, 1989. **7**(6): p. 725-36.
 37. Yamaguchi, M., et al., *High-performance liquid chromatographic determination of phenylephrine in human serum using column switching with fluorescence detection.* J Chromatogr B Biomed Appl, 1994. **661**(1): p. 93-9.
 38. Marin, A., et al., *Validation of a HPLC quantification of acetaminophen, phenylephrine and chlorpheniramine in pharmaceutical formulations: capsules and sachets.* J Pharm Biomed Anal, 2002. **29**(4): p. 701-14.
 39. Kiser, T.H., A.R. Oldland, and D.N. Fish, *Stability of phenylephrine hydrochloride injection in polypropylene syringes.* Am J Health Syst Pharm, 2007. **64**(10): p. 1092-5.
 40. Amer, S.M., et al., *Simultaneous determination of phenylephrine hydrochloride, guaifenesin, and chlorpheniramine maleate in cough syrup by gradient liquid chromatography.* J AOAC Int, 2008. **91**(2): p. 276-84.

41. Bogner, R. and J. Walsh, *Sustained-release principle in human subjects utilizing radioactive techniques*. Journal of Pharmaceutical Sciences, 1964. **53**(6): p. 617-620.
42. Cavallito, C.J., L. Chafetz, and L.D. Miller, *Some studies of a sustained release principle*. Journal of Pharmaceutical Sciences, 1963. **52**(3): p. 259-263.
43. Corporation, S.-P., *Understanding Phenylephrine Metabolism, Pharmacokinetics, Bioavailability and Activity*. 2007.
44. Hengstmann, J., U. Weyand, and H. Dengler, *The physiological disposition of etilefrine in man*. European journal of clinical pharmacology, 1975. **9**(2-3): p. 179-187.
45. Eisenhofer, G., *The role of neuronal and extraneuronal plasma membrane transporters in the inactivation of peripheral catecholamines*. Pharmacol Ther, 2001. **91**(1): p. 35-62.
46. Cases, O., et al., *Plasma membrane transporters of serotonin, dopamine, and norepinephrine mediate serotonin accumulation in atypical locations in the developing brain of monoamine oxidase A knock-outs*. J Neurosci, 1998. **18**(17): p. 6914-27.
47. Horvath, G., et al., *Norepinephrine transport by the extraneuronal monoamine transporter in human bronchial arterial smooth muscle cells*. Am J Physiol Lung Cell Mol Physiol, 2003. **285**(4): p. L829-37.
48. Yasuda, S., et al., *Sulfation of chlorotyrosine and nitrotyrosine by human lung endothelial and epithelial cells: role of the human SULT1A3*. Toxicol Appl Pharmacol, 2011. **251**(2): p. 104-9.
49. Baranczyk-Kuzma, A., *Phenol sulfotransferase in human lung*. Biochem Med Metab Biol, 1986. **35**(1): p. 18-30.
50. Baranczyk-Kuzma, A. and T. Szymczyk, *Lung phenol sulfotransferases. Thermal stability of human and bovine enzymes*. Biochem Pharmacol, 1986. **35**(6): p. 995-9.
51. Pacifici, G.M. and M.W.H. Coughtrie, *Human Cytosolic Sulfotransferases*. 2005: Taylor & Francis Group.
52. Mizuma, T., et al., *Differentiation of organ availability by sequential and simultaneous analyses: intestinal conjugative metabolism impacts on intestinal availability in humans*. J Pharm Sci, 2005. **94**(3): p. 571-5.
53. Mizuma, T., *Assessment of presystemic and systemic intestinal availability of orally administered drugs using in vitro and in vivo data in humans: intestinal sulfation metabolism impacts presystemic availability much more than systemic availability of salbutamol, SULT1A3 substrate*. J Pharm Sci, 2008. **97**(12): p. 5471-6.
54. Meerman, J.H., et al., *Sulfation of carcinogenic aromatic hydroxylamines and hydroxamic acids by rat and human sulfotransferases: substrate specificity, developmental aspects and sex differences*. Chem Biol Interact, 1994. **92**(1-3): p. 321-8.

55. Yang, C.H., et al., *Sulfation of selected mono-hydroxyflavones by sulfotransferases in vitro: a species and gender comparison*. J Pharm Pharmacol, 2011. **63**(7): p. 967-70.
56. Wang, Q., et al., *Inter-species comparison of 7-hydroxycoumarin glucuronidation and sulfation in liver S9 fractions*. In Vitro Cell Dev Biol Anim, 2006. **42**(1-2): p. 8-12.
57. Vaidyanathan, J.B. and T. Walle, *Glucuronidation and sulfation of the tea flavonoid (-)-epicatechin by the human and rat enzymes*. Drug Metab Dispos, 2002. **30**(8): p. 897-903.
58. Thomae, B.A., et al., *Human catecholamine sulfotransferase (SULT1A3) pharmacogenetics: functional genetic polymorphism*. J Neurochem, 2003. **87**(4): p. 809-19.
59. Klaassen, C.D. and J.W. Boles, *Sulfation and sulfotransferases 5: the importance of 3'-phosphoadenosine 5'-phosphosulfate (PAPS) in the regulation of sulfation*. FASEB J, 1997. **11**(6): p. 404-18.
60. Chen, G., et al., *Human gastrointestinal sulfotransferases: identification and distribution* ☆. Toxicology and applied pharmacology, 2003. **187**(3): p. 186-197.
61. Whittemore, R.M., L.B. Pearce, and J.A. Roth, *Purification and kinetic characterization of a dopamine-sulfating form of phenol sulfotransferase from human brain*. Biochemistry, 1985. **24**(10): p. 2477-82.
62. Lin, W.H. and J.A. Roth, *Characterization of a tyrosylprotein sulfotransferase in human liver*. Biochem Pharmacol, 1990. **40**(3): p. 629-35.
63. Mizuma, T., M. Hayashi, and S. Awazu, *p-Nitrophenol sulfation in rat liver cytosol: multiple forms and substrate inhibition of aryl sulfotransferase*. J Pharmacobiodyn, 1983. **6**(11): p. 851-8.
64. Honma, W., et al., *Enzymatic characterization and interspecies difference of phenol sulfotransferases, STIA forms*. Drug Metab Dispos, 2001. **29**(3): p. 274-81.
65. Veronese, M.E., et al., *Functional characterization of two human sulphotransferase cDNAs that encode monoamine- and phenol-sulphating forms of phenol sulphotransferase: substrate kinetics, thermal-stability and inhibitor-sensitivity studies*. Biochem J, 1994. **302** (Pt 2): p. 497-502.
66. Negishi, M., et al., *Structure and function of sulfotransferases*. Arch Biochem Biophys, 2001. **390**(2): p. 149-57.
67. Glatt, H., et al., *Human cytosolic sulphotransferases: genetics, characteristics, toxicological aspects*. Mutat Res, 2001. **482**(1-2): p. 27-40.
68. Riches, Z., et al., *Quantitative evaluation of the expression and activity of five major sulfotransferases (SULTs) in human tissues: the SULT "pie"*. Drug Metab Dispos, 2009. **37**(11): p. 2255-61.

69. Shih, J.C., K. Chen, and M.J. Ridd, *Monoamine oxidase: from genes to behavior*. *Annu Rev Neurosci*, 1999. **22**: p. 197-217.
70. Suzuki, O., et al., *Oxidation of synephrine by type A and type B monoamine oxidase*. *Experientia*, 1979. **35**(10): p. 1283-4.
71. Glover, V., et al., *Dopamine is a monoamine oxidase B substrate in man*. 1977.
72. O'Carroll, A.-M., et al., *The deamination of dopamine by human brain monoamine oxidase*. *Naunyn-Schmiedeberg's archives of pharmacology*, 1983. **322**(3): p. 198-202.
73. Peng, H., et al., *Vanillin cross-linked chitosan microspheres for controlled release of resveratrol*. *Food Chemistry*, 2010. **121**(1): p. 23-28.
74. Lu, Z., et al., *Complexation of resveratrol with cyclodextrins: solubility and antioxidant activity*. *Food Chemistry*, 2009. **113**(1): p. 17-20.
75. Kumar, G.N., et al., *Metabolism and disposition of the HIV-1 protease inhibitor lopinavir (ABT-378) given in combination with ritonavir in rats, dogs, and humans*. *Pharmaceutical research*, 2004. **21**(9): p. 1622-1630.
76. Shoba, G., et al., *Influence of piperine on the pharmacokinetics of curcumin in animals and human volunteers*. *Planta Med*, 1998. **64**(4): p. 353-6.
77. Atal, C., R. Dubey, and J. Singh, *Biochemical basis of enhanced drug bioavailability by piperine: evidence that piperine is a potent inhibitor of drug metabolism*. *Journal of Pharmacology and Experimental Therapeutics*, 1985. **232**(1): p. 258-262.
78. Johnson, J.J., et al., *Enhancing the bioavailability of resveratrol by combining it with piperine*. *Mol Nutr Food Res*, 2011. **55**(8): p. 1169-76.
79. Moon, Y.J. and M.E. Morris, *Pharmacokinetics and bioavailability of the bioflavonoid biochanin A: effects of quercetin and EGCG on biochanin A disposition in rats*. *Mol Pharm*, 2007. **4**(6): p. 865-72.
80. Volak, L.P., et al., *Curcuminoids inhibit multiple human cytochromes P450, UDP-glucuronosyltransferase, and sulfotransferase enzymes, whereas piperine is a relatively selective CYP3A4 inhibitor*. *Drug Metab Dispos*, 2008. **36**(8): p. 1594-605.
81. Marchetti, F., et al., *Differential inhibition of human liver and duodenum sulphotransferase activities by quercetin, a flavonoid present in vegetables, fruit and wine*. *Xenobiotica*, 2001. **31**(12): p. 841-7.
82. Walle, T., E.A. Eaton, and U.K. Walle, *Quercetin, a potent and specific inhibitor of the human P-form phenosulfotransferase*. *Biochem Pharmacol*, 1995. **50**(5): p. 731-4.
83. Prusakiewicz, J.J., et al., *Parabens inhibit human skin estrogen sulfotransferase activity: possible link to paraben estrogenic effects*. *Toxicology*, 2007. **232**(3): p. 248-56.

84. Nishimuta, H., et al., *Inhibitory effects of various beverages on human recombinant sulfotransferase isoforms SULT1A1 and SULT1A3*. *Biopharm Drug Dispos*, 2007. **28**(9): p. 491-500.
85. Bamforth, K.J., et al., *Common food additives are potent inhibitors of human liver 17 alpha-ethinyloestradiol and dopamine sulphotransferases*. *Biochem Pharmacol*, 1993. **46**(10): p. 1713-20.
86. Ravindranath, V. and N. Chandrasekhara, *Absorption and tissue distribution of curcumin in rats*. *Toxicology*, 1980. **16**(3): p. 259-65.
87. Garcea, G., et al., *Consumption of the putative chemopreventive agent curcumin by cancer patients: assessment of curcumin levels in the colorectum and their pharmacodynamic consequences*. *Cancer Epidemiol Biomarkers Prev*, 2005. **14**(1): p. 120-5.
88. Ireson, C., et al., *Characterization of metabolites of the chemopreventive agent curcumin in human and rat hepatocytes and in the rat in vivo, and evaluation of their ability to inhibit phorbol ester-induced prostaglandin E2 production*. *Cancer Res*, 2001. **61**(3): p. 1058-64.
89. Ireson, C.R., et al., *Metabolism of the cancer chemopreventive agent curcumin in human and rat intestine*. *Cancer Epidemiol Biomarkers Prev*, 2002. **11**(1): p. 105-11.
90. *Evaluation of certain food additives. Fifty-first report of the Joint FAO/WHO Expert Committee on Food Additives*. *World Health Organ Tech Rep Ser*, 2000. **891**: p. i-viii, 1-168.
91. Cheng, A.L., et al., *Phase I clinical trial of curcumin, a chemopreventive agent, in patients with high-risk or pre-malignant lesions*. *Anticancer Res*, 2001. **21**(4B): p. 2895-900.
92. Mamer, O.A., et al., *Identification of urinary 3-ethoxy-4-hydroxybenzoic and 3-ethoxy-4-hydroxymandelic acids after dietary intake of ethyl vanillin*. *Biomed Mass Spectrom*, 1985. **12**(4): p. 163-9.
93. Fischer, I.U., G.E. von Unruh, and H.J. Dengler, *The metabolism of eugenol in man*. *Xenobiotica*, 1990. **20**(2): p. 209-22.
94. Ogata, N., N. Matsushima, and T. Shibata, *Pharmacokinetics of wood creosote: glucuronic acid and sulfate conjugation of phenolic compounds*. *Pharmacology*, 1995. **51**(3): p. 195-204.
95. Kuge, T., T. Shibata, and M.S. Willett, *Wood creosote, the principal active ingredient of seirogan, an herbal antidiarrheal medicine: a single-dose, dose-escalation safety and pharmacokinetic study*. *Pharmacotherapy*, 2003. **23**(11): p. 1391-400.

96. Badger, D.A., et al., *Disposition and metabolism of isoeugenol in the male Fischer 344 rat*. Food Chem Toxicol, 2002. **40**(12): p. 1757-65.
97. Abbas, S., et al., *Metabolism of parabens (4-hydroxybenzoic acid esters) by hepatic esterases and UDP-glucuronosyltransferases in man*. Drug Metab Pharmacokinet, 2010. **25**(6): p. 568-77.
98. Bobka, M.S., *The 21 CFR (Code of Federal Regulations) online database: Food and Drug Administration regulations full-text*. Med Ref Serv Q, 1993. **12**(1): p. 7-15.
99. Yu, K.U., et al., *Metabolism of saikosaponin c and naringin by human intestinal bacteria*. Arch Pharm Res, 1997. **20**(5): p. 420-4.
100. Sharma, A.K., et al., *Up-regulation of PPARgamma, heat shock protein-27 and -72 by naringin attenuates insulin resistance, beta-cell dysfunction, hepatic steatosis and kidney damage in a rat model of type 2 diabetes*. Br J Nutr, 2011. **106**(11): p. 1713-23.
101. *Final report on the amended safety assessment of Propyl Gallate*. Int J Toxicol, 2007. **26** **Suppl 3**: p. 89-118.
102. Soni, M.G., et al., *Safety assessment of propyl paraben: a review of the published literature*. Food Chem Toxicol, 2001. **39**(6): p. 513-32.
103. Nakagawa, Y. and P. Moldeus, *Mechanism of p-hydroxybenzoate ester-induced mitochondrial dysfunction and cytotoxicity in isolated rat hepatocytes*. Biochem Pharmacol, 1998. **55**(11): p. 1907-14.
104. Lin, H.S., B.D. Yue, and P.C. Ho, *Determination of pterostilbene in rat plasma by a simple HPLC-UV method and its application in pre-clinical pharmacokinetic study*. Biomed Chromatogr, 2009. **23**(12): p. 1308-15.
105. Kapetanovic, I.M., et al., *Pharmacokinetics, oral bioavailability, and metabolic profile of resveratrol and its dimethylether analog, pterostilbene, in rats*. Cancer Chemother Pharmacol, 2011. **68**(3): p. 593-601.
106. Remsberg, C.M., et al., *Pharmacometrics of pterostilbene: preclinical pharmacokinetics and metabolism, anticancer, antiinflammatory, antioxidant and analgesic activity*. Phytother Res, 2008. **22**(2): p. 169-79.
107. Walle, T., U.K. Walle, and P.V. Halushka, *Carbon dioxide is the major metabolite of quercetin in humans*. J Nutr, 2001. **131**(10): p. 2648-52.
108. Walle, T., et al., *Quercetin glucosides are completely hydrolyzed in ileostomy patients before absorption*. J Nutr, 2000. **130**(11): p. 2658-61.
109. Manach, C., et al., *Quercetin is recovered in human plasma as conjugated derivatives which retain antioxidant properties*. FEBS Lett, 1998. **426**(3): p. 331-6.

110. Moon, J.H., et al., *Accumulation of quercetin conjugates in blood plasma after the short-term ingestion of onion by women*. Am J Physiol Regul Integr Comp Physiol, 2000. **279**(2): p. R461-7.
111. Day, A.J., et al., *Human metabolism of dietary flavonoids: identification of plasma metabolites of quercetin*. Free Radic Res, 2001. **35**(6): p. 941-52.
112. Caccia, S., *Antidepressant-like components of Hypericum perforatum extracts: an overview of their pharmacokinetics and metabolism*. Curr Drug Metab, 2005. **6**(6): p. 531-43.
113. Erlund, I., et al., *Pharmacokinetics of quercetin from quercetin aglycone and rutin in healthy volunteers*. Eur J Clin Pharmacol, 2000. **56**(8): p. 545-53.
114. Graefe, E.U., H. Derendorf, and M. Veit, *Pharmacokinetics and bioavailability of the flavonol quercetin in humans*. Int J Clin Pharmacol Ther, 1999. **37**(5): p. 219-33.
115. Ferry, D.R., et al., *Phase I clinical trial of the flavonoid quercetin: pharmacokinetics and evidence for in vivo tyrosine kinase inhibition*. Clin Cancer Res, 1996. **2**(4): p. 659-68.
116. Walle, T., et al., *High absorption but very low bioavailability of oral resveratrol in humans*. Drug Metab Dispos, 2004. **32**(12): p. 1377-82.
117. Vitaglione, P., et al., *Bioavailability of trans-resveratrol from red wine in humans*. Mol Nutr Food Res, 2005. **49**(5): p. 495-504.
118. Aumont, V., et al., *Regioselective and stereospecific glucuronidation of trans- and cis-resveratrol in human*. Arch Biochem Biophys, 2001. **393**(2): p. 281-9.
119. Boocock, D.J., et al., *Phase I dose escalation pharmacokinetic study in healthy volunteers of resveratrol, a potential cancer chemopreventive agent*. Cancer Epidemiol Biomarkers Prev, 2007. **16**(6): p. 1246-52.
120. Miksits, M., et al., *Sulfation of resveratrol in human liver: evidence of a major role for the sulfotransferases SULT1A1 and SULT1E1*. Xenobiotica, 2005. **35**(12): p. 1101-19.
121. Almeida, L., et al., *Pharmacokinetic and safety profile of trans-resveratrol in a rising multiple-dose study in healthy volunteers*. Mol Nutr Food Res, 2009. **53 Suppl 1**: p. S7-15.
122. Strand, L.P. and R.R. Scheline, *The metabolism of vanillin and isovanillin in the rat*. Xenobiotica, 1975. **5**(1): p. 49-63.
123. Dajani, R., A.M. Hood, and M.W. Coughtrie, *A single amino acid, glu146, governs the substrate specificity of a human dopamine sulfotransferase, SULT1A3*. Mol Pharmacol, 1998. **54**(6): p. 942-8.
124. Monge, P., R. Scheline, and E. Solheim, *The metabolism of zingerone, a pungent principle of ginger*. Xenobiotica, 1976. **6**(7): p. 411-23.

125. van de Kerkhof, E.G., I.A. de Graaf, and G.M. Groothuis, *In vitro methods to study intestinal drug metabolism*. *Curr Drug Metab*, 2007. **8**(7): p. 658-75.
126. Prueksaritanont, T., et al., *Comparative studies of drug-metabolizing enzymes in dog, monkey, and human small intestines, and in Caco-2 cells*. *Drug Metab Dispos*, 1996. **24**(6): p. 634-42.
127. Meinel, W., et al., *Sulfotransferase forms expressed in human intestinal Caco-2 and TC7 cells at varying stages of differentiation and role in benzo[a]pyrene metabolism*. *Drug Metab Dispos*, 2008. **36**(2): p. 276-83.
128. Nagar, S., S. Walther, and R.L. Blanchard, *Sulfotransferase (SULT) 1A1 polymorphic variants *1, *2, and *3 are associated with altered enzymatic activity, cellular phenotype, and protein degradation*. *Mol Pharmacol*, 2006. **69**(6): p. 2084-92.
129. Adjei, A.A., et al., *Interindividual variability in acetaminophen sulfation by human fetal liver: implications for pharmacogenetic investigations of drug-induced birth defects*. *Birth Defects Res A Clin Mol Teratol*, 2008. **82**(3): p. 155-65.
130. Brandon, E.F., et al., *Validation of in vitro cell models used in drug metabolism and transport studies; genotyping of cytochrome P450, phase II enzymes and drug transporter polymorphisms in the human hepatoma (HepG2), ovarian carcinoma (IGROV-1) and colon carcinoma (CaCo-2, LS180) cell lines*. *Toxicol Appl Pharmacol*, 2006. **211**(1): p. 1-10.
131. Lennernas, H., et al., *The effect of L-leucine on the absorption of levodopa, studied by regional jejunal perfusion in man*. *British journal of clinical pharmacology*, 1993. **35**(3): p. 243-250.
132. Hu, M. and R.T. Borchardt, *Transport of a large neutral amino acid in a human intestinal epithelial cell line (Caco-2): uptake and efflux of phenylalanine*. *Biochimica et Biophysica Acta (BBA)-Molecular Cell Research*, 1992. **1135**(3): p. 233-244.
133. Strazielle, N. and J.-F. Ghersi-Egea, *Demonstration of a coupled metabolism-efflux process at the choroid plexus as a mechanism of brain protection toward xenobiotics*. *The Journal of neuroscience*, 1999. **19**(15): p. 6275-6289.
134. Fry, J.R., *Influence of substrate concentration on the phase I and phase II metabolism of 4-methoxybiphenyl by rat isolated hepatocytes*. *Xenobiotica*, 1987. **17**(6): p. 751-758.
135. Koster, H., et al., *Dose-dependent shifts in the sulfation and glucuronidation of phenolic compounds in the rat in vivo and in isolated hepatocytes: The role of saturation of phenolsulfotransferase*. *Biochemical pharmacology*, 1981. **30**(18): p. 2569-2575.
136. Galinsky, R.E. and G. Levy, *Dose- and time-dependent elimination of acetaminophen in rats: pharmacokinetic implications of cosubstrate depletion*. *J Pharmacol Exp Ther*, 1981. **219**(1): p. 14-20.

137. Koster, H., et al., *Kinetics of sulfation and glucuronidation of harmol in the perfused rat liver preparation. Disappearance of aberrances in glucuronidation kinetics by inhibition of sulfation.* Biochem Pharmacol, 1982. **31**(19): p. 3023-8.
138. Kempen, G.M. and G.S. Jansen, *Enzymatic sulfation of 4-methylumbelliferone.* Cellular and Molecular Life Sciences, 1971. **27**(4): p. 485-486.
139. Walle, U.K. and T. Walle, *Stereoselective sulfation of terbutaline by the rat liver cytosol: evaluation of experimental approaches.* Chirality, 1989. **1**(2): p. 121-126.
140. Wong, K.P., *Measurement and kinetic study of the formation of adrenaline sulphate in vitro.* Biochem. J, 1978. **174**: p. 777-782.
141. Foldes, A. and J.L. Meek, *Rat brain phenolsulfotransferase: partial purification and some properties.* Biochim Biophys Acta, 1973. **327**(2): p. 365-74.
142. Ung, D. and S. Nagar, *Variable sulfation of dietary polyphenols by recombinant human sulfotransferase (SULT) 1A1 genetic variants and SULT1E1.* Drug Metab Dispos, 2007. **35**(5): p. 740-6.
143. Kurogi, K., et al., *A comparative study of the sulfation of bile acids and a bile alcohol by the Zebra danio (Danio rerio) and human cytosolic sulfotransferases (SULTs).* J Steroid Biochem Mol Biol, 2011. **127**(3-5): p. 307-14.
144. Yoshinari, K., et al., *Clioquinol is sulfated by human jejunum cytosol and SULT1A3, a human-specific dopamine sulfotransferase.* Toxicol Lett, 2011. **206**(2): p. 229-33.
145. Itaaho, K., et al., *Regioselective sulfonation of dopamine by SULT1A3 in vitro provides a molecular explanation for the preponderance of dopamine-3-O-sulfate in human blood circulation.* Biochem Pharmacol, 2007. **74**(3): p. 504-10.
146. Arakawa, Y., K. Imai, and Z. Tamura, *Improved Synthesis of Sulfoconjugate Isomers of Norepinephrine and Epinephrine, and Separation of All Sulfoconjugates of Catecholamines by Thin-Layer and High-Performance Liquid Chromatography.* Chemical & pharmaceutical bulletin, 1981. **29**(7): p. 2086-2089.
147. Lernhardt, U., et al., *Modified syntheses of dopamine-4-sulfate, epinephrine-3-sulfate, and norepinephrine-3-sulfate: determination of the position of the sulfate group by 1H-NMR spectroscopy.* Int J Sports Med, 1988. **9 Suppl 2**: p. S89-92.
148. Dusza, J.P., J.P. Joseph, and S. Bernstein, *The preparation of estradiol-17 beta sulfates with triethylamine-sulfur trioxide.* Steroids, 1985. **45**(3-4): p. 303-15.
149. Wuts, P.G.M. and T.W. Greene, *Greene's Protective Groups in Organic Synthesis.* 2006: Wiley.
150. Bowden, K., et al., *13. Researches on acetylenic compounds. Part I. The preparation of acetylenic ketones by oxidation of acetylenic carbinols and glycols.* Journal of the Chemical Society (Resumed), 1946. **0**(0): p. 39-45.

151. Tozzi, F., et al., *Enzymatic Oxidative Cyclisation Reactions Leading to Dibenzoazocanes*. 2010.
152. Fernandez, M.A. and R.H. de Rossi, *On the Mechanism of Ester Hydrolysis: Trifluoroacetate Derivatives*. *The Journal of Organic Chemistry*, 1999. **64**(16): p. 6000-6004.
153. Fendler, E.J. and J.H. Fendler, *Hydrolysis of nitrophenyl and dinitrophenyl sulfate esters*. *The Journal of Organic Chemistry*, 1968. **33**(10): p. 3852-3859.
154. Suominen, T., et al., *Determination of Serotonin and Dopamine Metabolites in Human Brain Microdialysis and Cerebrospinal Fluid Samples by UPLC-MS/MS: Discovery of Intact Glucuronide and Sulfate Conjugates*. *PLoS One*, 2013. **8**(6): p. e68007.
155. Uutela, P.i., et al., *Analysis of Intact Glucuronides and Sulfates of Serotonin, Dopamine, and Their Phase I Metabolites in Rat Brain Microdialysates by Liquid Chromatography–Tandem Mass Spectrometry*. *Analytical Chemistry*, 2009. **81**(20): p. 8417-8425.
156. Tornkvist, A., et al., *Analysis of catecholamines and related substances using porous graphitic carbon as separation media in liquid chromatography-tandem mass spectrometry*. *J Chromatogr B Analyt Technol Biomed Life Sci*, 2004. **801**(2): p. 323-9.
157. Koivisto, P., et al., *Separation of L-DOPA and four metabolites in plasma using a porous graphitic carbon column in capillary liquid chromatography*. *Chromatographia*, 2002. **55**(1-2): p. 39-42.
158. Taylor, R.L. and R.J. Singh, *Validation of liquid chromatography-tandem mass spectrometry method for analysis of urinary conjugated metanephrine and normetanephrine for screening of pheochromocytoma*. *Clin Chem*, 2002. **48**(3): p. 533-9.
159. Ji, C., et al., *Diethylation labeling combined with UPLC/MS/MS for simultaneous determination of a panel of monoamine neurotransmitters in rat prefrontal cortex microdialysates*. *Anal Chem*, 2008. **80**(23): p. 9195-203.
160. Okumura, T., et al., *Study of salivary catecholamines using fully automated column-switching high-performance liquid chromatography*. *Journal of Chromatography B: Biomedical Sciences and Applications*, 1997. **694**(2): p. 305-316.
161. Rinne, S., et al., *Limitations of porous graphitic carbon as stationary phase material in the determination of catecholamines*. *J Chromatogr A*, 2006. **1119**(1-2): p. 285-93.
162. Snyder, L.R., J.J. Kirkland, and J.L. Glajch, *Practical HPLC Method Development*. 2012: Wiley.
163. Rand, M. and F.R. TRINKER, *The mechanism of the augmentation of responses to indirectly acting sympathomimetic amines by monoamine oxidase inhibitors*. *British journal of pharmacology and chemotherapy*, 1968. **33**(2): p. 287-303.

164. Cuthbert, M.F., M.P. Greenberg, and S.W. Morley, *Cough and cold remedies: a potential danger to patients on monoamine oxidase inhibitors*. Br Med J, 1969. **1**(5641): p. 404-6.
165. Mason, A.M. and R.M. Buckle, "*Cold*" cures and monoamine-oxidase inhibitors. Br Med J, 1969. **1**(5647): p. 845-6.
166. Smookler, S. and A.J. Bermudez, *Hypertensive crisis resulting from an MAO inhibitor and an over-the-counter appetite suppressant*. Ann Emerg Med, 1982. **11**(9): p. 482-4U.
167. Elis, J., et al., *Modification by monoamine oxidase inhibitors of the effect of some sympathomimetics on blood pressure*. Br Med J, 1967. **2**(5544): p. 75-8.
168. Hodge, J.V., E.R. Nye, and G.W. Emerson, *Monoamine-Oxidase Inhibitors, Broad Beans, and Hypertension*. Lancet, 1964. **1**(7342): p. 1108.
169. Blackwell, B., et al., *Hypertensive interactions between monoamine oxidase inhibitors and foodstuffs*. The British Journal of Psychiatry, 1967. **113**(497): p. 349-365.
170. Xu, Y., et al., *The effects of curcumin on depressive-like behaviors in mice*. Eur J Pharmacol, 2005. **518**(1): p. 40-6.
171. Tao, G., et al., *Eugenol and its structural analogs inhibit monoamine oxidase A and exhibit antidepressant-like activity*. Bioorganic & medicinal chemistry, 2005. **13**(15): p. 4777-4788.
172. Kong, L., C.H. Cheng, and R. Tan, *Inhibition of MAO A and B by some plant-derived alkaloids, phenols and anthraquinones*. Journal of ethnopharmacology, 2004. **91**(2): p. 351-355.
173. Yoshino, S., et al., *Effect of quercetin and glucuronide metabolites on the monoamine oxidase-A reaction in mouse brain mitochondria*. Nutrition, 2011. **27**(7): p. 847-852.
174. Bandaruk, Y., et al., *Evaluation of the inhibitory effects of quercetin-related flavonoids and tea catechins on the monoamine oxidase-A reaction in mouse brain mitochondria*. Journal of agricultural and food chemistry, 2012. **60**(41): p. 10270-10277.
175. Ryu, S.Y., Y.N. Han, and B.H. Han, *Monoamine oxidase-A inhibitors from medicinal plants*. Archives of Pharmacal Research, 1988. **11**(3): p. 230-239.
176. Food, U., *Drug administration approved GRAS list. EAFUS: A food additive database*.
177. Food, U., *Drug Administration. EAFUS: a food additive database*. 2004.
178. Burdock, G.A., *Fenaroli's Handbook of Flavor Ingredients, Fifth Edition*. 2010: Taylor & Francis.
179. Matsumoto, T., et al., *A sensitive fluorometric assay for serum monoamine oxidase with kynuramine as substrate*. Clinical biochemistry, 1985. **18**(2): p. 126-129.
180. Herraiz, T. and C. Chaparro, *Analysis of monoamine oxidase enzymatic activity by reversed-phase high performance liquid chromatography and inhibition by beta-*

- carboline alkaloids occurring in foods and plants*. J Chromatogr A, 2006. **1120**(1-2): p. 237-43.
181. Herraiz, T. and C. Chaparro, *Human monoamine oxidase enzyme inhibition by coffee and β -carbolines norharman and harman isolated from coffee*. Life sciences, 2006. **78**(8): p. 795-802.
 182. Yan, Z., et al., *A high-throughput monoamine oxidase inhibition assay using liquid chromatography with tandem mass spectrometry*. Rapid communications in mass spectrometry, 2004. **18**(8): p. 834-840.
 183. Jones, C.K., et al., *The metabotropic glutamate receptor 4-positive allosteric modulator VU0364770 produces efficacy alone and in combination with l-DOPA or an adenosine 2A antagonist in preclinical rodent models of Parkinson's disease*. Journal of Pharmacology and Experimental Therapeutics, 2012. **340**(2): p. 404-421.
 184. Naoi, M., et al., *4-(O-benzylphenoxy)-N-methylbutylamine (bifemelane) and other 4-(O-benzylphenoxy)-N-methylalkylamines as new inhibitors of type A and B monoamine oxidase*. J Neurochem, 1988. **50**(1): p. 243-7.
 185. Copeland, R.A., *Evaluation Of Enzyme Inhibitors In Drug Discovery: A Guide For Medicinal Chemists And Pharmacologists*. 2005: Wiley-Interscience.
 186. Nishimura, M. and S. Naito, *Tissue-specific mRNA expression profiles of human phase I metabolizing enzymes except for cytochrome P450 and phase II metabolizing enzymes*. Drug metabolism and pharmacokinetics, 2006. **21**(5): p. 357-374.
 187. Anand, P., et al., *Bioavailability of curcumin: problems and promises*. Molecular pharmaceutics, 2007. **4**(6): p. 807-818.
 188. Hong, S.P., et al., *Toxicokinetics of Isoeugenol in F344 rats and B6C3F mice*. Xenobiotica, 2013.
 189. Burkon, A. and V. Somoza, *Quantification of free and protein-bound trans-resveratrol metabolites and identification of trans-resveratrol-C/O-conjugated diglucuronides - two novel resveratrol metabolites in human plasma*. Mol Nutr Food Res, 2008. **52**(5): p. 549-57.
 190. Huang, S., et al., *Drug interaction studies: study design, data analysis, and implications for dosing and labeling*. Clinical Pharmacology & Therapeutics, 2007. **81**(2): p. 298-304.
 191. Goon, D. and C.D. Klaassen, *Dose-dependent intestinal glucuronidation and sulfation of acetaminophen in the rat in situ*. Journal of Pharmacology and Experimental Therapeutics, 1990. **252**(1): p. 201-207.

VITA

Zhenxian Zhang

EDUCATION

School of Pharmacy, Virginia Commonwealth University
Ph.D. in Pharmaceutics Richmond, VA
August 2013

College of Pharmacy, The University of Toledo
M.S. in Pharmacology and Toxicology Toledo, OH
May 2009

College of Pharmacy, China Pharmaceutical University
B.Eng. in Pharmaceutical Engineering Nanjing, P. R. China
July 2006

PROFESSIONAL CONFERENCE PRESENTATIONS

Zhang Z., Gerk P. “*In Vitro* Inhibition of Phenylephrine Sulfation by Phenolic Dietary Compounds” (Poster presentation) American Society for Clinical Pharmacology and Therapeutics Annual Meeting, March, 2013, Indianapolis, IN.

Zhang Z., Gerk P. “Dietary Inhibitors of 2-Methoxyestradiol Glucuronidation in LS180 Cells” (Poster presentation) American Association of Pharmaceutical Scientists Annual Meeting, October, 2011, Washington, D.C.

Zhang Z., Gerk P. “Phenolic Inhibitors of *Trans*-Resveratrol Metabolism in LS180 Cells” (Poster presentation) American Association of Pharmaceutical Scientists Annual Meeting, October, 2011, Washington, D.C.

Zhang Z., Gerk P. “Inhibition of 2-Methoxyestradiol Metabolism” (Poster presentation) Graduate Research Association of Students in Pharmacy 31st Annual Conference, June, 2011, Boston, MA.

Zhang Z., Nauli S. “Shear Stress Induces Actin Rearrangement in Endothelial Cells” (Poster presentation) Experimental Biology Conference, April, 2009, New Orleans, LA.

JOURNAL PAPER

Yuan Y., Elbegdorj O., Chen J., Akubathini S., Zhang F., Stevens D., Beletskaya I., Scoggins K., Zhang Z., Gerk P., Selley D., Akbarali H., Dewey W., Zhang Y. “Design, Synthesis, and Biological Evaluation of 17-Cyclopropylmethyl-3,14 β -dihydroxy-4,5 α -epoxy-6 β -[(4'-pyridyl)carboxamido]morphinan Derivatives as Peripheral Selective Mu Opioid Receptor Agents” *Journal of Medicinal Chemistry*, November, 2012.

AWARDS & HONORS

Graduate School Thesis/Dissertation Assistantship Award	2012-2013
Virginia Commonwealth University Teaching Assistantship	2009-2012
The University of Toledo Graduate Rocket Award	2007-2009
The University of Toledo Graduate Scholarship	2007-2009
The Third Class Scholarship of China Pharmaceutical University	2004
The Third Class Scholarship of China Pharmaceutical University	2003
The Second Class Scholarship of China Pharmaceutical University	2003